The 2006 RBSE Journal

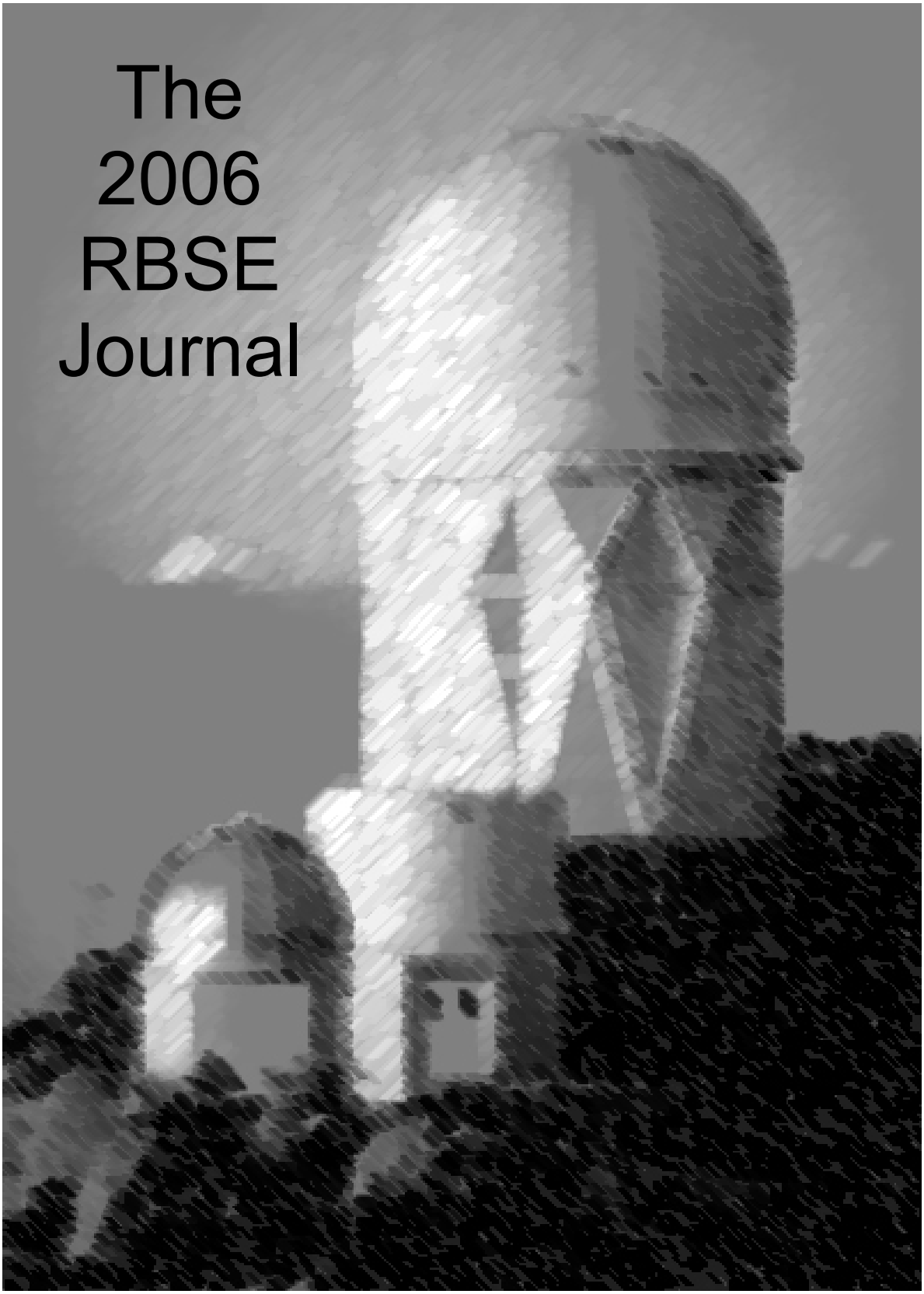

NOAO

AURA

NSF

The RBSE Journal 2006

The RBSE Journal is an annual publication that presents the research of students and teachers who have participated in the Teacher Enhancement program TLRBSE, "Teacher Leaders in Research Based Science" at the National Optical Astronomy Observatory in Tucson. This program, funded by the NSF, consists of a distance learning course and a summer workshop for high school teachers interested in incorporating research and leadership mentoring within their class and school. TLRBSE brings the research experience to the classroom with datasets, materials, support and mentors during the academic year. The journal publishes papers that make use of data from the TLRBSE program, or from its related programs such as New Mexico Skies and the SPITZER teacher observing program.

These papers represent a select set of those submitted for publication by many students. All papers are reviewed both by the Senior Editor and the Astronomer responsible for the particular research project. In addition to papers representing classroom work, a number of these papers are based on observing done at part of the Teacher Observing Program (TOP) at Kitt Peak during the fall and winter. More information about both the TLRBSE and the TOP program can be found on the website, www.noao.edu/outreach/tlrbse

I want to thank Dr. Travis Rector, Dr. Connie Walker, Dr. Steve Howell, and Dr. Jeff Lockwood for their generous help in reviewing these papers and working with the young scientists. Special thanks are due to Kathie Coil for her efficient editing of the final copy.

Dr. Katy Garmany
Senior Editor, RBSE Journal

Table of Contents

SOLAR

OTHER

Microvariability of AGN Target AO 0235+164

Crystal Ewen
Deer Valley High School, Antioch, CA
Teacher: Jeff Adkins, TLRBSE 2002

ABSTRACT
I predicted that if you watch a Polar or AGN object that there might be some variation in the magnitude over a short period of time. A Polar is two stars that orbit each other and one of the stars pulls matter from the other which emits energy. This is also true with an AGN because, as material is pulled into the black hole of an AGN, some is redirected outward at a 90° angle in a jet, which can be measured. I eventually ended up using an AGN object for this project. I originally selected a Polar object, but due to the Polar AM Her being too close to the horizon, it was no longer possible. I used a ground-based telescope to observe AO 0235+164 on December 8, 2005, for 6 hours. After my data was reduced, I did see significant variation for the time period observed, which lead to the size of the event.

BACKGROUND
The NASA website has a page on active galaxies and quasars (NASA, 2006), which states *that the black hole of an active galaxy may be highly variable and very bright compared to the rest of the galaxy.* A Polar also shows some variation since one star pulls material from the other one it would too emit energy. Therefore, an AGN and a Polar should both show variation in magnitude as the energy is absorbed or released.

With an AGN, normally it is hard to notice a lot of variation. AGNs (Fig.1) are powered by violent accretion disks surrounding supermassive black holes with masses from thousands to tens of billons of solar masses (Hester, Burnstein, Blumenthal, Greeley, Smith, Voss, Wegner, 448-456). An AGN (Fig.2) has a few specific characteristics. The black hole is located in the center of the active galaxy, surrounding the black hole is the accretion disk, which is then surrounded by an obscuring Torus. Shooting out from the accretion disk, before the event horizon, two jets are directed out at a 90° angle perpendicular to the active galaxy. When matter falls toward the black hole, before the event horizon some of it is redirected in the jets. The jets shoot out of the galaxy for hundreds, maybe thousands, of light years. On the following page is a picture of the parts of an Active Galactic Nuclei.

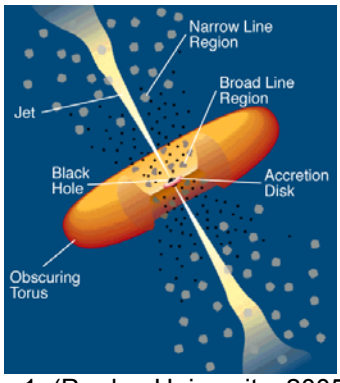

Fig.1. (Purdue University, 2005)

Unlike an AGN, a Polar (Fig.3) typically shows more variation in its magnitude. A Polar is two stars that orbit each other and one of the stars pulls matter from the other which emits energy. Steve Howell is an astronomer at the WIYN Observatory located on Kitt Peak in Arizona; he stated in an interview with CVnet (Mind Spring, 2006), that a polar is a binary star containing a white dwarf and a normal late type star. The two are very close together and the white dwarf has a very strong magnetic field. The gravitational field of the white dwarf is extremely strong that material is pulled from the secondary star. This pulled material falls onto the white dwarf at one or both of its magnetic poles, which then releases tremendous energy. If it was a regular binary star system with a white dwarf and a normal star, the material would be pulled and fall onto the equator. The energy that is emitted can be measured in magnitudes. A magnitude is a measurement of brightness that can be measured on a numerical scale.

Below are pictures of and AGN on the left (NASA, 2006) and a Polar on the right (NASA, 2006).


Fig.2 Active Galactic Nuclei, NASA, 2006

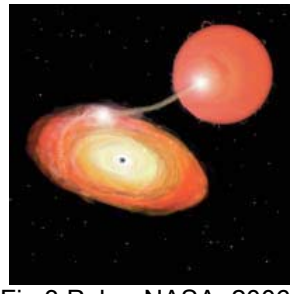
Fig.3 Polar, NASA, 2006

The targets on the Sonoma State University website are a list of objects that the GLAST (The Gamma Ray Large Area Space Telescope) telescope is going to take pictures after it is launched fall of 2007 (Myers, Newman). "With GLAST, astronomers will have a superior tool to study how black holes accelerate jets of gas outward at astonishing speeds." (NASA, 2006) The objects are also visible from a ground-based telescope. When students (like me) and several other students and teachers around the world

observe these targets from the ground, it would be possible to gain previous knowledge of any one object before GLAST points to it.

ANALYSIS AND RESULTS

To pick a target I went to http://gtn.sonoma.edu/participants/catalog and looked the objects listed. I decided to use the target AO 0235+164, an AGN, for my project. I used Starry Night Pro 3.1 to locate and predict where the target would be for observation. After imputing the Right Ascension (RA) and Declination (Dec), I could see where the target would be on any given date. The coordinates of AO 0235+164 are RA: 02h 38m 38.9s and Dec: 16h 36m 59s.

At the time I planned to observe, it was within 20° above the horizon and beyond 15° of the meridian, the range allowed for pointing the New Mexico Skies Telescope. New Mexico Skies is a commercial observatory that rents out time on a remote control telescope. The telescope I operated was a 14" Celestron SCT on a Bisque Paramount GT-1100ME. The CCD of the telescope has a field of view of about 10 arc minutes. The meridian line is a circle that passes through the two poles of the celestial sphere and the zenith of any observer. To receive time on the New Mexico Skies telescopes, I had to send a proposal to Dr. Steven Croft at the National Optical Astronomy Observatory to get a grant to use one of the telescopes. Within a week I was notified that my proposal got approved and I received seven hours of observation time. I scheduled the date for observation on December 7, 2005.

I scheduled my time in two separate time blocks. I left an hour and half for any changes with the telescope that would have to be made had an hour to start with. Right Ascension is the angular distance of a celestial body or point on a celestial sphere measured eastward from the celestial equator. Declination is the angular distance to a point on a celestial object measured north to south from the celestial equator.

To take a picture with the New Mexico Skies remote control telescope, I had to login into the telescope 07:00 Mountain Time. I then entered the coordinates and clicked slew to move the telescope. I entered different exposure times and shifted the RA and Dec a few times to rule out bad pixels. I checked the settings again to make sure everything was at the correct setting. After I took a picture, I referred to my finder chart (Fig.6), found below, to check the picture and make sure that my target was showing up. With the polar object AM Her, I could not locate the object or its standard stars.

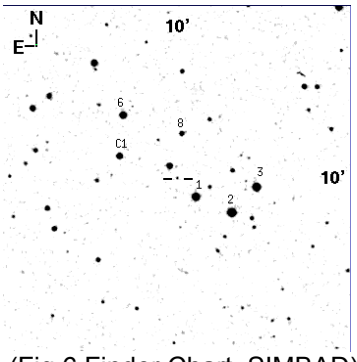

(Fig.6 Finder Chart. SIMBAD)
Coordinates are Right Ascension: 02h38m38.9s and Declination: 16h36m59s.

After I took every picture I checked the object by identifying with the standard stars, which are labeled 1, 2, 3, 6, 8, and C1. I repeated taking pictures of the object for many hours. About a week or two after the observing, I was able to access my pictures and start to record the data. For each picture, I used Image J to measure the magnitude. I measured the magnitude of AO 0235+164 in every picture I could identify it, although in some picture, it did not matter how much I changed the setting, I could not find the target. I changed the brightness and contrast to make dimmer objects, such as AO 0235+164, to be visible. After the object was visible, I used the aperture tool to get the brightness counts and x and y coordinates of the object.

When I had the brightness counts on each standard star and the target, I copied the information to a Microsoft Word Document. I used equation to convert the brightness counts to magnitudes.
Equation 1

$$\log\left(\frac{b_1}{b_2}\right) = \log(2.512)^{(m_1 - m_2)}$$

So the inputting of information would be smoother. With the help of another classmate Jennifer Becker, I rearranged the equation to be equation 2.
Equation 2

$$m_2 = \frac{m_1 + \left(\log\left(\frac{b_1}{b_2}\right)\right)}{(\log(2.512))}.$$

DISCUSSION

Collection 1

	STAR	MAGNITÉ	BRIGHTNESSCOUNTS	LOGBRIGHT
=				log (BRIGHTNESSCOU
1	1	13.03	251027.016	5.39972
2	2	12.71	325151.063	5.51209
3	3	12.92	268540.875	5.42901
4	6	14.02	104674.313	5.01984
5	8	16.48	9139.947	3.96094
6	C1	14.78	49227.504	4.69221

Fig.7 Fathom Table

With the brightness counts and magnitudes, I created a mathematical model of this relationship using a program called Fathom. I used Fathom to find the magnitudes, and, using its regression line analysis function, estimated the error of each measurement. An example of one of the models is below.

The table (Fig.7) above is the magnitude, brightness counts and the log of the brightness counts of all the standard stars. The magnitude and the log brightness are then graphed on the graph below left. The standard stars then make a least square regression line (Fig.8), which predicts where the object would fit on the line. The model (Fig.9) below on the right represents the line then gives the best estimate for the slope at a 95% confidence level and states the standard error for the slope. To get the magnitude and error of the object, I entered the log bright of the object in that picture. Fathom then predicts the value for a future observation of the magnitude and error.

Fig.8 Fathom Graph

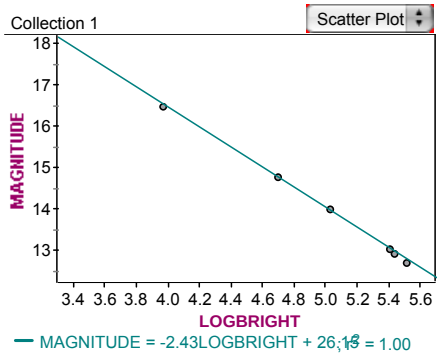

Fig.9 Fathom Model

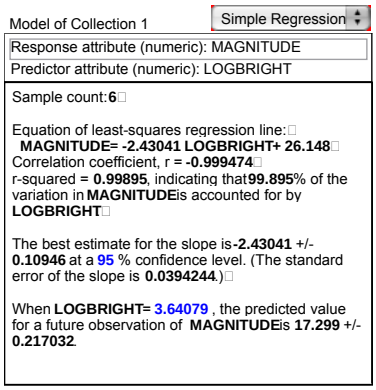

PICTURE	JULIAN DATE 2453712 +	MAGNITUDE	ERROR
28	0.72324	17.299	0.217032
29	0.72586	18.5558	0.137187
30	0.72898	17.5436	0.132601
31	0.72985	16.9926	0.196479
32	0.73201	17.2711	0.31464

PICTURE	JULIAN DATE 2453712 +	MAGNITUDE	ERROR
33	0.73492	17.5271	0.119445
34	0.73689	17.2379	0.092385
35	0.7387	17.0907	0.151131
36	0.74052	17.7923	0.707542
40	0.74726	18.3454	0.585858
43	0.75172	17.0002	0.574534
44	0.75405	17.3165	0.360194
45	0.75613	19.2069	0.3291
46	0.75841	19.2494	0.261124
47	0.76262	15.9438	0.0728273
48	0.76733	17.4236	1.00475
49	0.77225	17.6311	0.142875
50	0.78126	17.0862	0.124239
51	0.78454	17.6712	0.194272
52	0.7881	18.31372	0.17052
53	0.78983	17.7426	0.217554
54	0.79275	17.6642	0.210237
56	0.80127	17.1886	0.192085
57	0.80282	17.1683	0.19033
59	0.80693	17.6191	0.0955259
65	0.81426	16.7401	0.460569
68	0.82753	15.4695	0.08177
70	0.83705	17.2516	0.291948

Julian dates are a continuous count of days and fractions since noon Universal Time on January 1, 4713 BCE, which was almost 2.5 millions days ago. I used Julian Dates rather than a regular yearly date because it is less problematic and it can be accepted in every country of the world. Unlike calendar dates, leap years are not a problem since it is just an increasing list of dates. If an astronomer would like to use this information again it would be simpler.

The light curve (Fig. 10) represents the change in magnitude over a short period of time. The Julian dates are in decimal form because the changes all occurred within one night and about five hours of taking pictures with a telescope. As you can see, in the graph the points increase and decrease throughout the graph. If the points increase, then the object is dimmer, for example something blocking the jet. If the points decrease, then the object had something fall into it or an explosion is also possible.

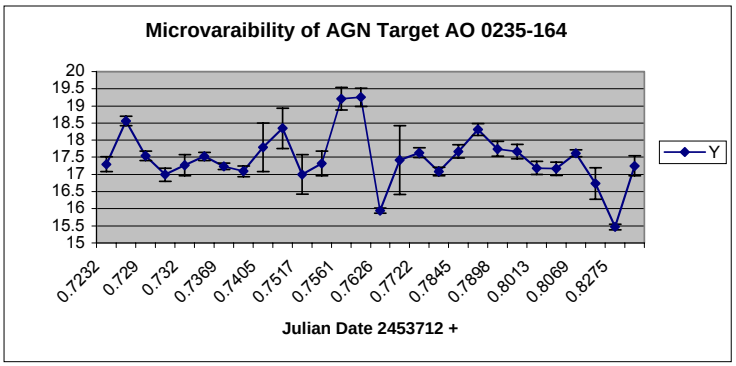

(Fig.10 Light Curve)

SUMMARY AND AKNOWLEDGEMENTS

Significant variation was detected; and there were a couple of microvariability events in the graph. The time scale if the change is such that something exceptionally small must have interfered with the flux to cause it. With changes happening over the course of just a few minutes could be caused by material moving close to the speed of light in front of the jet, or by a sudden influx of matter falling toward the black hole at the center of the AGN.

The time of the change leads to the size of what possibly caused the flux of brightness. There are three of these events throughout the light curve. For example, in the graph between the first three pictures the magnitude goes from about a magnitude of 17 to the magnitude approximately 18.5, then back to about 17. This could have been caused by something going by the jet; the size of this object can also be estimated. The speed of light is 299, 792, 458 meters per second, and will always travel at that speed. The time the change took place was within a few minutes. By multiplying the speed of light by the amount of time the flux happened, it is predictable to find the maximum size of what caused it, and the object cannot be larger.

299, 782, 458m/s x .00574s = 1720751.309m is the maximum size the object could be for the flux between the first three pictures.

I would like to thank my teacher Jeff Adkins for helping me with my project, getting me where I am and pushing me to be my best. Thanks to Lynn Rice for helping me with my telescope program I encountered. I was also helped and encouraged by my classmate and friend Jennifer Becker. With some of my complications with my research, Brielle Hinckley was a great help. Last but no least, I would like to thank my mom for pushing me and never letting me give up.

REFERENCES

"By Identifier." SIMBAD Astronomical Database. Centre de Donnees astronomiques de Strasbourg. 28 Dec. 2005 <*http://simbad.u-strasbg.fr/Simbad*>.

Comins, Neil F. and William J. Kaufmann lll. Discover the Universe. 5th ed. New York: W. H. Freeman and Company

Cui, Wei. "Active Galactic Nuclei." Purdue University. Department of Science: Physics, Purdue University. 16 Feb. 2006 <*www.physics.purdue.edu/ ~cui/pics/astro/agn.png*>.

Ferris, Timothy. Galaxies. New York: Harrison House, 1987. 106.

Gatland, Kenneth. The Illustrated Encyclopedia of Space Technology. 2nd ed. New York. Salamandr Books Limited.

Hester, Jeff; Burnstein, David; Blumenthal, George; Greeley, Ronald; Smith, Bradford; Voss, Howard, and Wegner, Gary. 21st Century Astronomy. New York & London: W.W. Norton & Company, 2002. 448-456.

Howell, Steve. "CVnet Steve Howell." CVnet. 9 Feb. 2006 <*http://home.mindspring.com/~mikesimonsen/cvnet/id32.html*>.

"Image Processing and Analysis in Java." Image J. Reaserch Service Branch. 17 Mar. 2006 <*http://rsb.info.nih.gov/ij/*>.

Levy, David H. The Scientific American Book of the Cosmos. New York: St. Martin P, 2000. 85-96.

Masetti, M, Phil Newman, and Paul J. Green. "Nasa's Imagine the Universe." NASA. NASA, Space Telescope Science Institute. 12 Jan. 2006 <*http://imagine.gsfc.nasa.gov*>.

Mitton, Simon, and Jacqueline Mitton. The Young Oxford Book of Astronomy. New York: Oxford Unversity P, 1995. 136-141.

Myers, J D., and Phil Newman. "GLAST." NASA. 01 Dec. 2005. NASA. 7 Feb. 2006 <*http://glast.gsfc.nasa.gov/*>.

"Program Object Catalog." GTN GLOBAL TELESCOPE NETWORK. Sonoma State University. 12 Jan. 2006 <*http://gtn.sonoma.edu/participants/catalog/*>.

"Tlrbse." Noao. National Science Foundation. 17 Mar. 2006 <*http://www.noao.edu/outreach/tlrbse/*>.

Yost, Dr., and Dr. Daunt. "Stellar." Astronomy 162. Dept. Physics & Astronomy: University of Tennessee. 12 Jan. 2006 <*http://csep10.phys.utk.edu/astr162/lect/stars/magnitudes.html*>.

Micro- Variability of 4c29.45 Using the Spitzer Space Telescope, and Ground Based Telescopes

Brielle Hinckley
Deer Valley High School, Antioch, CA
Teacher: Jeff Adkins, TLRBSE 2002

ABSTRACT
By observing the object 4C 29.45, an Active Galactic Nuclei in infrared and optical light, I hoped to find micro variability when observed over short periods of time. The observations using the Spitzer Space Telescope were taken on May 14, 2005, and June 9, 2005. The observations taken using the new Mexico Skies ground based telescopes were May 14, 2005, May 17, 2005, and June 10, 2005. AGN objects are known to be violent and fluctuate extensively over time. By using IRAF, an Image Data Reduction program, I reduced the optical pictures taken using both the Spitzer Space Telescope and ground optical telescopes. My light curves showed no significant change, which indicates no fluctuation in the magnitude of the object. An SED was also constructed and compared to typical graphs for these objects. No unusual emissions in the infrared were seen.

INTRODUCTION
Last year several students, including myself, were given the opportunity to observe various objects in space by Jeff Adkins, a teacher in the TOP (Teachers Observing Program). This allowed Mr. Adkins and I to observe the object 4C 29.45 with the Spitzer Space Telescope. This program provides observing time for teachers to use as a resource to create projects for themselves and their students, using the Spitzer Space Telescope. The purpose of this project was to observe this particular Active Galactic Nuclei (AGN) to determine if it fluctuates in magnitude over time. The variations that may be observed in 4C 29.45 could be caused by particles falling into the black hole. Objects such as the interstellar medium interfere with the radiation on its way to Earth. The "interstellar medium" is a very low-density material, which exists between stars and galaxies, typically just a few molecules per cubic m or less.

Active Galactic Nuclei 4C 29.45 is an AGN in a far away galaxy millions of light years away, that contains a black hole in its center. An AGN is also known as a blazar or quasar. The AGN that I observed, like others, is a black hole that has a jet that shoots out the center and is aimed directly at the earth, instead of being turned to the side or pointed away from us. These are sometimes called blazars. Quasar 4C29.45 pulsates on time scales of 30 minutes and less.

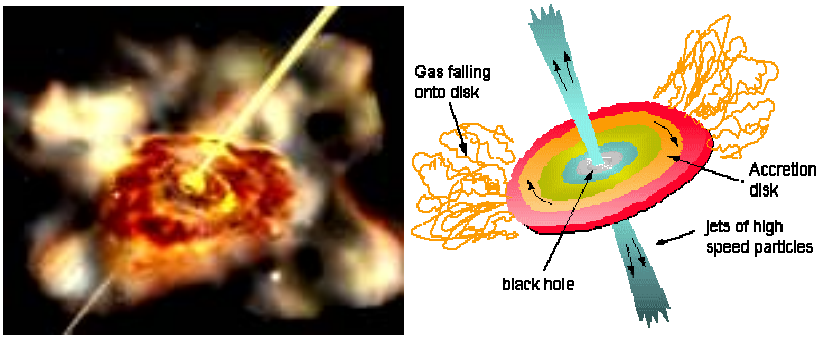

Here is an artist's impression of what a black hole may look like. Aurore Simonnet drew this picture for the GLAST Education and Public Outreach office. There are many parts of a black hole that can be seen above. The outer layer of the AGN is called the accretion disk, which is the part that is surrounding the center. It is a field of debris that has collected around the outer edge of the hole, waiting to be pulled by the immense gravitational force surrounding the center (Wikipedia, online encyclopedia). Next is the jet that shoots out of the center. It is created from particles that are redirected just before they fall into the oblivion that is the center of the hole. The particles are torn apart by the immense gravitational pull around a black hole. It is all of the particles colliding together that cause radiation to be created. The jet is the portion that is aimed directly at the Earth, as observed in this case in the object 4C 29.45.

OBSERVATIONS

When observing 4C 29.45 two methods of observation were used. One method was a remote controlled optical ground based telescope located in New Mexico, and the other was using the Spitzer Space Telescope, which gets the extended infrared part of the spectrum. Both observations were made simultaneously because there needed to be a secondary confirmation of any findings produced. Another reason that they were done simultaneously is that the Spitzer Space Telescope could not image in all channels simultaneously, and the ground based telescope observations were able to be used as a way of measuring the difference in time that elapsed between observations.

FINDER CHART

On this page is a finder chart of the coordinates and standard measurements. This came from Gordon Spear, (Spear, 2005).

4C29.45 (Coordinates: RA: 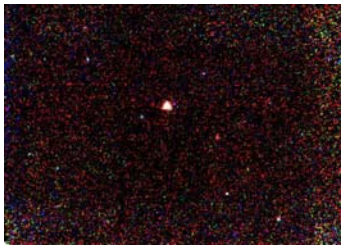 **11:59:31.8 Dec: 29:14:44)**

Star	U	B	V	R	I
1	0	14.01	13.39	13.01	0
13	16.17	16.02	15.36	14.97	14.62
13	16.38	16.41	15.89	15.53	15.16
15	17.07	17.14	16.6	16.3	15.88

Ground Based Observations

When using New Mexico Skies, a ground based observatory in New Mexico, for observations, there were a few things that I needed to know to operate the telescope. I had to learn how to measure the distance of my object from the meridian. If my object came to close to the meridian, the telescope would break, so it was crucial I not let that happen. The telescope had been pre-calibrated, so it was not necessary to calibrate my pictures for darks, flats or biases. The time on New Mexico Skies came from a grant of telescope time awarded Deer Valley High School by TLRBSE. TLRBSE an acronym that stands for Teacher Leaders in Research Based Science Education, the NOAO, or National Optical Astronomy Observatory created this program, which partners with the Spitzer Space Science Center on the California Institute of Technology campus in the Teacher Observing Program. Here is the data table that was produced using IRAF as my data reduction program.

Filter	Date	Maximum	
V	5/14/05	787.9146432	1265.549603
I	5/14/05	327.0700005	358.4600092
V	5/14/05	50.17045264	52.58332196
I	5/14/05	862.8718846	1078.316668
R	5/14/05	127.1785001	134.7143
R	5/14/05	161.6009734	176.6216641
V	5/14/05	657.3430808	926.3862405
R	5/14/05	109.0200608	118.5513271
I	5/17/05	43.32280132	45.34365571
V	5/17/05	100.9957347	104.256474
V	5/17/05	25.93581807	26.74853193
I	5/17/05	28.23681858	29.52675792
R	6/10/05	507.0678785	584.8790964
I	6/10/05	41.28375249	43.58922683
I	6/10/05	530.0031617	659.9005045
V	6/10/05	104.2406177	110.1125896
R	6/10/05	518.1311939	704.4330759
R	6/10/05	843.0051147	1302.057638
R	6/10/05	75.51945556	82.99632265
I	6/10/05	45.9917021	47.62987949
I	6/10/05	50.40067656	52.02790832

Here are the 3 light curves that were generated from that data:

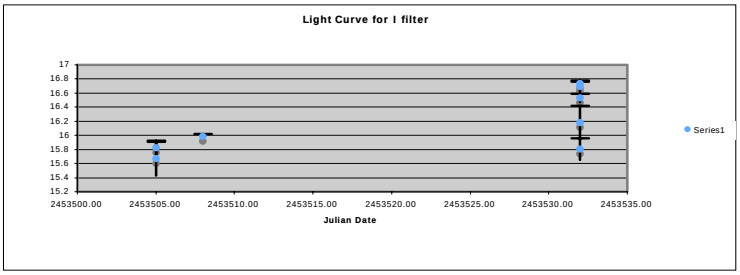

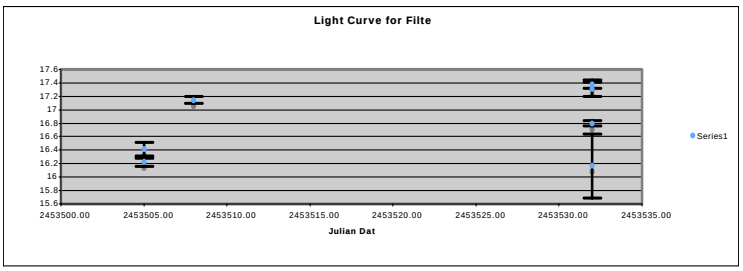

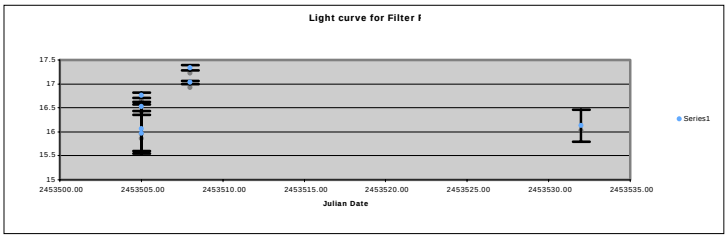

Light Curve

The first method that was used to detect variation in the objects was a light curve. A light curve is a graph of brightness vs. time, made when you observe an object over time. The way that variation is shown through a light curve is when the light curve shows spikes. If the light curve remained flat, it would prove that there was no change or flux during the observations. Some of the things that might cause the brightness to change would be an object passing over the jet radiation which would block the light from bring exposed on the CCD. Many astronomers believe super massive black holes may lie at the center of these galaxies and power their explosive energy output. The filters that I used to produce each the light curve were, V, R, I. A change in the magnitude of the objects would show one of two things, that when observed an object was passing over the jet blocking some of its light, or that extensive particles were being ripped apart causing a change in the amount of radiation that was observed.

Spitzer Space Telescope

The Spitzer Space Telescope orbits the sun and takes pictures using infrared light. Having a space telescope in space is very useful because it orbits above most of the Earth's atmosphere and can take more accurate pictures. It was especially helpful with relation to this project because the infrared part of the spectrum needs to be observed out in space away from most of the Earth's atmosphere, because the atmosphere absorbs most of the infrared radiation. I took a trip down to Pasadena, California to the Spitzer Space Science Center and with the help of Dr. Mark Lacy, reduced the Spitzer data using IRAF on a Unix machine. I am a student working in conjunction with a group of teachers, (Linda Stefaniak, Dr. Steve Rapp, and Jeff Adkins) who were also there learning how to reduce the data. Seven images were collected from the telescope.

I reduced four photos, which took about a day of work. I was able to take turns with the teachers reducing the data on the computer and we checked each other's work. The teachers reduced three of the seven images. Here is a copy of the data table produced.

Channels/ filters	Wavelength (microns)	Flux (microJanskys)	Date
IRAC 1	3.6	7011.366101	6/9/05
IRAC 2	4.5	9423.291907	6/9/05
IRAC 3	5.8	14662.31834	6/9/05
IRAC 4	8	21587.51461	6/9/05
MIPS 24	24	79033.18438	5/14/05
MIPS 70	70	234415.3588	5/14/05
MIPS 160	160	290783.9593	5/14/05

Here is the SED that was created with the help of my teacher Jeff Adkins. (Adkins, 2006)

SED

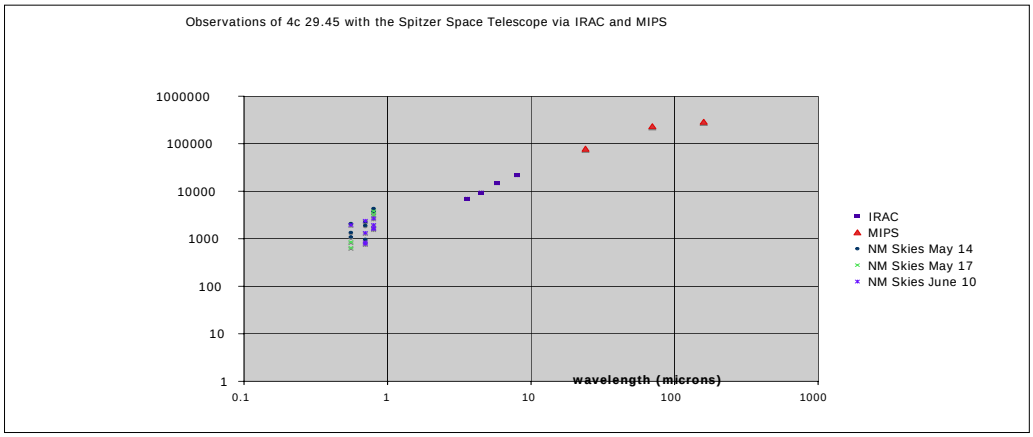

Mainly the filters that have been used in observing the objects 4C 29.45 were U, B, V, R, I. Occasionally when reducing the data collected in those filters it was discovered by both myself, and by my advising astronomer Dr. Gordon Spear, from Sonoma State University, that often the B, and V filters would not produce usable data. The object is dim and very far away, so those filters if used would block to much light from coming through to be exposed on a CCD, and would therefore make the data reduction difficult and sometimes impossible.

This graph, which is an SED, which graphs the flux of a star plotted against the wavelengths that it is measured in. This SED shows that there are no visible spikes which would indicate micro-variability. Though there may appear to be some movement among the optical data, the errors are as large as the spike, which indicates that it is not accurate enough to call it significant. This SED looks like a normal SED for an AGN.

DATA REDUCTION

After taking the New Mexico Skies pictures, I downloaded and installed IRAF, the Image Reduction and Analysis Facility Software from NOAO, onto a Macintosh computer, for data reduction purposes. Installing IRAF was a considerable challenge and took several days of effort to accomplish the first time. My teacher assisted me with this process. This project was expected to yield results that could show a change in the magnitude of both the objects over a period of time. I learned how to use IRAF and the proper commands that go along with it. Because it was unknown territory for a high school student I have produced a manual for others to use. (See appendix number 1.)

DISCUSSION

The observations of 4C29.45 do not show an unusual “spike” in the infrared end of the spectrum. The data that was collected and the graphs that were created, line up reasonably well with the Spitzer data that was analyzed. When observing an AGN in the optical spectrum any apparent variation that is observed may not prove any true variation.

The error bars on the graphs show that there is little known variation. This project has proven that these AGN were not as variable as they had been known to be in the past. My hypothesis was incorrect and was proved wrong.

SUMMARY AND ACKNOWLEDGEMENTS

I would like to thank Mr. Adkins for all of his patient effort on my behalf for an entire two years of working on this project. He was never harsh and helped me right along. I really appreciate him for that. I would also like to thank my parents for their never ending encouragement and support, even when I would want to give up, they just kept pushing me right along and now it all seems worth it. To Deer Valley High School for opening the school for late night observing, and to my classmates, Crystal Ewen and Jennifer Shankey, thanks for being great competition in the science fair and being a great help throughout the year. Thank you to you all I would NOT have gotten this far without you all!

REFERENCES

"Active Galactic Nuclei." Wikipedia. Wikipedia. Th Jan. 2006. Keyword: Active Galactic Nuclei.

Adkins, Jeff, comp. AGN Spectral Energy Distributions of GLAST Telescope Network Program Objects. Vers. 5.0. Mo Dec. 2005. NOAO, TOP, GLAST, NASA. W Dec. 2005 <*http://astronomyteacher@mac.com*>.

Krolik, Julian K. Active Galactic Nuclei: From the Central Black Hole to the Galactic Environment. Princeton: Princeton: Princeton UP, 1999. Pg.441.

Spear, Gordon. Sonoma State University. Finder Chart Credit: Landessternwarte Heidelberg-Konigstuhl.

APPENDIX 1

Procedures For Reducing Data With IRAF
These instructions for Differential Photometry assume that IRAF, XGTERM, DS9 and X11are installed and functioning but has not ever been used for photometry on New Mexico Skies fits files. Dr. Mark Lacy gave settings to us.

Getting Magnitudes From IRAF
These instructions are for you if you have already downloaded the software and IRAF package from the proper source.

Once you open up IRAF you need to type *maces login.cl*

A group of commands will appear. Go all the way down until you see the command *imtype*. Arrow over and change the default to *"fits"*. Once you have done that delete the # sign from in front of the row. CONTROL D deletes a character or mistake.

BEFORE: #set imtype "fits"
AFTER: set imtype = "fits"

Next you will go down right below to the next line *imextn* and remove the # sign there. You will next go over and ADD in the line with a bunch of stock commands (Do not delete the whole message) but ADD *fit, FIT*.

Hit *CONTROL X and S* to save the changes you have just completed.
Next hit *Ctr X C.*

Now using *cd* and .. commands you can maneuver into the directory where the files are kept.

You next type in the IRAF window *display* (the filename that you named the picture) *fill* +

Now the picture should load into the DS9 window.

Use your left click button on your mouse or on the trackpad, and in the image itself draw a green circle around your object or its standard stars.

Switch back to the IRAF window and type *digiphot.*
Next type *apphot*
Then type *epar photpars* (epar means to edit the parameters).
Then you will get a bunch of commands. You need to find the one that says *aperture* and set it to *5,10,15* (all on the same line not split up).
Next find *zmag,* another command on the page, and change it to Zero.

Now hit *CONTROL D.*

That should have saved the changes that you just made and exited you back into the IRAF window.

Next type *epar fitskypars.* When that comes up change the *annulus (annulus is a command that will pop up in the screen)* to *15* and do a CONTROL D to save and exit.

When the IRAF window comes back up you will then type the command *phot* (that opens your picture in the DS9 window) take the blinky dot and place it over your standard stars and center finely with the up and down arrows. Remember the order in which you took the phots. Once you have centered approximately in the middle you will press the SPACE bar to capture the photometry data.

A row of numbers will appear in the IRAF window.

-9.750	-9.665	-9.455
Number in IRAF standard Magnitude 1	Better magnitude for standard star	Another magnitude measurement

Of the last three in each row select the middle number. This is the photometry measurement of that star. Record the magnitudes of the standards and also measure the object.

You take the magnitude of the standard and subtract from it that of the magnitude of your target. Record this in a table.
Ex.: 13 -9.665 - -8.431= -1.234

13	-9.665	- (-8.431)	= -1.234
Standard star number	Number received from DS9	Object mag from DS9	Answer

Repeat for each standard star.

Reducing Data
Add to each result the magnitude in the finder chart under the proper filter for each standard

13	(-)1.234	+15.36	= 16.594
Standard Star	Previous answer NO NEGITIVE SIGN it is not necessary it cancels out according to M Lacy if you standard is brighter you subtract and if dimmer then you add.	Finder chart calculation of magnitude	Magnitude for standard num 13

Estimate the error for each picture by finding the range (which is the largest number by the smallest) and dividing by two. EX: 16.594, 16.456,17.011, 16.233
(16.233 – 17.011) ÷ 2 = -0.4 error bar.
Converting Magnitudes into Micro Jansky's

We must convert magnitudes to Micro Janskys to compare to the data given by Spitzer.

The Spitzer Space web page has given this table and data for conversion use.

Band	**Zero Point (Jy)**	**Central Wavelength**
U	1900	3650
V	4400	4400
B	3540	5556
R	2880	7000
I	2500	8000

Star of magnitude m has a flux in Jy if given by: $f = 100^{-0.4m} * fo$

1. Convert Central Wavelength of filter in A to nm.

in A $A * \frac{1m}{10^{10}A} * \frac{10^6 nm}{1m}$

2. Take $f_o * 10^{-.4*magnitude}$ this answer is now in Janskys.
3. Take the answer and multiply it by $\frac{10^6 mJy}{Jy}$

A Spectral Analysis of Starburst Galaxies

Aaron J. Greene, Amana A. Harris, Michael B. Roberts, and John C. Stewart
Graves County High School, Mayfield, KY
Teacher: Velvet Dowdy, TLRBSE 2003

ABSTRACT

The spectrum of emission lines of starburst galaxies was analyzed, thus determining the elements in the galaxies emitting energy. It was expected that a higher amount of H and He in the spectra of emission lines of starburst galaxies would be found. A higher amount of He I and O III, lighter elements, emitting energy was found; this was in concordance with the hypothesis. However, a lesser number of heavier elements was also found.

INTRODUCTION

A starburst galaxy is a galaxy that is in the process of an intense burst of star formation. They are studied by the scientific community because studies of nearby starburst galaxies can give a unique insight into the processes and causes of high star formation rates, which is not readily accessible in galaxies with high star formation rates at high redshift. (University of Calgary Radio Astronomy Laboratory, 2006)

Spectroscopy is the analysis of the intensity of electromagnetic radiation (such as ultraviolet, visible light, and infrared, etc.) across a range of wavelengths. Each element has a series of specific wavelengths from which it is identifiable. Spectral graphs of starburst galaxies show tall, spiky lines, known as emission lines, where energy is emitted. When analyzed, these emission lines can tell us what elements the galaxy is emitting at that time. An example of a spectral graph of a starburst galaxy is shown below.

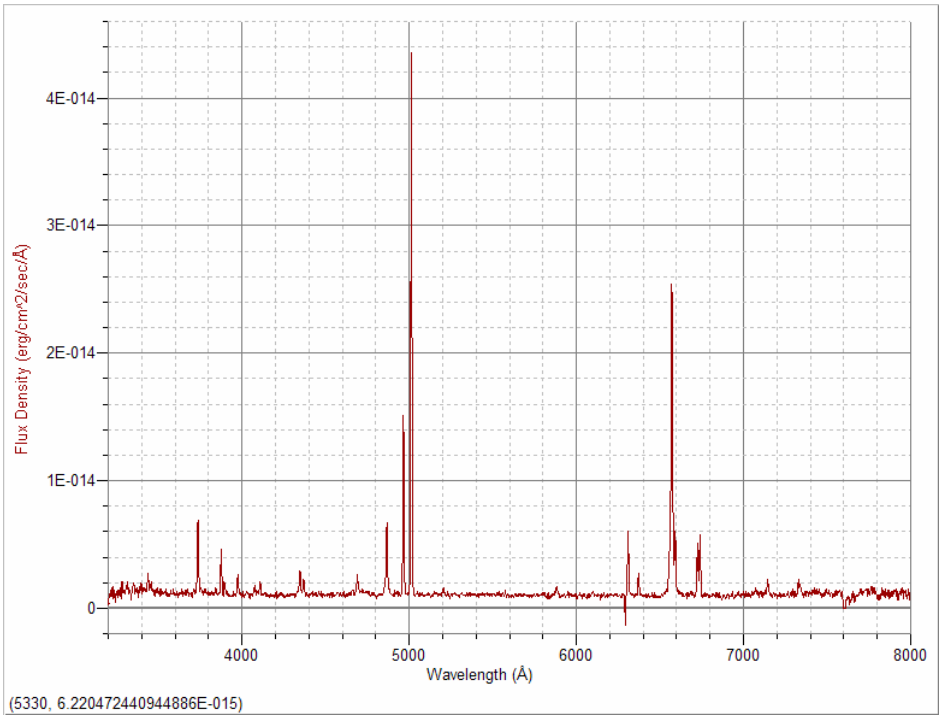

A redshift is a shift in the frequency of a photon toward lower energy or longer wavelength (MacMath, 2003). Another way to describe redshift is the elongation of a wavelength due to an object moving away from the observer.

Previous research projects found in earlier publications of the RBSE Journal were examined. More about starburst galaxies was learned while reading a research paper in the 2005 RBSE Journal by Mark Ashley, Joseph Dublin, and Josh Keeling. From this paper we found that the redshifts of starburst galaxies are somewhat smaller that those of radio and elliptical galaxies. Also, a research paper, entitled *Starbursts and Their Redshifts* (MacMath, 2003), led more research on this topic to be found. This research project led to the belief that light elements would be found in these galaxies because the stars in them would be too young to have yet fused heavier elements.

OBSERVATIONS AND DATA REDUCTION

In order to find the elements emitting energy in starburst galaxies the wavelengths of emission lines of their graphs needed to be found. This was done using graphical analysis, and data obtained from NOAO (National Optical Astronomer's Organization), NSF (National Science Foundation), and AURA (Association of Universities for Research in Astronomy). The spectra of starburst galaxies was collected by the Goldcom Spectrograph found on the 2.1-meter telescope on Kitt Peak, near Tucson, Arizona.

After the wavelengths were found, they had to be manipulated by using the redshift formula. The wavelengths of recorded starburst galaxies are skewed due to their redshift. The redshift had to be calculated in order to correct this skew in the data. This allowed the wavelength at rest for each galaxy to be found. The formula used to do this is

$$Z+1=\frac{\lambda \text{observed}}{\lambda \text{rest}}$$

A large part of the calculations made involved this formula used to find redshift, the variable Z. Obviously there are too many variables to simply solve for Z, so the observed wavelength ($\underline{\lambda}$) and the resting wavelength ($\underline{\lambda}$) needed to be found. A table was found in AGN Spectroscopy (Rector, 2001) with average value of wavelengths at rest, based on the ratio of wavelengths on any given galaxy's spectra. This wavelength and the observed wavelength were used in the formula above.

Once the final wavelength was found, it was entered into a Microsoft Excel program, *Star Classify* (written by DeVore, 2003 and used with his permission). This program gave us the known elements emitted at wavelengths near the one entered.

The data was then entered into a table using Excel, showing the galaxy, its redshift, and the elements emitted from its three tallest emission lines.

ANALYSIS AND RESULTS

Galaxy	Redshift (z)	Elements		
ngc 4631	0.0075	C II	C IV	Fe
ngc 4300	0.3835	He I	C III	He I
ngc 4395	0.011	Ca I	O III	He I
ngc 5585	0.0095	Ca I	Fe I	H X
ic 4355	0.4596	Mg	N III	N III
gb 172243	0.18	N I	O III	O III

The above graph lists each galaxy, its redshift, and the element emitted by the galaxy's the most prominent emission lines.

The chart below shows each element found and the number of times it was found emitting energy.

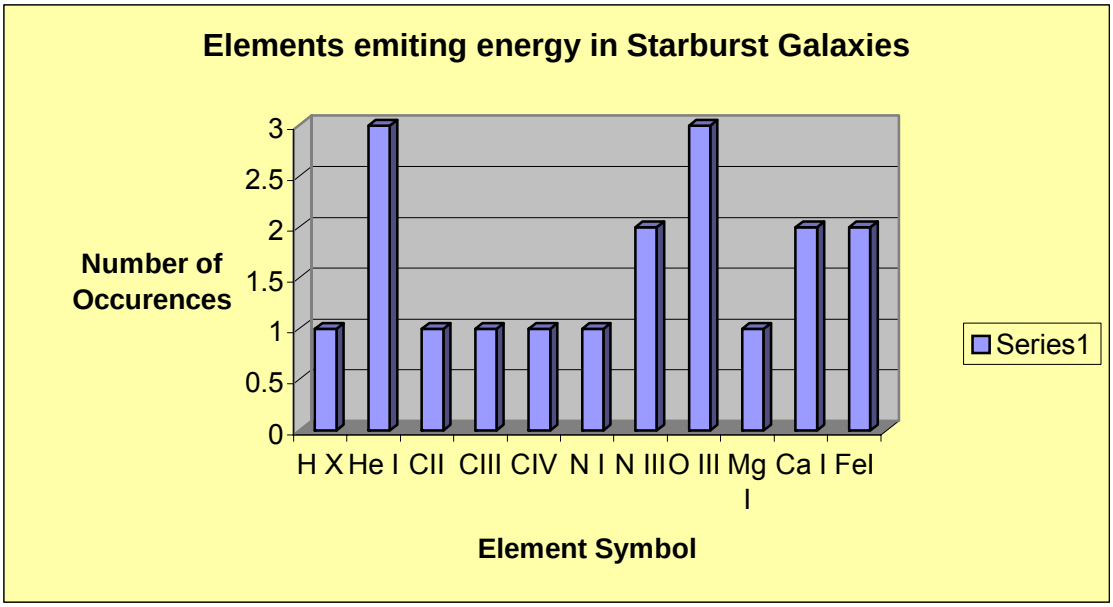

DISCUSSION

As evident in the chart, the two elements that were seen being emitted the most number of times were Helium I and Oxygen III. As both of these are lighter elements, the original hypothesis appears to be correct. However, heavier elements, such as iron and magnesium, were also found. This could be from older stars present in the galaxies.

Possible downfalls in the outcome of the data could have come from the inaccuracy of the Star Classify program. When a wavelength is entered, the program lists the top four best matches for known elements emitted at that wavelength. Then, one must choose the element whose listed wavelength is closest to the actual wavelength entered. In addition, the information found could simply be an anomaly of the fact that only six starburst galaxies were found in this study.

SUMMARY AND ACKOWLEDGEMENTS

It was concluded that although the majority of elements emitted from starburst galaxies are lighter elements, both heavier and lighter elements are emitted. This is because both young and old stars are present in starburst galaxies.

For further research on this topic, one might compare the elements that are being emitted to the redshift of the galaxy. Also, the elements could also be compared to the flux of the wavelengths.

Acknowledgements for the research project are Mrs. Velvet Dowdy for guidance throughout this project; NOAO, NSF, and AURA for giving us access to the data; and Harlan DeVore for allowing us use of he program Star Classify.

REFERENCES

Dublin, Joseph. "Redshifts of Starbursts and Elliptical/Radio Galaxies." RBSE Journal 7 (2005). 2006 <*http://www.noao.edu/outreach/tlrbse/rbsejournal05.pdf*>.

Keel, Bill. "Starburst Galaxies." The University of Alabama Arts and Sciences. Feb 2003. 2006 <*http://www.astr.ua.edu/keel/galaxies/starburst.html*>.

MacMath, Amie. "Starbursts and their Redshifts." RBSE Journal 5 (2003). 2006 <*http://www.noao.edu/outreach/tlrbse/rbsejournal03.pdf*>.

Rector, Travis A., AGN Spectroscopy, 1 Oct. 2001

"Spectra." Answers.com. 30 Mar. 2006 <*http://www.answers.com/spectra*>.

"Starburst Galaxies." Chandra X-Ray Observatory. 2006 *http://chandra.harvard.edu/xray_sources/starburst.html*

"Starburst Galaxy." Wikipedia. 2006 <*http://en.wikipedia.org/wiki/Starburst_galaxies*>.

"Starburst and Galaxy Evolution." Space Telescope Science Institute. 8 Sep 2005. Space Telescope Science Institute. 2006 <*http://www.stsci.edu/science/starburst/*>.

Stevens, Ian. "Galaxies: Starburst Galaxies." Astrophysics and Space Research Group. 25 Feb 2005. University of Birmingham. 2006 <*http://www.sr.bham.ac.uk/research/starburst.html*>.

Tremonti , Christy. "The Structure and Kinematics of Starburst Galaxies." Physics & Astronomy at John Hopkins University. 21 Jun 1998. 2006 <*http://www.pha.jhu.edu/~cat/gbo/*>.

AGN: Distance vs. Luminosity

Jessica Nicole Ortiz
Teacher: Cindy Weehler, RBSE 1999

ABSTRACT
Using Graphical Analysis for Windows, I researched and analyzed the Active Galactic Nuclei (AGN): a category of galaxies that emit a large amount of energy from an exceptionally bright nucleus. Giving the nucleus its brightness is an accretion disk located around a black-hole at its center itself. Using the RBSE CD version 7.0, I was able to find the AGN's red-shift, velocity, distance, luminosity, flux, and elemental composition configuration as well as classify it into one of five AGN groups: Radio, Quasar, BL Lac, Elliptical and Starburst. I also looked for a relationship within the data between the AGN's distance with its luminosity.

HYPOTHESIS
Regardless of the type of AGN, the farther the distance, the less intense its luminosity will be.

PURPOSE
The purpose of this project was to analyze the AGN spectral data on the RBSE CD version 7.0, classify the AGN and test my hypothesis of distance vs. luminosity.

PROCEDURE
I first searched for emission lines on the graph. Emission lines play a big role in the identification of a galaxy. They help identify the calcium break, elemental composition and red-shift of the object. These help classify the type of galaxy. Use the Analyze/Examine tool on Graphical Analysis for Windows. Using this tool provides the wavelength (X) and the flux (Y) of the point closest to the cursor.

In order to determine the element making the line, divide the longer wavelength by the shorter to get a ratio. After finding the ratio refer to the emission line ratios chart to find a ratio which closely matches your lines and attempt to identify them. For instance, if you measure 2 lines at 7605 & 7833, their ratio will be 1.029, which is close to the ratio found between the known lines for H β & [O III] of 1.03. They may be the emission lines for these 2 elements at a different red-shift. Because the object is moving, any emission lines will be shifted, but the ratio of distance between the two will stay the same, and this is how you identify the element in the spectral lines you see.

EMISSION LINE RATIOS

	Ly α	C IV	CIII]	Mg II	H β	[O III]	Hα
Lyα							
C IV	1.28						
C III]	1.57	1.23					
Mg II	2.31	1.81	1.47				
H β	4.01	3.14	2.55	1.74			
[O III]	4.13	3.23	2.62	1.79	1.03		
H α	5.41	4.24	3.44	2.35	1.35	1.31	

Once both the rest and observed wavelengths are found, determine the red-shift by using the equation:

$$1+z=\lambda obs/\lambda rest$$

Having measured the red-shift, the velocity, distance and luminosity of the object can be determined.

In order to determine velocity use the equation:

$$V= c((1+z)^2-1)/((1+z)^2+1)$$

With c=3.0x10^5 km s^-1

In measuring distance, use the equation:

$$D= (cz/Ho)(1+0.5z/1+z)$$

With Ho=75 km s^-1 Mpc^-1

In measuring luminosity use:

$$L=4\pi f d^2 (1+z)^2$$

These equations are to be used specifically with distant objects, such as AGN. To measure flux, use the Analyze/Integrate tool around the V Band (5000-6000A). To measure the intensity of the calcium break, find a range blue-ward (3750-2950A) and red-ward (4050-4250A) at the red-shift for the object, and determine the intensity of the break using the formula:

$$1+z=\lambda obs/\lambda rest$$

In order to measure flux, draw a rectangle with the cursor around the V-Band (5000-6000A) and activate the Analyze/Integrate tool, which then gives the flux. Measuring the calcium break takes two steps. First find the blue-ward and red-ward flux. To do this convert the given lines (3750-3950A blue-ward, 4050-4250A red-ward) for blue-ward and red-ward into the range in which they would be with the red-shift of the data being researched. This can be done by using:

Fb (1+z)(3750) to **(1+z)(3950)** and **Fr (1+z)(4050)** to **(1+z)(4250)**

After finding the new range for blue-ward and red-ward, use the Analyze/Integrate tool to find the mean flux and insert them into the following equation:

Break=(Fr-Fb)/Fr

Using a flow chart helps identify the class of object the spectrum shows.

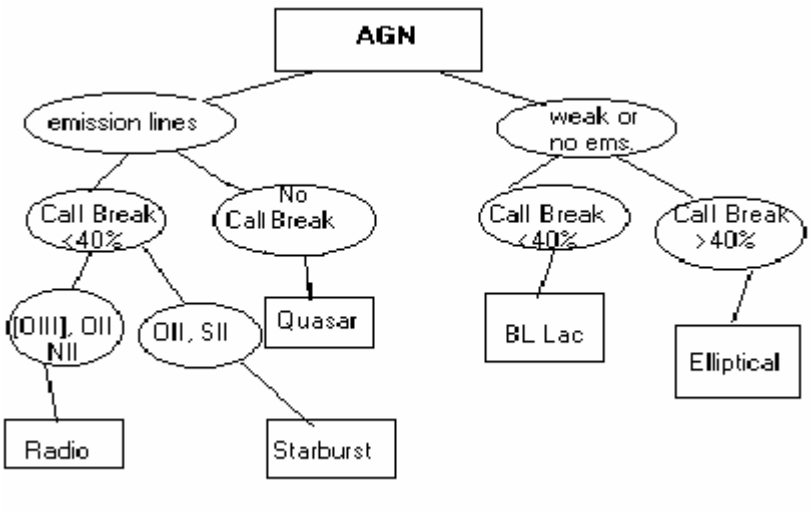

Data was recorded in Microsoft Excel.

Flux (blueward)	Flux (redward)	CA II Break	Flux	Elemental Composition	Class
2.28E-16	2.19E-16	4.1%	2.028E-13	Hβ, [O III]	BL Lac
		no break	1.093E-13	Hβ, [O III]	Quasar
		no break	1.942E-13	MgII, Hβ	Quasar
3.33E-17	4.20E-17	20.7%	5.362E-14	Hβ, [O III]	Elliptical
4.24E-16	4.71E-16	10.0%	4.843E-13	Hβ, [O III], CaII	Elliptical
5.38E-16	5.51E-16	2.4%	5.699E-13	Hβ, [O III], MgII	BL Lac
1.68E-16	2.08E-16	19.2%	4.895E-13	CaII, Hβ, [O III]	Elliptical
1.10E-16	1.09E-16	0.9%	1.263E-13	CaII, Hβ, [O III]	BL Lac
		no break	4.107E-14	CIV, CIII]	Quasar
		no break	9.123E-14	MgII	Quasar
		no break	1.164E-13	CIV, CIII]	Quasar
		no break	2.251E-13	MgII, CaII, Na"D"	Starburst
		no break	4.956E-13	CIV, CIII]	Quasar
		no break	7.004E-14	Hβ, Hα	Quasar
		no break	1.012E-13	[O III], Hα	Radio
2.35E-14	4.30E-14	45.0%	3.227E-13	CaII, MgII, Mg"b"	Starburst
7.42E-17	9.87E-17	24.8%	2.227E-13	CaII, MgII	Elliptical
1.44E-16	1.81E-16	20.4%	5.662E-13	CaII, Na"D"	Elliptical
		no break	8.372E-14	Lα, CIV	Quasar
		no break	2.201E-13	MgII, Na"D"	Quasar
		no break	1.072E-13	Lα, CIII]	Quasar
		no break	4.613E-14	Lα, CIV	Quasar

Flux (blueward)	Flux (redward)	CA II Break	Flux	Elemental Composition	Class
		no break	7.261E-14	Lα, CIV	Quasar
		no break	2.627E-13	CIII], MgII	Quasar
		no break	1.275E-13	Hβ, [O III]	Quasar
8.54E-18	3.64E-17	76.5%	9.807E-14	CaII, [O III]	Elliptical
3.96E-17	4.92E-17	19.5%	1.136E-13	MgII	Elliptical
		no break	6.259E-14	MgII	Elliptical
		no break	2.449E-13	CIV, CIII]	Quasar
		no break	8.231E-14	CIII], MgII	Quasar
3.79E-17	1.31E-16	71.1%	3.982E-13	MgII, CaII	Starburst
		no break	2.058E-13	MgII, Hβ	Quasar
8.83E-17	1.02E-16	13.4%	3.375E-13	CaII	Elliptical
4.99E-17	7.71E-17	35.3%	1.575E-13	CaII	Elliptical
		no break	1.864E-13	CIII], MgII	Quasar
3.74E-17	5.37E-17	30.4%	1.387E-13	MgII	Elliptical
4.15E-17	4.68E-17	11.3%	1.032E-13	Hβ, [O III]	BL Lac
5.95E-17	6.09E-17	2.3%	1.322E-13	CaII. Mg"b"	BL Lac

DATA ANALYSIS

My survey gathered data on 38 objects, as shown in the table. Using the flow chart in the procedure, I was able to identify the objects easily and categorize them as BL Lacs, Quasars or Radio galaxies (AGNs) or as starburst or elliptical (regular galaxies).
I found that there was a loose correlation between distance and luminosity (refer to graphs), but opposite to what my hypothesis said. It seems that the more distant objects such as ffs1001 and 0800 are more luminous. However despite that, the graphs weren't similar enough to be dependable.

SOURCE OF ERROR

We found that some of the objects contained characteristics of more than one category, so we placed them with the best fit. These classifications are limited by what we presently know and may not always apply.

EXTENSION

I would like to investigate the difference in luminosity between the different AGN categories.

REFERENCES

Chaisson, Eric, Steve McMillan. Astronomy: A Beginner's Guide to the Universe. 2nd Edition. Upper Saddle River: Prentice-Hall, Inc., 1998.

Quasars: Another Look at Redshift Vs. Luminosity

Eric C. Naumann and Cameron J. DeLemos
Orangevale Open K-8 School, Orangevale, CA
Teacher: Jim Carvalho, TLRBSE 2004

ABSTRACT

We studied a total of 119 Active Galactic Nuclei in this project. We began by analyzing spectra from TLRBSE data that had not been previously investigated. We also included data that other scientists had evaluated for previous studies. The data was then analyzed to find the redshift and luminosity of the AGN by calculating the values via analysis of the spectral lines emitted from the AGN. Finally, the redshift and luminosity were graphed to determine if a trend in the data was present. Our graph demonstrated that there was a correlation between luminosity and redshift. Furthermore, the slope found was similar to the slope that has been observed in other studies.

INTRODUCTION

AGN, active galactic nuclei, consist of super massive black holes that emit jets of energy near the speed of light from groups of particles swirling around their poles. These AGN are located at the center of some galaxies and emit light as the matter swirls around and falls into the black hole, which is expressed as luminosity. Luminosity is the amount of energy released as photons over the entire electromagnetic spectrum, not just as visible light.

Most of these objects are more or less distant from the Milky Way. Because of this they exhibit redshift, which is the displacement of spectral lines towards the long wavelengths of the spectrum, which is proportional to the velocity of the AGN moving away from Earth. Thus, the AGN's distance and age can be determined based on the redshift. Our primary goal was to find a possible correlation, if any, between luminosity and redshift. If we find that these objects change luminosity in a regular way, they may be telling us something about the history of the universe.

OBSERVATIONS AND DATA REDUCTION

Using the Graphical Analysis application, we studied the spectral lines of the data to find the primary absorption and emission lines from the AGN. These values were then examined to find redshift. To find the luminosity, the spectral values between 5000 and 6000 angstroms were taken and calculated using Graphical Analysis to find the integral. This integral was then entered into Microsoft Excel as the flux value (see figures 1 & 2). This flux (f) value is then used in unison with the average redshift to find the luminosity, given Luminosity=4*(3.1416)*f*((d*3.09E+24)^2)*((1+z)^2).
f=flux
d=distance (mpc)
z=redshift average

ANALYSIS AND RESULTS

A graph was constructed from the values in the Microsoft Excel chart to determine if a correlation was present between luminosity and redshift. The dependent variable, luminosity, was graphed on the y-axis, and the independent variable, redshift, was graphed on the x-axis. The y-axis was adjusted to fit only the data values in the table.

When graphed, we found two approximately parallel curves. After close scrutiny, we found one curve belonged to our range of data, and the other to Coon and Thomas' data set. Coon and Thomas used a different equation to calculate the luminosity of the AGN observed. Our form of the equation calculated luminosity based upon the distance in centimeters. Koon and Williams' equation however used a different variation using millions of light years. Both of our equations ended with ergs per second, the unit for luminosity, but their distance was measured in millions of light years, and ours measured distance in centimeters. Their equation did not correct the units for distance when input into the formula for luminosity. Because luminosity is measured in ergs per square centimeter, in order to get accurate results, distance must be converted into centimeters from either mpc or M.L.Y.

When we corrected, their values for luminosity and redshift, their data fit into our trend perfectly. The trend we found was very similar to other articles that also studied the correlation between luminosity and redshift. Our trend showed that as redshift increases, luminosity also increased, though the rate of increase tapers off with distance.

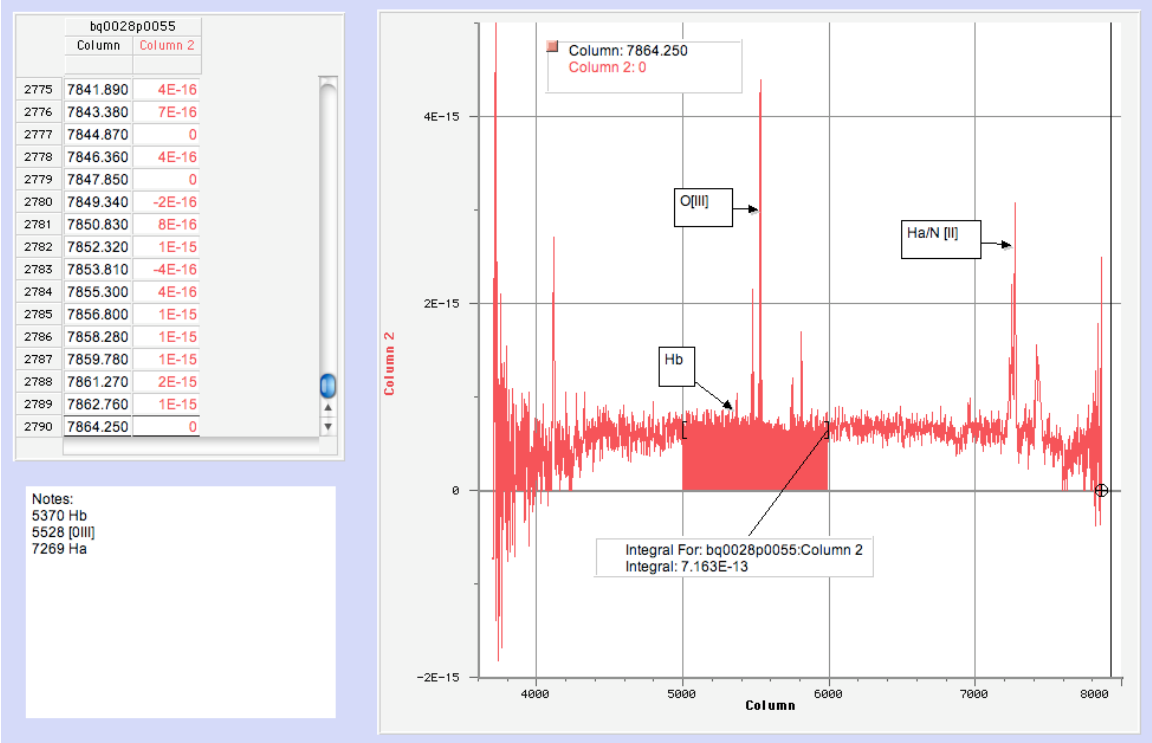

Figure 1

	A	B	C	D	E	F	G	H	I	J	K	L	M
1	Credits:												
2	William Lutschak		**Rest wavelength**			**Corrected Table**							
3													
4	**bq0028p0055**				Ly apha	C IV	C III]	Mg II 2798	H beta	[O III]	H alpha		
5	RA		1213	Ly apha									
6	Dec		1400	Si IV	1.154								
7			1549	C IV	1.280								
8			1909	C III]	1.570	1.230							
9	Peak Flux (mJy/bm)		2326	C II	1.918	1.502	1.218						
10			2796	Mg II	2.305	1.805	1.465						
11			2803	Mg II	2.311	1.810	1.468						
12	Classification:		4340	H gamma	3.578	2.802	2.273	1.552					
13			4861	H beta	4.010	3.140	2.550	1.740					
14			4959	[O III]	4.088	3.201	2.598	1.774	1.020				
15			5007	[O III]	4.128	3.232	2.623	1.791	1.030				
16			6563	H alpha	5.410	4.240	3.440	2.347	1.350	1.323			
17			6584	[N II]	5.428	4.250	3.449	2.355	1.354	1.328	1.003		
18													
19													
20				**line**	**lambda**	**z**		**f**	**v** (km/s)	**v/c**	**d** (Mpc)	**time** (ly)	**Lum**
21			**bq0028p0055**	line a		3.024732		1.30E-13	1.87E+05	62%	3,193.0	1.05E+10	6.86E+44
22				[O III]		0.103611		1.30E-13	1.87E+05	62%	3,193.0	1.05E+10	6.86E+44
23				H alpha		0.105053		1.30E-13	1.87E+05	62%	3,193.0	1.05E+10	6.86E+44
24					Average	1.0778							
25													
26		**Observed**											
27		a	4882	line a									
28		b	5533	[O III]	b÷a	1.133347							
29		c	7243	H alpha	c÷a	1.483613	c÷b	1.309055					
30													
31		**ion**	**observed**	**rest**		**ion**	**observed**	**rest**		**ion**	**observed**	**rest**	
32		**line a**	4882	1213		**[O III]**	5533	5007		**H alpha**	7243	6563	
33		**redshift:**	3.024732069			**redshift:**	0.105053			**redshift**	0.1036112		
34													

Figure 2

Name	RA	DEC	z	f	v (km/s)	v/c	d (Mpc)	time (ly)	Lum
bq0001m0041	RA 00 01 00	Dec - 00 41 00	0.0211	3.752E-12	6262.802051	0.020876007	83.52222915	275623356.2	3.27439E+42
bq0232p0040	RA 02 32 00	Dec 00 40 00	0.02351791	1.167E-12	6972.43157	0.023241439	92.99087284	306869880.4	1.26844E+42
bq0018m1022.2	RA 00 18 00	Dec - 10 22 20	0.026931598	3.712E-13	7970.721146	0.02656907	106.3138129	350835582.4	5.30882E+41
bq0043m1035	RA 00 43 00	Dec - 10 35 00	0.052317167	4.61E-13	15285.12039	0.050950401	204.06665	673419945.1	2.55074E+42
bq0004p0051	RA 00 04 00	Dec 00 51 00	0.0655	1.731E-13	24547.28309	0.081824277	328.3983023	1083714398	2.63911E+42
FFS 0817+3128	RA 08 17 00	Dec 31 28 00	0.1200	5.97E-13	33853.79702	11.28%	454.2857143	1499142857	1.85437E+43
FFS 1424+4705	RA 14 24 00	Dec 47 05 00	0.1300	6.78E-13	36483.81571	12.16%	490.0884956	1617292035	2.49496E+43
bq0059m0215.01	RA 00 59 00	Dec - 02 15 01	0.1920	1.02E-13	5.22E+04	17%	706.3	2.33E+09	6.68E+42
bq0043m0026	RA 00 43 00	Dec - 00 26 00	0.193579089	4.613E-12	52539.66907	0.17513223	711.5256053	2348034497	3.99204E+44
bq0100m0200	RA 01 00 00	Dec - 02 00 00	0.227178969	1.18E-13	60571.58473	0.201905262	824.6038017	2721192546	1.44983E+43
bq0058m1114	RA 00 58 00	Dec - 11 14 00	0.245280055	3.456E-14	64772.52239	0.215908408	884.4966822	2918835751	5.0336E+42
ffs 0905+2849	09 05 00	28 49 00	0.27						2.13E+43
bq0012p0125	RA 00 12 00	Dec 01 25 00	0.289834834	3.773E-14	74747.20158	0.249157339	1029.083542	3395975688	7.97598E+42
ffs 0859+3802	08 59 00	38 02 00	0.31						2.61E+43
bq0212m0030	RA 02 12 00	Dec - 00 30 00	0.391473266	1.832E-15	95654.09729	0.318846991	1345.621037	4440649421	7.70635E+41
ffs 0816+4910	08 16 00	49 10 00	0.45						6.07E+43
ffs 1537+2300	15 37 00	23 00 00	0.46						2.17E+44
ffs 1157+3244	11 57 00	32 44 00	0.485						3.23E+44
ffs 0742b			0.5						6.40E+44
ffs 1706+5049	17 06 00	50 49 00	0.54						6.55E+44
ffs 1534b			0.555						4.20E+44
bq0051p0041_2	RA 00 51 00	Dec 00 41 00	0.5567	1.298E-13	124730.8905	0.415769635	1828.623935	6034458986	1.262E+44
ffs 0811			0.61						5.57E+44
ffs 0740+2852	07 40 00	28 52 00	0.71						2.04E+44
ffs 1533+2608	15 33 00	26 08 00	0.766						7.95E+44
ffs 1639+4705	16 39 00	47 05 00	0.79						1.40E+45
FFS 1047			0.8000	4.83E-13	158490.566	52.83%	2488.888889	8213333333	1.16314E+45
ffs 0847+2714	08 47 00	27 14 00	0.88						1.80E+45
ffs 1606+5405	16 06 00	54 05 00	0.88						3.18E+45
ffs 0737+3036	07 37 00	30 36 00	0.92						1.04E+45
ffs 1608+5613	16 08 00	56 13 00	0.96						2.13E+44
ffs 1448+3416	14 48 00	34 16 00	0.975						9.53E+44
bq0004p0000.2	RA 00 04 00	Dec 00 00 20	1.0061	6.58E-14	180582.7867	0.601942622	3015.218369	9950220617	2.88863E+44
ffs 1630+5221	16 30 00	52 21 00	1.01						3.13E+45
ffs 1030+4113	10 30 00	41 13 00	1.025						2.52E+45
bq0028p0055	RA 00 28 00	Dec 00 55 00	1.0778	1.30E-13	1.87E+05	62%	3,193.0	1.05E+10	6.86E+44
ffs 1557+4007	15 57 00	40 07 00	1.1						2.66E+45
ffs 1620+5448	16 20 00	54 48 00	1.14						5.02E+45
bq0041m1108	RA 00 41 00	Dec - 11 08 00	1.20291998	1.03E-13	197485.953	0.65828651	3497.954054	11543248378	7.33822E+44
ffs 0301+0118	03 01 00	01 18 00	1.22						4.61E+44
ffs 1349+3524	13 49 00	35 24 00	1.221						2.09E+45
ffs 1546+2621	15 46 00	26 21 00	1.23						2.38E+45
ffs 1628+5641	16 28 00	56 41 00	1.25						3.67E+45
bq0057m0932.01	RA 00 57 00	Dec - 09 32 01	1.266592229	1.369E-13	202239.3755	0.674131252	3650.802539	12047648379	1.12475E+45
ffs 1534c			1.29						2.99E+45
bq0014m0107	RA 00 14 00	Dec - 01 07 00	1.2937	8.24E-14	204168.4001	0.680561334	3715.406502	12260841457	7.1793E+44
ffs 1143+4823	11 43 00	48 23 00	1.318						1.12E+45
ffs 1708+3346	17 08 00	33 46 00	1.35						5.63E+45
ffs 1343a			1.356						7.36E+45
ffs 1517+3612	15 17 00	36 12 00	1.37						4.35E+45
bq0019m0104	RA 00 19 00	Dec - 01 04 00	1.388935995	2.612E-13	210541.4282	0.701804761	3940.679196	13004241347	2.77749E+45
ffs 0733+3515	07 33 00	35 15 00	1.42						1.77E+45
ffs 0732+2548	07 32 00	25 48 00	1.43						1.78E+45
ffs 1408+5613	14 08 00	56 13 00	1.46						1.33E+45
ffs 1501+5619	15 01 00	56 19 00	1.46						4.15E+45
ffs 1257+2454	12 57 00	24 54 00	1.489						1.04E+46
ffs 1614b			1.54						5.21E+45
FFS 0749+4748	RA 07 49 00	Dec 47 48 00	1.5600	2.86E-13	220567.6763	73.52%	4338.75	14317875000	4.23353E+45
ffs 1306+5529	13 06 00	55 29 00	1.599						1.23E+46
ffs 0722+3722	07 22 00	37 22 00	1.61						6.55E+45
ffs 0800+5010	08 00 00	50 10 00	1.62						3.20E+46
FFS 0754b			1.6400	9.54E-14	224713.9129	74.90%	4522.424242	14924000000	1.63165E+45
ffs 1254+4536	12 54 00	45 36 00	1.647						6.34E+45
bq0015m0008.2	RA 00 15 00	Dec - 00 08 20	1.695001525	3.653E-13	227387.4395	0.757958132	4647.888443	15338031862	6.87713E+45
ffs 0747+4920	07 47 00	49 20 00	1.71						6.46E+45
ffs 1334b			1.712						4.19E+45
ffs1335+5407	13 35 00	54 07 00	1.718						1.22E+46
FFS 0912+4422	RA 09 12 00	Dec 44 22 00	1.7200	1.55E-13	228557.8205	76.19%	4704.705882	15525529412	3.04553E+45
ffs 1545+3941	15 45 00	39 41 00	1.76						1.25E+46
ffs 1011+3415	10 11 00	34 15 00	1.78						5.84E+45
ffs 1602+2418	16 02 00	24 18 00	1.78						1.70E+46
ffs 1210+5316	12 10 00	53 16 00	1.788						1.31E+46
FFS 1019+3750	RA 10 19 00	Dec 37 50 00	1.7930	5.47E-13	231824.7592	77.27%	4869.924096	16070749517	1.21423E+46
bq0102m0921	RA 01 02 00	Dec - 09 21 00	1.799794644	6.811E-14	232117.8664	0.773726221	4885.251182	16121328901	1.52685E+45
FFS 1039+2422	RA 10 39 00	Dec 24 22 00	1.8	2.14E-13	232126.6968	77.38%	4885.714286	16122857143	4.80523E+45
FFS 1152+2333	RA 11 52 00	Dec 23 33 00	1.8010	0.0000	232169.6739	77.39%	4887.969297	16130298679	1.18078E+46
FFS 1018+2650	RA 10 18 00	Dec 26 50 00	1.8100	1.03E-12	232554.715	77.52%	4908.256228	16197245552	2.35089E+46
FFS 1359+2708	RA 13 59 00	Dec 27 08 00	1.8230	2.54E-13	233105.3638	77.70%	4937.533829	16293861637	5.92111E+45

Figure 3.1

FFS 0811a			1.8700	5.82E-13	235043.1422	78.35%	5043.135689	16842348432	1.4629E+46
FFS 0957+2356	RA 09 57 00	Dec 23 56 00	1.9050	7.6E-13	236434.1126	78.81%	5121.531842	16901055077	2.01852E+46
FFS 0928+4446	RA 92 28 00	Dec 44 46 00	1.9100	3.86E-13	236629.3132	78.88%	5132.714777	16937958763	1.03323E+46
FFS 1106+5527	RA 11 06 00	Dec 55 27 00	1.9400	3.72E-13	237782.5708	79.26%	5199.727891	17159102041	1.0431E+46
FFS 1052+4241	RA 10 52 00	Dec 42 41 00	1.9600	4.16E-13	238534.6664	79.51%	5244.324324	17306270270	1.20277E+46
FFS 1047+4725	RA 10 47 00	Dec 47 25 00	1.9800	4.83E-13	239273.7136	79.76%	5288.85906	17453234899	1.43957E+46
FFS 1131+5128	RA 11 31 00	Dec 51 28 00	1.9800	1.2E-13	239273.7136	79.76%	5288.85906	17453234899	3.57656E+45
FFS 1119+4647	RA 11 19 00	Dec 46 47 00	1.9900	1.2E-13	239638.4342	79.88%	5311.103679	17526642140	3.63096E+45
FFS 1054+2703	RA 10 54 00	Dec 27 03 00	2.0200	4.43E-13	240713.8058	80.24%	5377.748344	17746569536	1.40199E+46
FFS 1036a			2.0300	3.6E-13	241066.114	80.36%	5399.933993	17819782178	1.15636E+46
FFS 1112+4513	RA 11 12 00	Dec 45 13 00	2.0500	6.76E-14	241761.7083	80.59%	5444.262295	17966065574	2.23641E+45
bq0221p0101	RA 02 21 00	Dec 01 01 00	2.06384251	1.298E-13	242236.2148	0.807454049	5474.909953	18067202845	4.38217E+45
FFS 1036b			2.0700	4.69E-13	242445.4911	80.82%	5488.534202	18112162866	1.59768E+46
FFS 0955+5001	RA 09 55 00	Dec 50 01 00	2.1100	2.92E-13	243778.6378	81.26%	5576.913183	18403813505	1.05395E+46
FFS 1658+3605	RA 16 58 00	Dec 36 05 00	2.1100	8.67E-13	243778.6378	81.26%	5576.913183	18403813505	3.12936E+46
bq0046p0104	RA 00 46 00	Dec 01 04 00	2.146365034	4.072E-13	244952.1736	0.816507245	5657.075916	18668350523	1.54788E+46
FFS 1351+3413	RA 13 51 00	Dec 34 13 00	2.1490	3.11E-13	245035.8234	81.68%	5662.877739	18687496539	1.18661E+46
FFS 1005+5019	RA 10 05 00	Dec 50 19 00	2.2400	1.84E-13	247815.1962	82.61%	5862.716049	19346962963	7.96587E+45
FFS 1318+3532	RA 13 18 00	Dec 35 32 00	2.2640	2.5E-13	248514.1881	82.84%	5915.254902	19520341176	1.11819E+46
FFS 1616+3621	RA 16 16 00	Dec 36 21 00	2.3500	5.95E-13	250910.2066	83.64%	6102.985075	20139850746	2.98414E+46
FFS 1619+5256	RA 16 19 00	Dec 52 56 00	2.3500	2.51E-13	250910.2066	83.64%	6102.985075	20139850746	1.25886E+46
FFS 1627+4955	RA 16 27 00	Dec 49 55 00	2.4100	2.5E-12	252486.9141	84.16%	6233.489736	20570516129	1.35531E+47
FFS 1238+2343	RA 12 38 00	Dec 23 43 00	2.4160	1.98E-13	252640.5124	84.21%	6246.519906	20613515691	1.0817E+46
FFS 1656+5321	RA 16 56 00	Dec 53 21 00	2.4500	1.57E-13	253497.3842	84.50%	6320.289855	20856956522	8.95653E+45
FFS 1001+2911	RA 10 01 00	Dec 29 11 00	2.5000	4.15E-13	254716.9811	84.91%	6428.571429	21214285714	2.52081E+46
FFS 1006+3236	RA 10 06 00	Dec 32 36 00	2.5000	2.95E-13	254716.9811	84.91%	6428.571429	21214285714	1.7919E+46
FFS 1723+5236	RA 17 23 00	Dec 52 36 00	2.5200	2.53E-13	255191.7792	85.06%	6471.818182	21357000000	1.57538E+46
FFS 1406+3433	RA 14 06 00	Dec 34 33 00	2.5600	3.75E-13	256119.8221	85.37%	6558.202247	21642067416	2.45261E+46
FFS 1535+4836	RA 15 35 00	Dec 48 36 00	2.5600	9.07E-13	256119.8221	85.37%	6558.202247	21642067416	5.93205E+46
FFS 1144+3315	RA 11 44 00	Dec 33 15 00	2.6050	3E-13	257130.6853	85.71%	6655.214979	21962209431	2.07197E+46
bq0000m1021	RA 00 00 00	Dec - 10 21 00	2.6445	9.32E-14	2.58E+05	86%	6,740.3	2.22E+10	6.75E+45
FFS 0811b			2.6800	4.58E-13	258741.3357	86.25%	6816.521739	22494521739	3.45792E+46
FFS 1641+3345	RA 16 41 00	Dec 33 45 00	2.7500	3.85E-13	260165.9751	86.72%	6966.666667	22990000000	3.15283E+46
FFS 1724+4636	RA 17 24 00	Dec 46 36 00	2.7900	1.45E-12	260947.9241	86.98%	7052.295515	23272575198	1.2429E+47
bq0044m0900	RA 00 44 00	Dec - 09 00 00	2.924022651	7.461E-14	263410.0688	0.878033563	7338.364248	24216602018	7.42312E+45
FFS 2341+0018	RA 23 41 00	Dec 00 18 00	2.9800	2.62E-13	264371.3926	88.12%	7457.487437	24609708543	2.76937E+46
FFS 0738b			3.0500	2.95E-13	265522.1951	88.51%	7606.17284	25100370370	3.35886E+46
FFS 1223+4611	RA 12 23 00	Dec 46 11 00	3.6170	8.95E-13	273114.2913	91.04%	8800.81628	29042700325	1.77303E+47
FFS 1410+4608	RA 14 10 00	Dec 46 08 00	3.6400	2.02E-13	273368.3687	91.12%	8848.965517	29201586207	4.09602E+46
FFS 1430+2512	RA 14 30 00	Dec 25 12 00	3.9800	2.46E-13	276744.5466	92.25%	9558.393574	31542698795	6.68793E+46
FFS 1450+4710	RA 14 50 00	Dec 47 10 00	4.5400	5.44E-13	281067.5384	93.69%	10718.98917	35372664260	2.30173E+47

Figure 3.1 (continued)

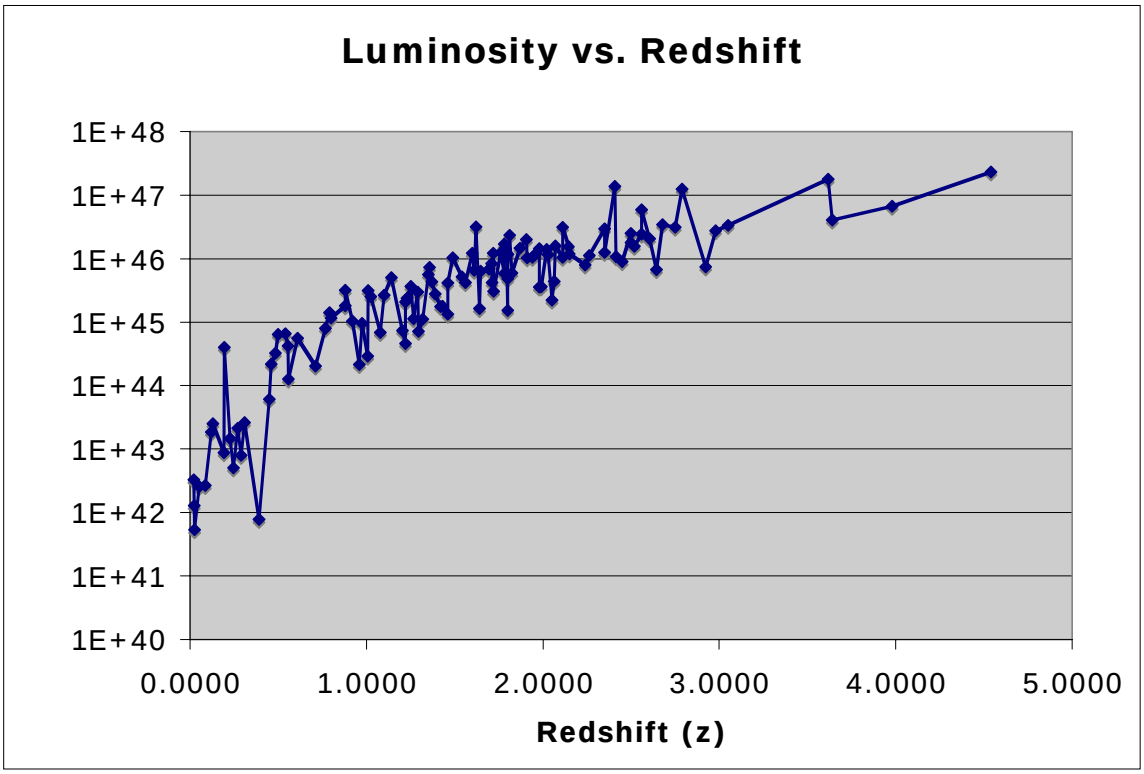

Figure 3.2

DISCUSSION

We found a definite trend between luminosity and redshift. This means that as the AGN have a higher value for redshift, i.e. more distant, the luminosity increases. The photons given off are caused by matter swirling around the AGN, which, over time, has been consumed by the AGN to the point at which there is not as much left. Therefore, AGN that are closer, have less matter surrounding the AGN and fewer photons are emitted. More distant quasars, since we're looking back in time, are younger and tend to have more matter surrounding them that has not yet fallen into the black hole.

SUMMARY AND ACKNOWLEDGEMENTS

Our primary goal was to find a possible correlation, if any, between luminosity and redshift. After studying the luminosity and redshift of various AGN we discovered that there was a correlation between luminosity and redshift. This trend revealed that, over time, AGN deplete their supply of matter, therefore causing the luminosity to decrease.
We would like to acknowledge our teacher Jim Carvalho and colleagues Joel Hatley, Kevin Hatley, and Leah DeFord for working with us on the early parts of this project, and thanks to Joe for "Starcraft" and pizza.

REFERENCES

Coon, Will, and Sarah Thomas. "Quasars: Redshift vs. Luminosity." TLRBSE (1999).

Montano, Artie. "The Correlation of Distance with Luminosity in Quasars." TLRBSE (2000).

Beaudry, Karyn, Stephanie McClain, Ryan McCusker, and Ethan Robinson. "Investigating and Categorizing AGN Objects." TLRBSE (1999).

Miller, Michelle, and Randy Buhram. "Does Distance Affect Types of AGN?." TLRBSE (2001).

Westerlin, Ryan. "The Correlation of Active Galactic Nucleus Type with Distance as Determined by the Redshift of Spectral Signatures." TLRBSE (1998).

Trickett, Riley, and Rachel Wolcott. "The Redshift of Unknown AGN." TLRBSE (2001).

Ransom, Cassiopea, and Alana Stednitz. "The Determination of the Look Back Time of Distant Active Galaxies." TLRBSE (1998).

Liou, Iva, and Ed Cazalas. "Distance of Active Galactic Nuclei." TLRBSE (2001).

Acevedo, Gissel. "Active Galactic Nuclei." TLRSE (2000).

X-ray Sources of M31

Corey F. Austin, Marilyn L. Feezor, Sarah E. Ikerd,
Graves County High School, Mayfield, KY
Teacher: Velvet Dowdy, TLRBSE 2003

ABSTRACT

In the project novae and their locations were compared to determine if novae are the source of x-rays from M31. Through the research, it was discovered that there appears to be a correlation between the locations of novae and the x-ray emissions of the Andromeda galaxy. It was concluded that the location and the concentration of novae increase the amount of x-rays from M31.

INTRODUCTION

The question that was explored in this research project was, "Are novae related to the x-ray sources of M31?" This project is a study of the x-ray emissions of the Andromeda galaxy compared with the presence of novae. Andromeda, also known as M31, is a spiral galaxy not far from the Milky Way Galaxy, which makes it one of the most studied and known galaxies of the universe (Burnham Jr., 2005) (Andromeda Galaxy, 2005). Novae occur in binary star systems where hydrogen from one star is transferred to the surface of the other star; this accumulation of hydrogen causes an explosion. This explosion, in turn, is the nova (NASA's Observatorium, 1999). The question is addressing if the novae in M31 release any amount of x-ray radiation. Previous research shows that novae occur in the center bulge of the galaxy, as well as the spiral arms (Herndon, Green, 2005) (Dudley, Derek, 2004). There has also been a study of the x-ray emissions from the boundary layer, which is formed between the accretion disc and a white dwarf (Pringle, 1979). As far as it is known, no specific research has been conducted on the x-ray emissions of novae in particular. This is why this topic was researched. The data that was used by the group came from the 0.9 meter telescope on Kitt Peak, near Tucson, Arizona. NOAO, NSF, and AURA made the information available.

OBSERVATIONS AND DATA REDUCTION

In order to determine whether or not the novae released x-rays, it had to first be found where the novae were located. To find this information, Scion Image was used. In Scion Image, images taken of M31 on specific dates and times, known as epochs, were observed. When looking at the epochs, novae were found by "blinking" the images. The novae would appear and disappear, providing the location of novae by allowing the coordinates of a nova in a certain field to be found by the researchers (see Figure 1). M31 is broken up into sixteen areas, or fields, due to its large size. The coordinates found were based upon the location of the nova in one field.

Figure 1

Galactic Coordinates	
x'	**y'**
592	-694
827	-769
770	-564
795	-670
767	-649
171	-984
220	-872
358	-556
59	-717
510	-739
-103	-734
-214	-780
-1024	-512
561	-105
364	-405
250	-223
67	-31
75	-134
233	-60
93	-106
201	-127
201	-127
390	-485
287	-446
405	-177
67	-241
-317	-347
-351	-100
-319	-6
-42	-440
-403	-198
-441	-124
-420	-167
-371	-94
-225	-140
-292	-42
-42	-288
-40	-117
-14	-84
-90	-91
-54	-88
-653	-33
-930	-409
-571	-223
706	310
112	419
112	419
411	13
228	39
-393	72
73	81
437	27
417	59
452	69
135	179
112	48
76	162
233	18
404	479
470	186
504	401
-653	487
-557	429
-737	493
-850	401
-864	270
-845	437
-842	432
-983	371
-721	418
-763	41
-377	179
-437	162
-333	303
-469	502
-280	18
-370	39
-400	48
-374	161
-342	226
-227	190
-306	225
-328	89
-328	89
182	655
-173	711
-428	832

After gathering the coordinates of the novae from each field in M31, further investigation was conducted to find the location of the novae based on their galactic coordinates. Galactic coordinates are the location of the novae in comparison to the entire galaxy. Using an excel spreadsheet, Excel Nova Data (DeVore, Harlan, 2003), which provided a formula was used to calculate the galactic coordinates. A graph was created using these galactic coordinates, showing where each nova was located in relation to each other (see Figure 2). The graph created in Graphical Analysis 3. After viewing the graph, spectral images of the Andromeda galaxy, courtesy of Chandra X-ray observatory, were analyzed (see Figure 3).

ANALYSIS AND RESULTS

Surprisingly, it was discovered that an image of x-ray emissions of M31 was very similar to the graph of novae locations. Could this mean that the novae in M31 give off high frequency x-ray emissions?

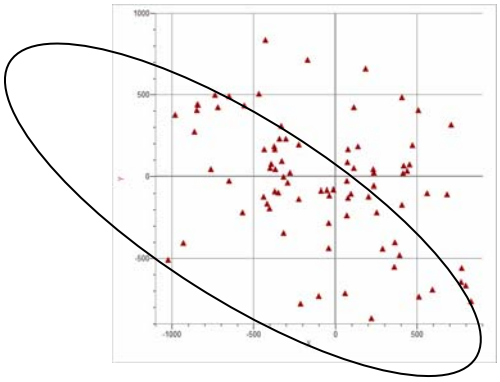

Location of Novae, created by researchers Fig. 2

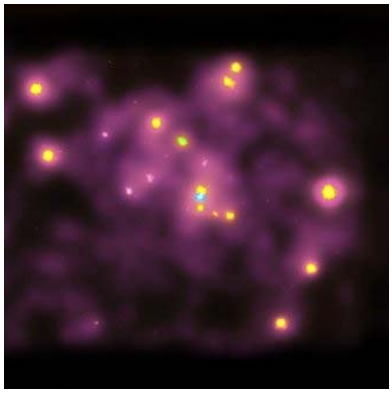

X-ray image of M31, Chandra (Kronberg, 2001) Fig. 3

Ultra-violet image of M31, GALEX
Fig. 4

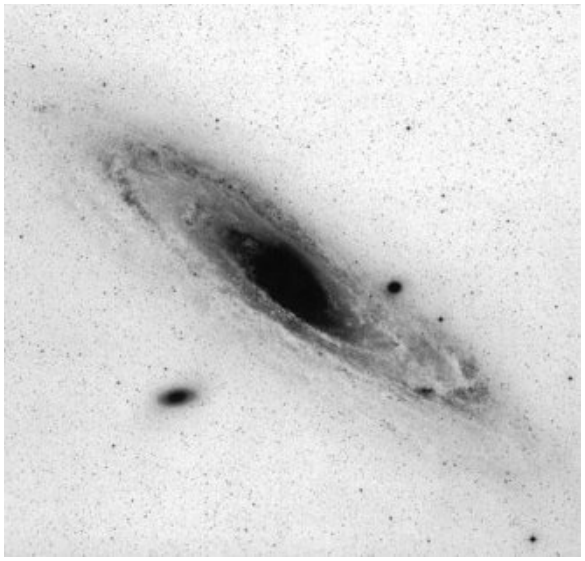

Optical image of M31, Palomar Observatory
Fig. 5

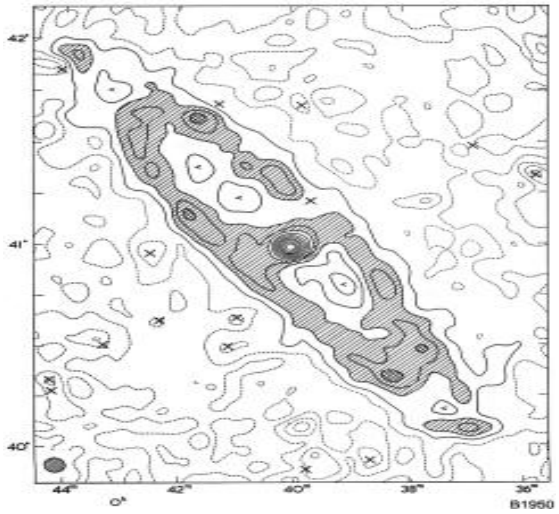

Radio image of M31, Pooley, MRAO
Fig. 6

Infrared image of M31, IRAS
Fig. 7

(Multi-wavelength Astronomy, 2006) (Multi-wavelength Viewer, 2006)

These images show the different spectral qualities of M31 (see Figures 3-7). Upon analyzing these images, it is easy to see that the x-ray image most closely correlates with the location of the novae in the graph shown above. Although the images take the same basic shape of the galaxy, the x-ray image most closely represents the location of novae in M31.

As you can see from the circle drawn on the researcher's graph (previous page), the correlation between the x-ray images of the galaxy and the location of the novae is more closely related than the remaining images, especially considering the novae not included in the spiral arms. But the optical, UV and radio do not show any point sources. How sure are you that the point sources in the X-ray image are really at the same position as the novae? It's a big galaxy.

DISCUSSION

The results of the research show that novae may be the source of x-rays in M31. Initially, the locations for the sources of x-rays in M31 were to be used. Unfortunately, no database had this information (SIMBAD Astronomical Database, 2006). Since the specific information was not available, the project had to be approached from a different angle. There were several images of M31 available, as well as the location of the novae. The only feasible solution was to juxtapose the images with the graph of the location of the novae; upon this action, it was made evident as to the correlation between the two.

With further research the group learned that it is possible for novae to give off x-ray emissions. In fact, through accretion, material from a sun-like star spirals onto the surface of white dwarfs, causing a nuclear reaction (Cataclysmic Variables, 2004) (Ness). In these nuclear reactions hydrogen nuclei is combined with helium nuclei causing an explosive event that is similar to the hydrogen bomb. In this explosive event highly energetic radiation, such as x-ray emissions are released.(Ness) It has also been proven that in three out of five novae explosions x-ray emissions were detected (Hernanz, Sala, 2003).

SUMMARY AND ACKNOWLEDGMENTS

This project was conducted in order to find out if the novae in the M31 galaxy, affect the x-rays given off by the galaxy. It is concluded that novae are the sources of x-rays from M31. In the future, projects dealing with this topic could include finding the exact values and locations for the radiation given off by the novae.

There are several people who helped us with the research of our project and we would like to include them in our paper. We would like to thank Mrs. Velvet Dowdy for everything she did in helping us find information, staying late after school with us, and providing us with software used to find data. We would like to thank the researchers at the astronomical observatories whose images of M31 we used to come to our conclusion. We would also like to thank the creators of the software that provided us with essential information about our topic as well as the NOAO, NSF, and the AURA for making the data accessible for our research.

REFERENCES

Pringle, Savonije,. "X-ray emission from dwarf novae." 1979. Smithsonian/NASA ADS. 15 01 2006 <*http://adsabs.harvard.edu/cgi-bin/nph-bib_query?bibcode=1979MNRAS.187..777P&db_key=AST&data_type=HTML&format=*>.

"M 31." Burnham's Celestial Handbook. 18 12 2005 <*http://www.csulb.edu/~gordon/m31hubl.html*>.

Frommert, Kronberg, . "Chandra X-ray Observatory Views the Center of the Andromeda Galaxy M31." 14 May 2001. Chandra X-ray Observatory Center. 27 12 2005 <*http://www.seds.org/messier/more/m031_cxo.html*>.

Walterbos, A. M. "Spectroscopy of the WIM and the Source of Ionization." 1997. Astronomical Society of Australia. 2 1 2006 <*http://www.atnf.csiro.au/pasa/15_1/walterbos/paper/node3.html*>.

"SIMBAD Astronomical Database." CDS. 3 1 2006 <*http://simbad.u-strasbg.fr/sim-id.pl?protocol=html&Ident=M+31&NbIdent=1&Radius=10&Radius.unit=arcmin&CooFrame=FK5&CooEpoch*

"Multi-wavelength Viewer." 27 1 2006 <*http://www.rigel.org.uk/astro/m31/Chandra.html*>.

"Multi-wavelength Astronomy." NASA/IPAC. 24 1 2006 <*http://coolcosmos.ipac.caltech.edu//cosmic_classroom/multiwavelength_astronomy/multiwavelength_museum/m31.html*>.

"Andromeda Galaxy." The Free Dictionary. 2005. Farflex. 31 01 2006 <*http://columbia.thefreedictionary.com/M31*>.

Herndon, Green, "Nova Rate in M31 Galaxy." 2005. 24 1 2006 <*http://www.noao.edu/outreach/tlrbse/rbsejournal05.pdf*>.

Herndon, Liz, "Nova Rate in M31 Galaxy" 2005. 19 12 2005, <*http://www.noao.edu/outreach/tlrbse/rbsejournal05.pdf*>

Dudley, Derek, "Patterns in the Distribution of Novae in M31." 2004. 24 1 2006 <*http://www.noao.edu/outreach/tlrbse/rbsejournal04.pdf*>

Ness, Jan-Uwe. "X-ray observations of Classical Novae." Jan-Uwe NessProjects at University of Oxford. University of Oxford. 30 Mar. 2006 <*http://www-thphys.physics.ox.ac.uk/user/Jan-UweNess/Novae/novae.html*>.

Hernanz, Sala, . "X-ray Observations of Recent Classical Novae: on the Fast Recovery of a Cataclysmic Variable after a Nova Explosion." Bulletin of the American Astronomical Society. 23 2003. The American Astronomical Soceity. 30 Mar. 2006 <*http://www.aas.org/publications/baas/v35n2/head2003/80.htm*>."Cataclysmic Variables." NASA's Imagine The Universe!. Nov 2004. NASA. 30 Mar. 2006 <*http://imagine.gsfc.nasa.gov/docs/science/know_l2/cataclysmic_variables.html*>.

Novae Brightness in Relation to Coordinates

Jennifer Searcy, Maggie Goff, Tawny Eckstein
Teacher: Jim Hoffman, RBSE 2000

ABSTRACT

In the search for novae, a question was raised on whether or not a nova's position affects its brightness. It was proposed that the brightest average magnitude novae would appear closest to the nucleus of the galaxy. Also because of the Andromeda Galaxy's upper left to lower right slant (negative correlation) the nova will be located in a similar slant in relation to the sixteen fields. Data was collected and novae were found in fields five, six, seven, ten, eleven, fourteen, and fifteen. Each nova was plotted onto a graph according to its magnitude. An average was taken of each nova's magnitude, and then all the averages were plotted onto a graph. Two other graphs were plotted with the minimum magnitude, and the maximum magnitude of each nova. Then the data was put onto a map to analyze the effects of a nova's coordinates on its brightness. When the averages were analyzed, the novae that appeared in fields six and seven were the brightest. Also, when the maximum magnitudes were plotted and the brightest nova was located in the same fields. However, when the minimum magnitudes were plotted the dimmest magnitudes of novae were found in fields seven and eleven, which are located near the nucleus. When all the novae had been plotted a pattern was found in relation to the fields that mirrored the slant of the Andromeda Galaxy.

INTRODUCTION

The Andromeda Galaxy, or M31, is about 2.37 million light years away from Earth's Milky Way galaxy. It is a spiral galaxy similar to the Milky Way. It is about 160,000 light years in diameter. The nucleus itself is about 70 light years across with 10 million stars and has a magnitude of 4.1. The best time to see the galaxy is October 2, in the northern hemisphere. (1) The novae pictures were taken at Kitt Peak Observatory, during the observatory's Research Based Science Education program.

QUESTION

Does a nova's position in relation to the different fields have any affect on its brightness?

HYPOTHESIS

Because of the Andromeda galaxy's slant, the novae are more likely to appear in a negative correlation similar to the slant of the galaxy. Also because of this slant, the highest average magnitudes will be focused closer to the center.

PROCEDURE

Using the Nova Search macros in Scion image, fields were searched through for novae.

- If a nova is found, then its coordinates are recorded.
- Then the known magnitudes of three surrounding stars in the field are recorded.
- Then the apparent magnitude is taken of the nova and recorded.
- This process is repeated until all the nova's epochs have been recorded.
- After the nova's magnitude has been recorded, the magnitudes are graphed and an average of the magnitudes if taken to use for comparing the brightness to position.
- By using the coordinates that were recorded the nova is plotted onto a large Andromeda map.
- When all novae have been plotted onto the map, with their brightness, the data is analyzed.

DATA

Field	Epoch	Magnitude	Field	Epoch	Magnitude
5	3	17.85	11	14	19.63
	4	18.06		15	17.05
	5	17.45		16	19.14
	6	17.55		17	18.45
	7	17.52	14	3	17.03
6	10	15.18		4	17.51
	11	15.82		5	17.68
	12	15.89		6	16.82
	13	16.18		7	16.55
	14	16.55		8	16.86
	15	17.34		9	17.83
	16	17.51		10	18.42
	17	18.01	14	25	17.1
7	10	15.68		26	19.19
	11	15.54		27	19.08
	12	15	15	13	15.13
	13	16.62		14	16.83
	14	19.61		15	16.82
10	20	17.03		16	17.28
	21	16.72		17	18.36
	22	17.4			
	23	17.29			
	24	17.93			
	25	17.07			

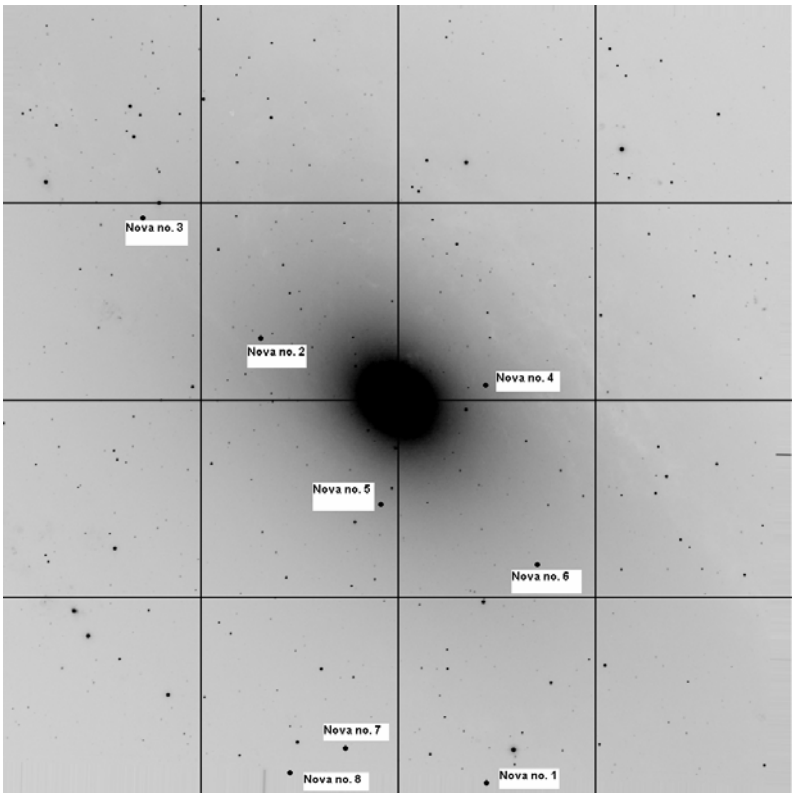
Nova no. 3
Nova no. 2
Nova no. 4
Nova no. 5
Nova no. 6
Nova no. 7
Nova no. 8
Nova no. 1

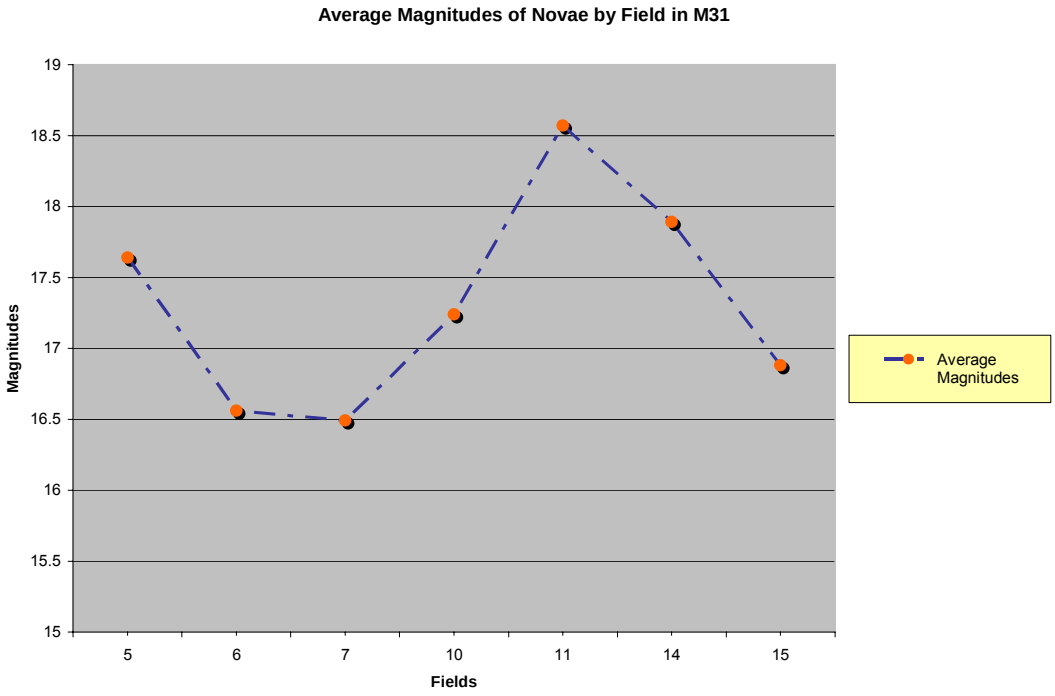
Average Magnitudes of Novae by Field in M31
Magnitudes
19
18.5
18
17.5
17
16.5
16
15.5
15
5
6
7
10
11
14
15
Fields
Average Magnitudes

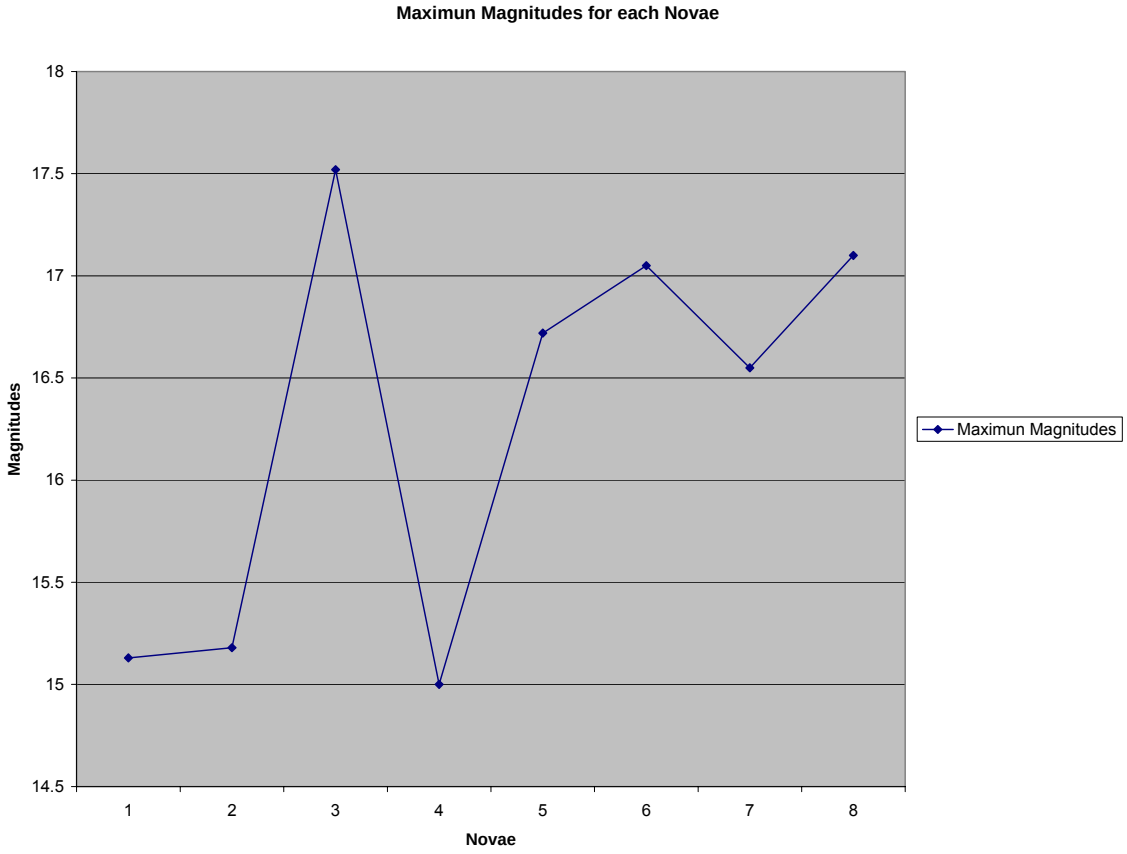
Maximun Magnitudes for each Novae
Magnitudes
18
17.5
17
16.5
16
15.5
15
14.5
1
2
3
4
5
6
7
8
Novae
Maximun Magnitudes

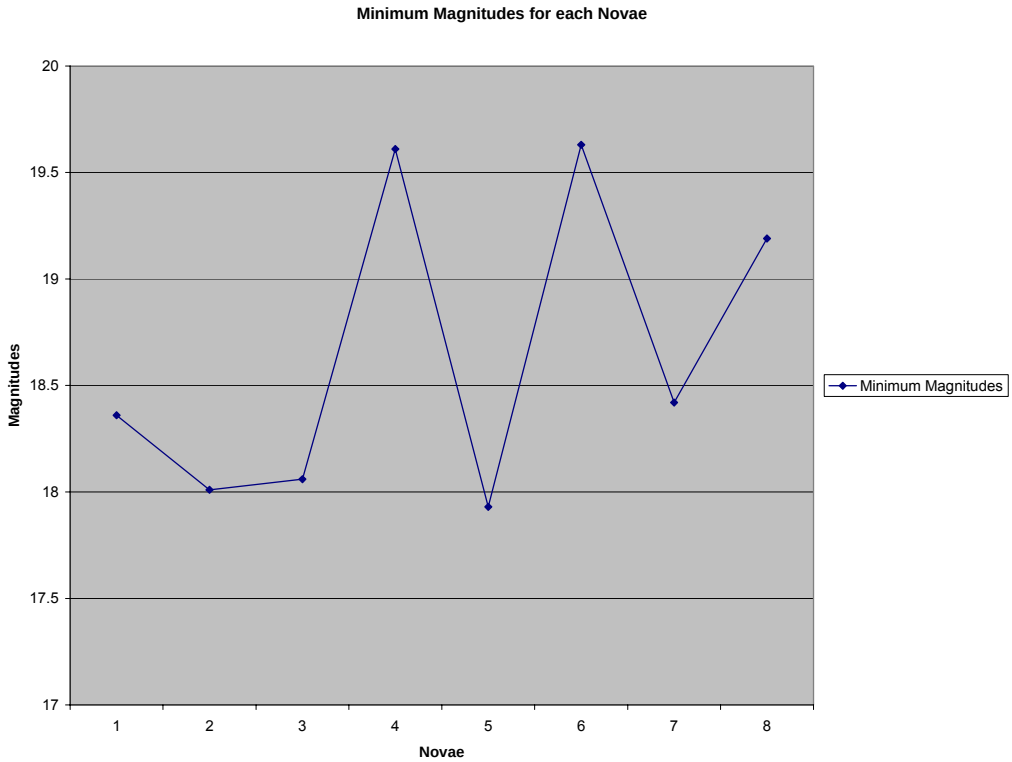
Minimum Magnitudes for each Novae
Magnitudes
20
19.5
19
18.5
18
17.5
17
1
2
3
4
5
6
7
8
Novae
Minimum Magnitudes

ERROR ANALYSIS

It is possible that the research could have had a few glitches. Many times the Scion Image program would give a macro error, and shut down. Unfortunately this caused in losing earlier recorded magnitude data that was not saved. When the magnitudes were average, it is very likely that the nova's life was not recorded in entirety. Since pictures were not taken everyday at Kitt Peak, the average magnitudes many have only come from a certain time period and could not have been a good picture of the nova's entire lifetime. This is why two more graphs were plotted showing the minimum and maximum magnitudes, to help give a better analysis. Human error could also be a factor. Each person is different, so one person could track a nova and get different magnitudes with someone who is tracking the same nova.

CONCLUSION

In conclusion, the data showed that the novae were located in fields that resembled the negative correlation similar to that of the galaxy. The brightest novae were found in fields six and seven which are located near the nucleus. However, these were only averages of magnitudes. When the maximum brightness was plotted it was discovered that the same fields held the brightest novae, but when the minimum magnitude was take fields seven and eleven emerged as the dimmest. This is strange because they are fields are located near the nucleus.

REFERENCES

1 http://www.starlore.net/m31.htm

Distribution of White Dwarf Masses in Close Binary Systems in M31

Teacher: Mary Dunn, Messalonskee Middle School, TLRBSE 2005
Teacher: Cynthia Gould, Southeast School, TLRBSE 2005
Teacher: Chris Martin, Howenstine Magnet High School, TLRBSE 2005
Teacher: Thomas Rutherford, Sullivan South High School, TLRBSE 2005
Teacher: Marcia Talkmitt, Slaton High School, TLRBSE 2005

ABSTRACT

The Andromeda Galaxy (M31) was imaged, using a H-α filter, for a ten-year time period running from September 1995 to December 2005. These images were examined for the presence of novae. When novae were discovered, the rates (t_2 times) of their decays were determined. Using these decay rates made it possible to determine the masses of the white dwarf stars which were the precursors of the novae. Most white dwarfs in binary systems in M31 were found to have masses less than one solar-mass.

INTRODUCTION

How do the masses of the white dwarf components of close binary systems compare to one another? Is there an upper or lower limit to their masses in these systems or can white dwarfs of any mass exist in close orbit around another star?

Novae are exploding stars that occur in binary star systems when the two members of the system are of different masses and are also very close together. They have very short orbital periods, often of around four hours (Zeilik, 1994). They are, in fact, so close that it is possible for matter to actually flow from one star to the other (Seeds, 2005). An area of gravitational control, known as the Roche lobe, surrounds every object with substantial mass, such as a star. In close binary systems, the Roche lobes of the two stars may touch. This provides a pathway for matter to flow from one star to the other.

The rate at which a star ages is determined by that star's mass, with a more massive star aging faster than a less massive one. In a binary system with stars of unequal masses, the more massive star, known as the primary, will reach the white dwarf stage while its companion, known as the secondary, is still in the red giant phase.

As the red giant swells it fills its Roche lobe and begins to dump matter, mostly hydrogen, onto the surface of the white dwarf. After a period of time, this accumulated hydrogen reaches a high enough temperature and a high enough pressure that it undergoes nuclear fusion. This produces large quantities of heat and light and blows much of the remaining hydrogen gas off into space (Shafter, 2000). The nuclear reactions then taper off and the entire process begins again. Most novae reoccur over time.

One mechanism that controls the duration of a nova explosion appears to be the mass of the white dwarf. More massive white dwarfs have shorter outbursts (Petz, 2006), although, if the white dwarf has a mass greater than 1.44 solar masses, known as the

Chandrasehkar Limit, then it will undergo gravitational collapse and become a neutron star (Nave, 2006). If the white dwarf is of too low a mass, then the temperatures and pressures on its surface never become great enough for hydrogen fusion to occur. If the mass of the white dwarf is between these two values, however, then a nova will be the outcome.

The study of novae is important because of their potential use as *standard candles* (Della Valle, 1995). A standard candle is an object whose true brightness is known and so which can be used to estimate distances by comparing this true brightness to its apparent brightness. In order to use a nova as a standard candle, the rate at which its brightness declines must be known. Typically, the value is given as the t_2 time, which is the length of time that it takes the nova to decline by two magnitudes in brightness (Della Valle, 1994). A nova classification system has been developed according to the t_2 times. This classification system can be seen in Table 1. It is these values which will be used in this paper.

Table 1. The classification of novae into speed classes showing the number of days taken for the novae to fade by two magnitudes (t_2 time) along with their rates (slopes) of decay (dV/dt) given in magnitudes per day (Darnley, 2004).

Speed Class	t_2 Time	Slope (mag/day)
Very Fast	< 10 Days	> 0.20
Fast	11 - 25	0.19-0.08
Moderately Fast	26 - 80	0.07-0.025
Slow	81 - 150	0.024-0.013
Very Slow	>151	0.013-0.008

The rate at which a nova decays appears to be related to the mass of the white dwarf component of the binary system. Using the system proposed by Livio (Rector, 2005), it is possible to determine the masses of the white dwarfs. This information is summarized in Table 2.

Table 2. The classification of white dwarfs into mass classes based upon their t_2 times. White dwarfs with masses below 0.4 solar masses are not large enough for hydrogen fusion to occur on their surfaces while white dwarfs with masses much above 1.4 solar masses cannot exist—*they collapse and become neutron stars*.

Speed Class	t2 (days)	White Dwarf Mass (sun=1)
Very Fast	≤10	1.1 – 1.4
Fast	11 - 25	0.96 – 1.1
Moderately Fast	26 - 80	0.67 - 0.95
Slow	81 - 150	0.57 – 0.66
Very Slow	≥151	0.4 – 0.56

OBSERVATIONS AND DATA REDUCTION

From 28 June 2005 through 1 July 2005, these researchers photographed the central region of the Andromeda Galaxy, M31, using the 0.9-meter WIYN telescope located at Kitt Peak, Arizona. All imaging was done using a hydrogen alpha (Hα) filter. Novae remain visible in Hα long after they have faded from visibility at other wavelengths (Ciardullo, 1990). Therefore, H-α offers a method of studying novae where constant monitoring is not feasible (Shafter, et al., 2001).

In addition to the data collected during the summer 2005 observing run, additional images taken by other groups stretching from September 1995 through December 2005 were utilized. A total of 103 epochs covering the 10-year period were examined. These additional data sets were taken with the 0.9-meter WIYN, the 1.3-meter MDM, and the 2.1-meter telescopes at Kitt Peak. The dates of all data sets are listed in Table 3.

Table 3. The images of M31 were taken over a ten-year period**,** although at irregular intervals. The M31 viewing season runs from June through February.

Epoch Number	Calendar Date	Epoch Number	Calendar Date	Epoch Number	Calendar Date
e001	3 Sep 1995	e036	21 Sep 2002	e071	6 Jan 2004
e002	18 Jun 1997	e037	23 Oct 2002	e072	31 Jan 2004
e003	23 Jul 1997	e038	10 Nov 2002	e073	2 Feb 2004
e004	24 Jul 1997	e039	11 Nov 2002	e074	3 Feb 2004
e005	25 Jul 1997	e040	11 Jun 2003	e075	24 Jun 2004
e006	31 Jul 1997	e041	13 Jun 2003	e076	25 Jun 2004
e007	1 Aug 1997	e042	14 Jun 2003	e077	26 Jun 2004
e008	18 Nov 1997	e043	15 Jun 2003	e078	27 Jun 2004
e009	6 Jun 1998	e044	16 Jun 2003	e079	30 Sep 2004
e010	24 Jul 1998	e045	17 Jun 2003	e080	1 Oct 2004
e011	25 Jul 1998	e046	18 Jun 2003	e081	2 Oct 2004
e012	26 Aug 1998	e047	4 Jul 2003	e082	23 Oct 2004
e013	5 Sep 1998	e048	5 Jul 2003	e083	24 Oct 2004
e014	14 Oct 1998	e049	6 Jul 2003	e084	17 Nov 2004
e015	30 Oct 1998	e050	7 Jul 2003	e085	20 Nov 2004
e016	11 Nov 1998	e051	8 Jul 2003	e086	28 Jun 2005
e017	27 Jan 1999	e052	9 Jul 2003	e087	29 Jun 2005
e018	24 Jun 1999	e053	2 Aug 2003	e088	30 Jun 2005
e019	20 Jul 1999	e054	3 Aug 2003	e089	1 Jul 2005
e020	14 Jun 2000	e055	30 Aug 2003	e090	29 Jul 2005
e021	17 Jul 2000	e056	31 Aug 2003	e091	27 Sep 2005
e022	13 Sep 2000	e057	17 Sep 2003	e092	28 Sep 2005
e023	14 Sep 2000	e058	18 Sep 2003	e093	29 Sep 2005
e024	15 Oct 2000	e059	19 Sep 2003	e094	21 Oct 2005
e025	10 Nov 2000	e060	20 Sep 3003	e095	22 Oct 2005
e026	12 Jan 2001	e061	21 Sep 2003	e096	23 Oct 2005

Epoch Number	Calendar Date	Epoch Number	Calendar Date	Epoch Number	Calendar Date
e027	15 Jan 2001	e062	9 Oct 2003	e097	14 Nov 2005
e028	2 Nov 2001	e063	13 Oct 2003	e098	15 Nov 2005
e029	22 Nov 2001	e064	6 Nov 2003	e099	16 Nov 2005
e030	23 Dec 2001	e065	5 Dec 2003	e100	16 Nov 2005
e031	25 Jun 2002	e066	9 Dec 2003	e101	17 Dec 2005
e032	21 Jul 2002	e067	10 Dec 2003	e102	18 Dec 2005
e033	14 Aug 2002	e068	11 Dec 2003	e103	20 Dec 2005
e034	17 Sep 2002	e069	13 Dec 2003		
e035	20 Sep 2002	e070	3 Jan 2004		

Each image of M31 was taken with the 2048 x 2048 pixel MOSAIC CCD camera. In order to make the images easier to examine, each was subdivided into sixteen smaller areas known as subrasters—each 512 pixels x 512 pixels in size (Rector, 2005). The subrasters were labeled as shown in Figure 1.

Fig. 1. The large 2048 pixel x 2048 pixel image of M31 was divided into sixteen smaller 512 pixel x 512 pixel subrasters for easier study. Subrasters 6, 7, 10, 11 contained the core of the galaxy and provided a greater occurence of novae than the outer areas.

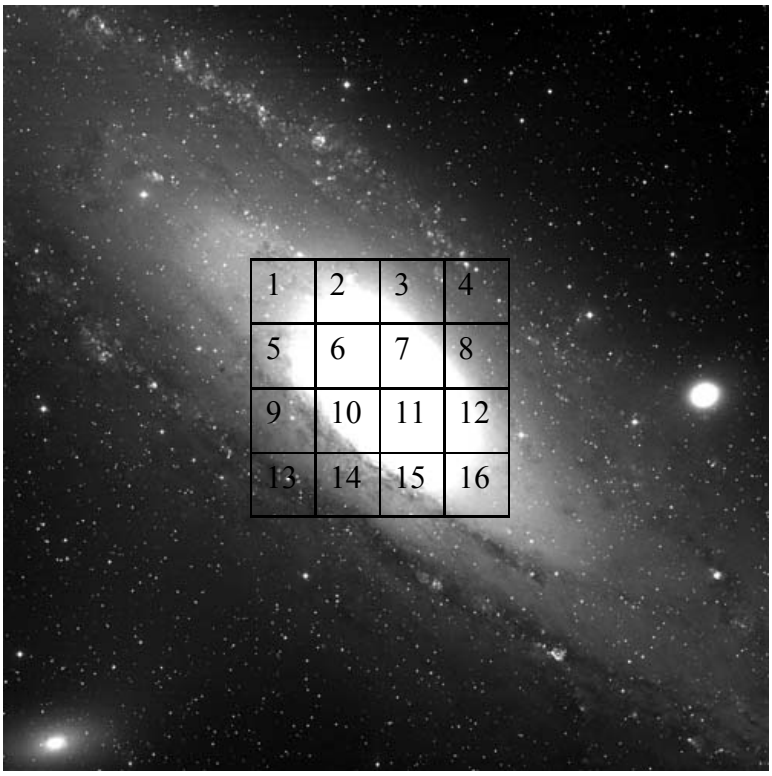

Each subraster was examined through all 103 epochs, making a total of 1648 images examined. The free JAVA-based program ImageJ was used to examine the images in

this study. ImageJ may be downloaded from *http://rsb.info.nih.gov/ij/*. In addition, a plug-in, called the Nova plug-in was also utilized.

ImageJ was used to "stack" the successive images from each epoch and then project them in rapid succession ("blinking"). Blinking is a common method used in astronomy for detecting transient events (Seeds, 2005). Ordinary stars in the frame remained stationary and were present in each frame, while any object that appeared in one subraster and then disappeared in a later one was deemed to be a possible nova.

These nova candidates were then examined more closely. Many objects that at first appeared to be novae turned out to be due to other events, such as plate defects, cosmic rays, or in a couple of cases, variable stars. Defects tended to have sharply defined edges while stars were round and with softer edges.

After examining all M31 images, a total of 92 novae were detected over the ten-year period. Their locations and dates of appearance are shown in Appendix 1.

After the novae were located, they were examined with the ImageJ Nova-plug-in. This allowed the coordinates (Right Ascension and Declination) of the novae to be determined. ImageJ was also used to measure the change in brightness of the novae from one frame to the next. The brightness values of the novae were determined by comparing their brightness to the brightness values of three standard stars which were present in the same frame, using the Image J software. This, along with the knowledge of the dates on which the images were taken, allowed the rate of decay of the novae to be determined. All dates were converted into Julian Days since this allows the differing lengths of the various months of the year to be ignored. The program *Graphical Analysis 3* was used to measure the slopes of the novae decay curves. Once the slope had been determined, the novae's t_2 time was calculated by using the following equation:

$$\mathbf{t_2 = (1/slope) \times 2}$$

Some of the novae appeared in only one frame, making it difficult to determine their t_2 times. It was suggested by Rector (personal communication, 2005) that a t_2 time of sorts could be measured for these objects. The method involved measuring the brightness of the nova, then measuring the faintest star-like object visible in the next frame—the nova could be no brighter than this value. After measuring several frames, it was determined that the faintest star-like objects visible were of approximately magnitude 19.5. This value was then used for all observations. This meant that a maximum value for the second brightness measurement could be determined and a maximum t_2 time could be assigned. Therefore, these novae decayed at a rate no slower than what is given and so a lower limit is placed on their masses. These single-image novae are listed in Table 4 and also in Appendix 1. There was no change in the overall distribution of white dwarf masses when these novae were included.

Table 4. Some novae appeared in only a single image - t_2 times for these novae were determined by using a method proposed by Rector (2005). A second magnitude measurement of 19.5 was assigned to each of these novae (see text for details).

Subraster	Init Date	Final Date	RA	Dec (dms)	Mag1	Mag2	Slope	T_2
f02	8/2/2003	8/3/2003	00h 42m 56.30s	41 22 22.1	17.87	19.5	1.6300	1.227
f02	6/26/2004	6/27/2004	00h 42m 54.72s	41 22 52.2	18.10	19.5	1.4000	1.429
f02	6/26/2004	6/27/2004	00h 43m 08.73s	41 22 51.6	18.72	19.5	0.7800	2.564
f02	6/27/2006	9/30/2004	00h 42m 53.56s	41 22 48.9	17.95	19.5	0.0163	122.549
f05	1/27/1999	6/24/1999	00h 43m 35.54s	41 20 41.3	17.91	19.5	0.0107	186.220
f07	12/23/2001	6/25/2002	00h 42m 41.49s	41 16 25.6	14.70	19.5	0.0261	76.658
f07	7/25/1998	8/26/1998	00h 42m 37.03s	41 16 57.4	15.49	19.5	0.1253	15.962
f09	7/25/1998	8/26/1998	00h 43m 19.69s	41 13 36.7	17.88	19.5	0.0506	39.502
f09	7/25/1998	8/26/1998	00h 43m 23.64s	41 15 46.0	17.11	19.5	0.0747	26.777
f10	7/25/1998	8/26/1998	00h 42m 45.24s	41 15 32.4	15.94	19.5	0.1113	17.969
f10	11/18/1997	6/6/1998	00h 43m 42.22s	41 15 00.4	15.32	19.5	0.0209	95.694
f10	7/20/1999	6/14/2000	00h 42m 44.82s	41 11 38.9	14.73	19.5	0.0145	138.408
f11	11/18/1997	6/6/1998	00h 42m 21.82s	41 12 17.0	16.97	19.5	0.0127	158.103
f11	6/14/2000	7/17/2000	00h 42m 30.17s	41 15 27.8	13.34	19.5	0.1867	10.712
f11	11/18/1997	6/6/1998	00h 42m 42.22s	41 15 12.0	15.88	19.5	0.0181	110.497

ANALYSIS AND RESULTS

Using the mass bins listed in Table 2, it was found that 85% of them fell into the 0.4-0.95 solar-mass categories. The remaining novae had masses greater than 0.95 solar masses. These results are in agreement with those of other researchers (Della Valle, 1994). This information is summarized in Figure 2.

Fig. 2. The majority of M31's binary white dwarfs appear to be less massive than the sun. Their masses range from 0.4 to 0.95 suns. There is a steady drop off in abundance as the masses of the white dwarfs increase.

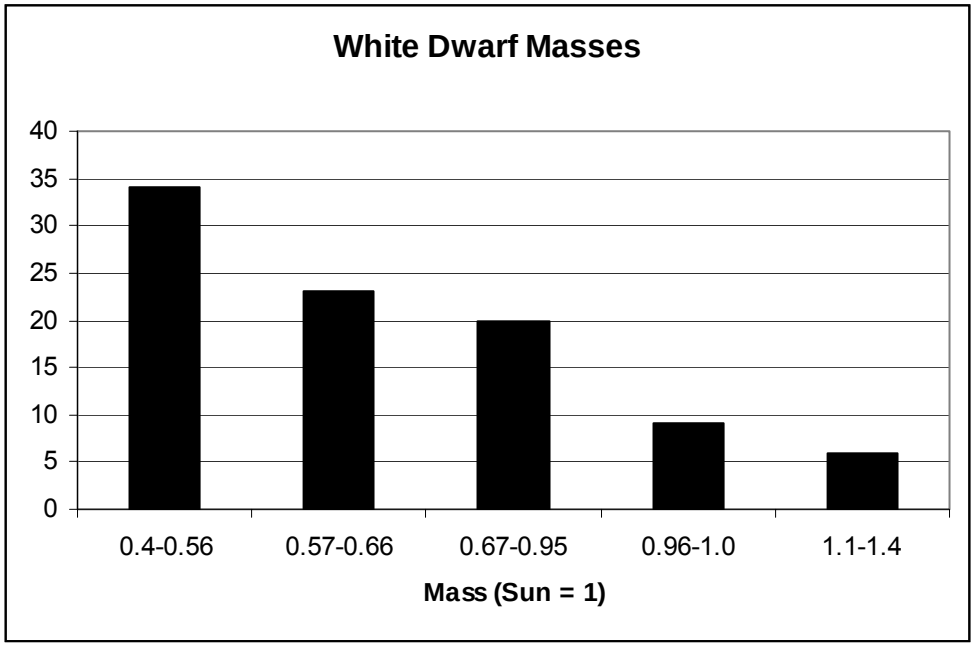

In close binary stars in M31, most white dwarfs have masses less than the mass of the sun. The numbers of white dwarf stars drop off steadily as their masses increase.

DISCUSSION

Close binary star systems containing white dwarfs with masses greater than the suns appear to be rare in M31. Some mechanism must therefore be limiting their numbers. Either white dwarfs with high mass do not often occur in M31's close binary star systems or some process is preventing their detection.

Due to the irregular timing of data collection over the 10-year period, it is possible that many fast novae, and hence, massive white dwarfs, went undetected. If images were taken on a more regular schedule, and also at shorter intervals, the detection rate for these massive white dwarfs should improve. There will be no increase in the numbers of slow novae detected since they often require many weeks or even months in order to fade away and so they are easily detected by the current method.

SUMMARY

The distribution of white dwarf masses in M31 is still uncertain. In order to determine the correct distribution of white dwarf masses, continual long-term monitoring should be carried out. The time between samples should be of short duration in order to catch novae with very short t_2 times.

ACKNOWLEDGEMENTS

The authors would like to thank the NOAO, Kitt Peak National Observatory and its support staff, the TLRBSE program, the Tohono O'odham Nation, Jeff Lockwood, Katy Garmany, Steve Howell, Travis Rector, Connie Walker, Stephen Pompea, Steven Croft, Kathy Stiles, Randy Accetta, and Kathie Coil for making this project possible.

Special thanks are offered to the spouses and members of the researchers' families for their patience and understanding.

REFERENCES

Ciardullo, Robin, et al. 20 June 1990. "The Hα Light Curves of Novae in M31". The Astrophysical Journal 356: 472-482.

Darnley, M J., et al. 26 May 2004. "Monthly Notices of the Royal Astronomical Society Vol 2. Classical Novae from the POINT-AGAPE Microlensing Survey of M31 – I". The Nova Catalogue.

Della Valle, Massimo, et al. June 1994. "The Nova Rate in Galaxies of Different Nova Types. Astron Astrophys. 287, 403-409 (1994)".

Della Valle, Massimo, et al. 20 October 1995. The Calibration of Novae as Distance Indicators. The Astrophysical Journal 452:704-709 1995 October 20.

Nave, Rod. 2005. Online. *http://hyperphysics.phy-astr.gsu.edu/HBASE/astro/whdwar.html.* 21 March 2006.

Petz, Alexander. Online. *http://www.hs.uni-hamburg.de/EN/For/ThA/phoenix/novae.html.* 18 March 2006

Rector, Travis and Jacoby, G. 2005. Nova Search: "Cosmic Easter Eggs", TLRBSE website, www.noao.edu/outreach/tlrbse/

Rector, Travis. 2005. Personal Communication. TLRBSE Final Session. 4 July 2005.

Rector, Travis. 2006 March 17. A TLRBSE 2005 Nova Question [email]. Accessed March 18 2006.

Seeds, Michael. 2005. "Foundations of Astronomy, 8th ed". Brooks/Cole. Canada.

Shafter, Allen, et al., 10 February 2000, "Novae in External Galaxies: M51, M87, and M101. The Astrophysical Journal, 530:193-206.

Shafter, Allen and Bryan Irby. 20 December 2001. "On the Spatial Distribution, Stellar Population, and Rate of Novae in M31". The Astrophysical Journal, 563:749-767.

Zeilik, Michael. 1994. Astronomy: "The Evolving Universe, 7th ed.", John Wiley and Sons. New York.

APPENDICES

Appendix 1. The locations and times of all novae images used in this study are shown. The highlighted novae are those whose slopes were determined using the single-image method described in the text (see Table 4).

Subraster	RA	Dec	Initial Epoch	Final Epoch	Date Start	Julian Date Start	Date End	Julian Date End
f02	00 42 53 56	41 22 48 9	78	79	6/27/2006	2453913	9/30/2004	2453278
f02	00 43 08 73	41 22 51 6	77	78	6/26/2004	2453182	6/27/2004	2453183
f02	00:42 54 72	41 22 52 2	77	78	6/26/2004	2453182	6/27/2004	2453183
f02	00 42 56 30	41 22 22 1	53	53	8/2/2003	2452853	8/3/2003	2452854
f05	00 43 23 62	41 21 40 1	2	7	6/18/1997	2450617	8/1/1997	2450661
f05	00 43 28 58	41 21 42 5	9	19	6/6/1998	2450970	7/20/1999	2451379
f05	00 43 23 5	41 21 40 1	1	8	9/3/1995	2449963	11/18/1997	2450770
f05	00 43 17 66	41 20 59 7	8	15	11/18/1997	2450770	10/30/1998	2451116
f05	00 43 28 77	41 21 43 3	10	16	7/24/1998	2451018	11/11/1998	2451128
f05	00 43 28 55	41 21 42 5	9	18	6/6/1998	2450970	6/24/1999	2451353
f05	00 43 17 71	41 20 59 4	8	17	11/18/1997	2450770	1/27/1999	2451205
f05	00 43 23 47	41 21 09 9	2	8	6/18/1997	2450617	11/18/1997	2450770
f05	00 43 35 54	41 20 41 3	17	18	1/27/1999	2451205	6/24/1999	2451353
f06	00 43 06 86	41 18 09 4	9	18	6/6/1998	2450970	6/24/1999	2451353
f06	00 43 06 84	41 18 09 4	9	18	6/6/1998	2450970	6/24/1999	2451353
f06	00 42 46 81	41 19 48	62	74	9/21/2003	2452903	2/3/2004	2453038
f06	00 42 45	41 17 54	61	65	9/20/2003	2452902	12/5/2003	2452978
f06	00 43 12 39	41 21 49 2	2	8	6/18/1997	2450617	11/18/1997	2450770
f06	00 43 12 38	41 21 48 3	2	8	6/18/1997	2450617	11/18/1997	2450770
f06	00 43 06 89	41 18 09 8	2	8	7/24/1998	2451018	10/14/1998	2451100
f06	00 43 06 9	41 18 10 4	10	14	7/24/1998	2451018	10/14/1998	2451100
f06	00 42 54	41 18 46.7	64	71	11/6/2003	2452949	1/6/2004	2453010
f06	00 41 27	41 08 37	14	16	10/14/1998	2451100	11/11/1998	2451128
f06	00 42 44 54	41 20 40 1	21	25	7/17/2000	2451742	11/10/2000	2451858
f06	00 43 07	41 18 06	84	85	11/17/2004	2453326	11/20/2004	2453329
f06	00 42 49	41 19 19.3	75	78	6/24/2004	2453180	6/27/2004	2453183
f06	00 42 49 6	41 18 02.1	61	61	9/20/2003	2452902	10/13/2003	2452925
f06	00 43 04 3	41 19 36 2	18	19	6/24/1999	2451353	7/20/1999	2451379
f07	00 41 28	41 08 13	3	7	7/23/1997	2450652	8/1/1997	2450661
f07	00 41 07	41 08 27	10	13	7/24/1998	2451018	9/5/1998	2451061
f07	00 41 15	41 08 49	10	12	7/24/1998	2451018	8/26/1998	2451051
f07	00 42 41 3	41 16 15.6	62	72	10/9/2003	2452921	1/31/2004	2453035
f07	00 42 19 3	41 16 16 8	3	9	7/23/1997	2450652	6/9/1998	2450973
f07	00 42 43 9	41 17 35.8	75	83	6/24/2004	2453180	10/24/2004	2453302
f07	00 42 19 3	41 16 17 3	3	8	7/23/1997	2450652	11/18/1997	2450770
f07	00 42 30 4	41 16 34	10	15	7/24/1998	2451018	10/30/1998	2451116
f07	00 42 41 49	41 16 25 6	30	31	12/23/2001	2452266	6/25/2002	2452450
f07	00 42 30 4	41 16 34 5	10	14	7/24/1998	2451018	10/14/1998	2451100
f07	00 42 34 04	41 16 56 7	10	12	7/24/1998	2451018	8/26/1998	2451051
f07	00 42 37 62	41 17 37 2	22	23	9/13/2000	2451800	9/14/2000	2451801
f07	00 42 37 0	41 16 56 9	10	12	7/24/1998	2451018	8/26/1998	2451051
f07	00 42 42 9	41 18 28.1	84	85	11/17/2004	2453326	11/20/2004	2453329

Subraster	RA	Dec	Initial Epoch	Final Epoch	Date Start	Julian Date Start	Date End	Julian Date End
f07	00 42 37 03	41 16 57 4	11	12	7/25/1998	2451019	8/26/1998	2451051
f07	00 42 32	41 19 25.3	84	85	11/17/2004	2453326	11/20/2004	2453329
f09	00 43 19 69	41 13 36 7	11	12	7/25/1998	2451019	8/26/1998	2451051
f09	00 43 18 69	41 13 35 3	11	12	7/25/1998	2451019	8/26/1998	2451051
f09	00 43 23 64	41 15 46 0	11	12	7/25/1998	2451019	8/26/1998	2451051
f09	00 43 23 58	41 15 45 3	11	12	7/25/1998	2451019	8/26/1998	2451051
f10	00 40 23	41 06 38	14	16	10/14/1998	2451100	11/11/1998	2451128
f10	00 42 46 51	41 15 56 5	62	66	10/9/2003	2452921	12/9/2003	2452982
f10	00 42 46 55	41 14 40 00	3	13	10/14/1998	2451100	11/11/1998	2451128
f10	00 42 46 5	41 14 49 7	14	17	10/14/1998	2451100	1/27/1999	2451205
f10	00 43 08 68	41 15 37 4	72	78	1/31/2004	2453035	6/27/2004	2453183
f10	00 42 44 82	41 11 38 9	19	20	7/20/1999	2451379	6/14/2000	2451709
f10	00 43 05 3	41 14 59 9	8	10	11/18/1997	2450770	7/24/1998	2451018
f10	00 43 05 22	41 15 38 7	8	10	11/18/1997	2450770	7/24/1998	2451018
f10	00 42 46 58	41 14 48 3	14	17	10/14/1998	2451100	1/27/1999	2451205
f10	00 42 47 37	41 15 07 3	20	24	6/14/2000	2451709	10/15/2000	2451832
f10	00 40 39	41 13 47	3	7	7/23/1997	2450652	8/1/1997	2450661
f10	00 42 54 16	41 15 13 5	70	74	1/3/2004	2453007	2/3/2004	2453038
f10	00 43 42 22	41 15 00 4	8	8	11/18/1997	2450770	6/6/1998	2450970
f10	00 43 03 17	41 15 59 7	3	7	7/23/1997	2450652	8/1/1997	2450661
f10	00 43 04 78	41 12 22 7	71	74	1/6/2004	2453010	2/3/2004	2453038
f10	00 42 47 4	41 15 53 0	79	82	9/30/2004	2453278	10/23/2004	2453301
f10	00 43 08 8	41 13 54 4	9	10	6/6/1998	2450970	7/24/1998	2451018
f10	00 43 01 75	41 15 37 9	18	19	6/24/1999	2451353	7/20/1999	2451379
f10	00 42 45 24	41 15 32 4	11	12	7/25/1998	2451019	8/26/1998	2451051
f10	00 43 06 8	41 11 58 9	75	78	6/24/2004	2453180	6/27/2004	2453183
f11	00 42 38 53	41 14 16 3	3	8	7/23/1997	2450652	11/18/1997	2450770
f11	00 40 59	41 03 24	14	16	10/14/1998	2451100	11/11/1998	2451128
f11	00 42 21 82	41 12 17 0	8	9	11/18/1997	2450770	6/6/1998	2450970
f11	00 42 32 1	41 14 42 2	3	9	7/23/1997	2450652	6/6/1998	2450970
f11	00 42 42 22	41 15 12 0	8	9	11/18/1997	2450770	6/6/1998	2450970
f11	00 42 31 93	41 07 47 8	3	8	7/23/1997	2450652	11/18/1997	2450770
f11	00 42 40 05	41 15 46 0	2	7	6/18/1997	2450617	8/1/1997	2450661
f11	00 42 19 6	41 11 58 7	14	17	10/14/1998	2451100	1/27/1999	2451205
f11	00 42 10 8	41 14 08 2	2	3	6/18/1997	2450617	7/23/1997	2450652
f11	00 42 37 14	41 14 29 4	75	78	6/24/2004	2453180	6/27/2004	2453183
f11	00 42 22 1	41 11 32 3	14	17	10/14/1998	2451100	1/27/1999	2451205
f11	00 41 09	41 06 33	3	7	7/23/1997	2450652	8/1/1997	2450661
f11	00 42 22 40	41 13 45 1	75	78	6/24/2004	2453180	6/27/2004	2453183
f11	00 42 38 54	41 14 18 4	18	19	6/24/1999	2451353	7/20/1999	2451379
f11	00 42 30 17	41 15 27 8	20	21	6/14/2000	2451709	7/17/2000	2451742
f12	00 41 47 24	41 15 33 7	1	8	9/3/1995	2449963	11/18/1997	2450770
f14	00 42 50 37	41 07 47 8	3	13	7/23/1997	2450652	9/5/1998	2451061
f14	00 42 50 35	41 07 49 10	9	18	7/23/1997	2450652	8/1/1997	2450661
f14	00 42 50 3	41 07 48 4	3	5	7/23/1997	2450652	7/25/1997	2450654
f15	00 42 13 30	41 07 41 3	12	19	8/26/1998	2451051	7/20/1999	2451379
f15	00 42 33 77	41 04 57 4	13	17	9/5/1998	2451061	1/27/1999	2451205

Subraster	RA	Dec	Initial Epoch	Final Epoch	Date Start	Julian Date Start	Date End	Julian Date End
f16	00 40 50	40 59 37	12	16	8/26/1998	2451051	11/11/1998	2451128
f16	00 42 08 36	41 08 15 7	2	7	6/18/1997	2450617	8/1/1997	2450661
f16	00 42 08 39	41 08 14 9	2	8	6/18/1997	2450617	11/15/1997	2450767

Project Glob

Kyle L. Hornbeck & Robert G. Johnson
Deer Valley High School, Antioch, CA
Teacher: Jeff Adkins, TLRBSE 2002

ABSTRACT

After initially searching for novas in globular clusters (and not finding any) we took our data from variable stars and created light curves. We selected variable stars inside M 3 and M 92. From the data consolidated and collected, we constructed models which enabled us to find the magnitudes of the variable stars in each epoch. Using these, we further speculated and arrived at likely periods, but the variations were of prime importance. The difference exceeded the errors calculated which leads us to believe that we have observed variations in the magnitudes which confirmed the validity of our procedure.

INTRODUCTION

We began this lab when our astronomy instructor approached us with a challenge as we began to look for novas in pictures taken of M31. He described a scientific task that would count for our nova search project and major research project for the year. It required taking pictures from a remote control observatory and then aligning, and calibrating these images to a form accepted universally. We blinked these images in search of a nova. None were found, and we have used the opportunity to track multiple variable stars to validate our technique. Light curves for the variables have been measured, and checked.

OBSERVATIONS AND DATA REDUCTION

We were selected by the Teacher Observing Program (TOP) to go to Kitt Peak observatory and take pictures of globular clusters in an ongoing search for novae. Only one of us, Robert, was able to represent our team. Robert took his pictures using the 0.9-meter telescope run by the National Optical Astronomy Observatory (NOAO) in Arizona. We made a schedule of targets (Table 1) to capture each of the three potentially observable nights. Much to our dismay the actual observable time was decreased significantly due to ill-tempered weather. Due to these unfortunate circumstances, the scheduled list of targets was not completed. After returning from Arizona, we compared the pictures obtained from Kitt Peak and those from Hands on Universe (HOU) (http://www.handsonuniverse.org/), and checked if there were any novae. HOU provided images through other astronomers taking pictures of objects on our behalf.

Selected Obj.	Time	Quantity	Captured
92	8:00	1	X
12	8:20	1	
15	8:40	1	X
2	8:45	1	X
30	8:50	1	
71	9:00	1	X
72	9:00	1	X
56	9:30	1	X
79	4:30 AM	1	

Table 1

Before our trip we had selected a smaller group of globular clusters. The reason we investigated the possibility of novae in globular clusters was that it had seldom been researched or proven. The clusters we selected were done so for their location in the sky relative to the observatory, New Mexico Skies (www.telescope2.net) in Mayhill, New Mexico, during the times we would observe. Our clusters had to fulfill prerequisites such as not only being above the horizon, but also 20° above that so the telescope was not pointed at the wall of the observatory, and at least 10° from due south orientation. The telescope does not track well near the meridian.

We then logged onto New Mexico Skies to use the telescope to photograph the selected objects (m3, m5, m13, m53, m68, m92) (Table 2) over time attempting to have one-week intervals between exposures. The photographs were taken with 60 seconds exposure times. Using the Simbad clickable star maps, (available at http://simbad.u-strasbg.fr/sim-fid.pl) (Fig. 2) we selected and located 5-10 standard stars (Table 3) and recorded magnitudes of each star to be used to calibrate our measurements. After this, we used NIH image processor (http://rsb.info.nih.gov/nih-image/download.html) to search for novas by blinking the epochs. However, before this was possible, the images had to be aligned so the stars lined up, these pictures did not need to be resized because they were all done as they came. We found it was most efficient to pick one star and correct any variation from one frame to another. No change was noticed, and the chance of finding a nova was greatly reduced if not eliminated, because the magnitude of a nova would be quite noticeable. We decided to move on to the secondary objective, finding and measuring variable stars. Again, using Simbad, a target variable star had to be selected. An ideal target is an easily identifiable star out of the main cluster, so it is easier to measure. If it is in the heart of the cluster, it is impossible to distinguish from the mess of other stars.

Globular Clusters Selected

M 3	13 42 11.23	+28 22 31.6 C ~
M 5	15 18 33.75	+02 04 57.7 D ~
M 13	16 41 41.44	+36 27 36.9 D ~
M 53	13 12 55.3	+18 10 09 D
M 68	12 39 28.01	-26 44 34.9 D ~
M 92	17 17 07.27	+43 08 11.5 D ~

Table 2

M3 Standard Stars

Object	RA	Dec
Cl* NGC 5272 KUST 906	13 42 28.23	+28 18 52.3 C ~
Cl* NGC 5272 KUST 928	13 42 35.56	+28 19 58.5 C ~
Cl* NGC 5272 KUST 917	13 42 32.04	+28 27 02.7 C ~
NGC 5272 1405	13 42 44.35	+28 23 09.0 D
Cl* NGC 5272 KUST 960	13 42 49.33	+28 23 52.6 C ~
Cl* NGC 5272 KUST 69	13 41 55.12	+28 19 14.9 C ~
Cl* NGC 5272 KUST 15	13 41 44.34	+28 26 04.7 C ~
Cl* NGC 5272 KUST 18	13 41 44.70	+28 26 20.7 C ~
Cl* NGC 5272 KUST 20	13 41 45.17	+28 26 38.7 C ~
Cl* NGC 5272 KUST 840	13 42 22.24	+28 17 06.6 C ~

Table 3

Our first method to find the magnitude of the target employed the formula (Fig. 1) in the application Hands on Universe Image Processing (http://www.handsonuniverse.org/about_hou/index.html). We

$$M_1 + 2.5 \times Log\left(\frac{B_2}{B_1}\right) = M_2$$

Fig. 1

attempted to calibrate all images by using the "sky" function for each image, and to each one, used the "add" function to standardize the interfering light from other sources. The Sky function averaged the pixels over an area of the image and when that same number is added to the image with the "add" function resulting in standardizing the sky counts to zero, meaning the anomalies are accounted for. This effort, however, was superfluous in the end because the tool used to measure the brightness counts of each selected star would account for this.

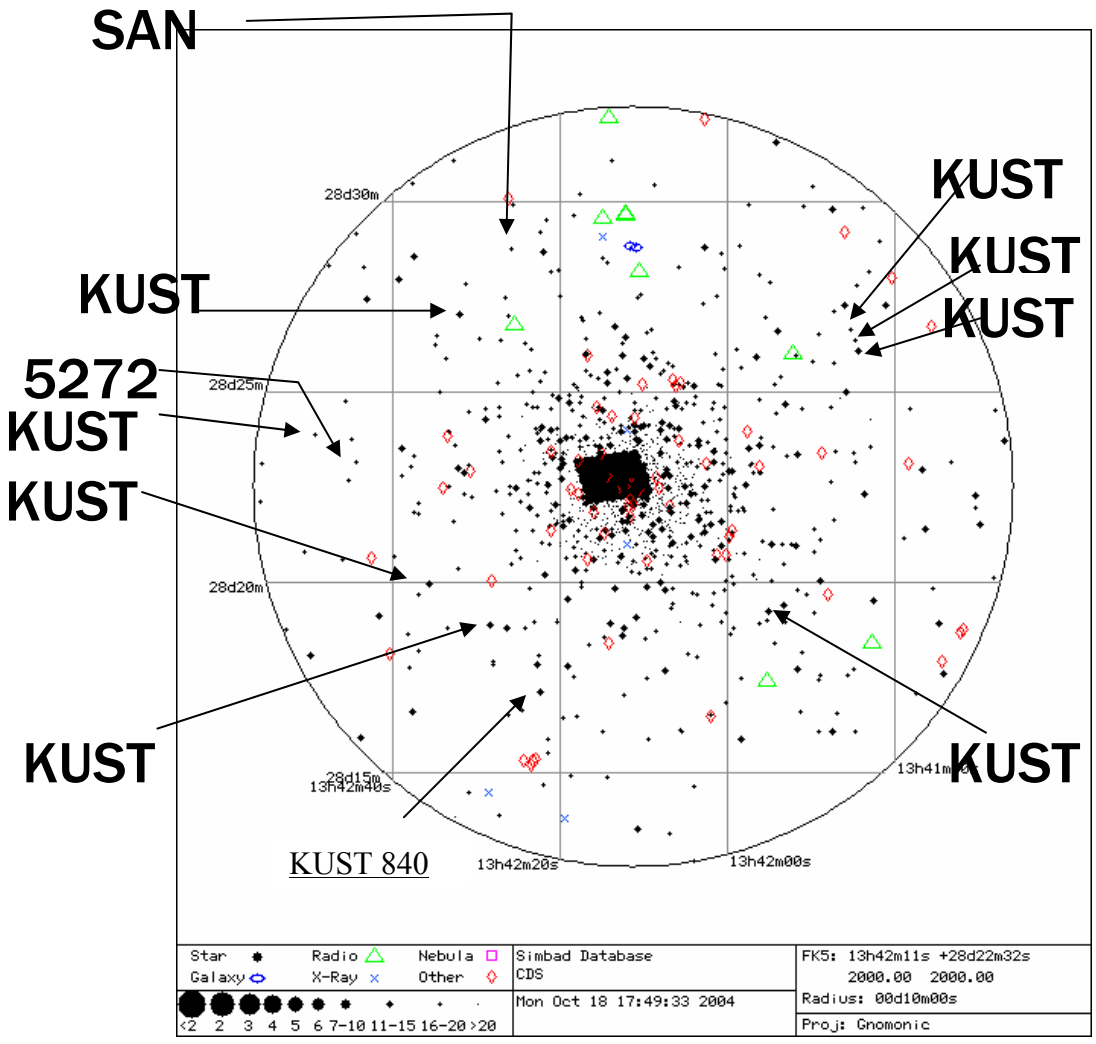

Fig. 2

Finding the brightness counts for each standard star using the auto aperture/"bull's-eye" function in each image was simple enough. The result yielded a sum of the white pixels in the selected area, which was used in an average to determine the brightness counts of the standard stars. Next we took the average ratio of a standard star in the first epoch and divided it by the same star in another epoch and multiplied each picture by the ratio. This method was determined with the intention of to finding the magnitude of a star measured in the picture. After we equalized all the pictures, we used this equation (Fig. 1) to convert the brightness counts into magnitudes. We discovered that this method did not work unless the stars were relatively similar in their magnitudes, which skewed our ratio due to the varied selection of standard stars to compensate for any error in magnitude specific issues. Instead, a mathematic model was computed by using the application Fathom 2.0 Beta (http://www.keypress.com/fathom/update.html).

The model was constructed based on a logarithm of the brightness counts of a star compared to the magnitude. We derived this conclusion from the original equation (Fig. 1) by, instead of trying to covert each brightness count into a magnitude, taking the log of the brightness counts and comparing it to known magnitudes of each of the standard stars. The comparison gave a line of best fit that we then used to get the magnitude of an arbitrary star's brightness count by moving the point on the model onto the line of best fit. We used this method to better understand where the magnitudes came from as apposed to letting automated software do all the work. By doing this, the magnitude would change on the spreadsheet to the actual magnitude within a small deviation from the projected ratio. This process was done to each epoch for every standard star.

$$M = a \sin(k(\text{Date} + \phi)) + b$$

Fig. 3

With these models, we had to then input the brightness counts of the variable stars into these models (separately, not in the spreadsheet) to ensure that the data is affected by, but not affecting the line of best fit. These variable magnitudes were put into yet another spreadsheet in fathom, this one for the actual variable star, but set against the Julian date (as the actual interval was a factor) and graphed the magnitude as a function of time (Fig. 3). The variables a, k, ϕ (phi), and b were modified with "slider" tools in fathom until the function accurately represented a plausible plot of the points. A residual plot was also used to ensure the integrity of the plot.

We do not completely trust our data because of a recent discovery that the fluctuations may not be sinusoidal but possibly tangential. We are investigating this now.

Data for M3 and M92

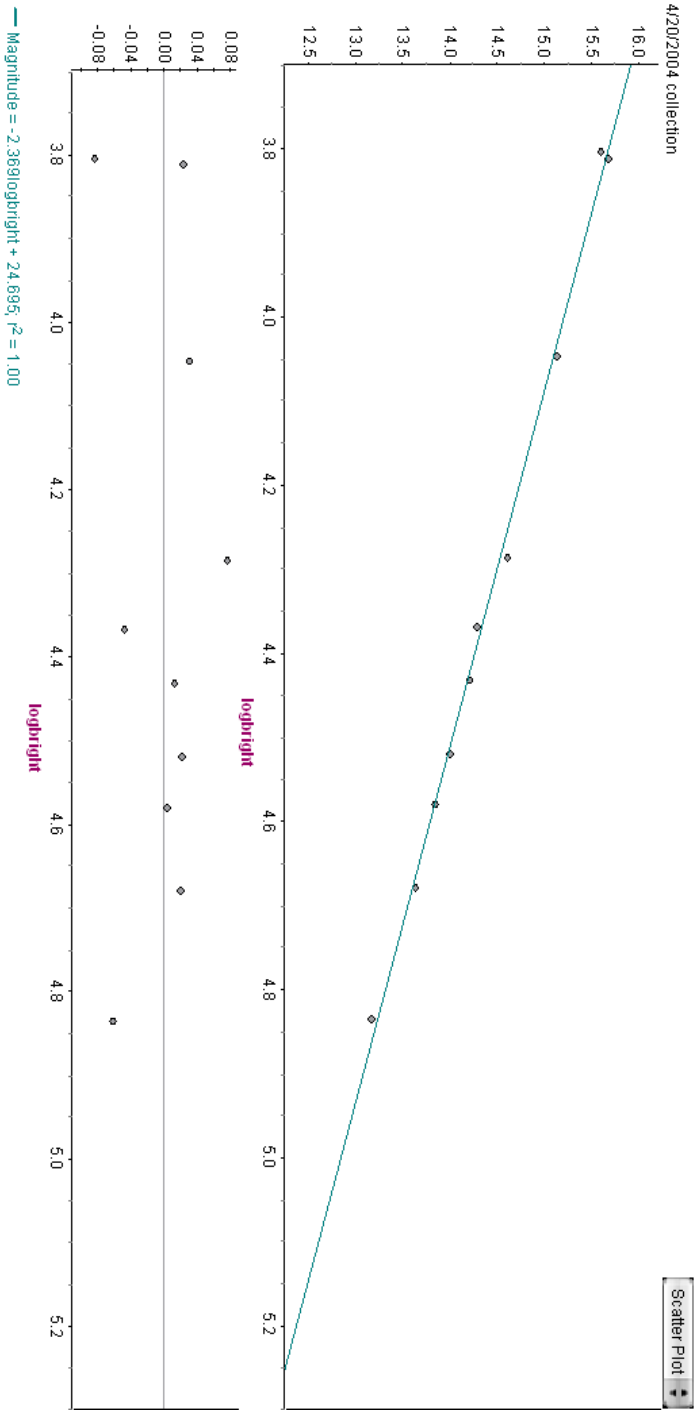

4/20/2004 collection

	star	Bright	MagnituÉ	logbright
=				log (Bright)
1	Cl* NGC 5272 KUST 906	27024	14.21	4.43175
2	Cl* NGC 5272 KUST 928	47795	13.63	4.67938
3	Cl* NGC 5272 KUST 917	33140	14.01	4.52035
4	NGC 5272 1405	6365	15.60	3.8038
5	Cl* NGC 5272 KUST 960	19295	14.62	4.28544
6	Cl* NGC 5272 KUST 69	68400	13.18	4.83506
7	Cl* NGC 5272 KUST 15	38042	13.85	4.58026
8	Cl* NGC 5272 KUST 18	11147	15.14	4.04716
9	Cl* NGC 5272 KUST 20	6484	15.69	3.81184
10	Cl* NGC 5272 KUST 840	23349	14.30	4.36827

Model of 4/20/2004 collection Simple Regression

Response attribute (numeric): Magnitude

Predictor attribute (numeric): logbright

Sample count: **10**

Equation of least-squares regression line:
Magnitude = -2.36875 logbright + 24.695
Correlation coefficient, r = **-0.998266**
r-squared = **0.99653**, indicating that **99.653**% of the variation in **Magnitude** is accounted for by **logbright** .

The best estimate for the slope is **-2.36875** +/- **0.113883** at a **95** % confidence level. (The standard error of the slope is **0.0493855**.)

When **logbright** = **5** , the predicted value for a future observation of **Magnitude** is **12.8509** +/- **0.147025**.

4/29/2004 collection

	star	Bright	MagnituÉ	logbright
=				log (Bright)
1	Cl* NGC 5272 KUST 906	19285	14.21	4.28522
2	Cl* NGC 5272 KUST 928	33983	13.63	4.53126
3	Cl* NGC 5272 KUST 917	24124	14.01	4.38245
4	NGC 5272 1405	5258	15.60	3.72082
5	Cl* NGC 5272 KUST 960	14030	14.62	4.14706
6	Cl* NGC 5272 KUST 69	49471	13.18	4.69435
7	Cl* NGC 5272 KUST 15	27520	13.85	4.43965
8	Cl* NGC 5272 KUST 18	8567	15.14	3.93283
9	Cl* NGC 5272 KUST 20	4231	15.69	3.62644
10	Cl* NGC 5272 KUST 840	17140	14.30	4.23401

Model of 4/29/2004 collection Simple Regression

Response attribute (numeric): Magnitude

Predictor attribute (numeric): logbright

Sample count: **10**

Equation of least-squares regression line:
Magnitude = -2.39854 logbright + 24.495

Correlation coefficient, r = **-0.997691**

r-squared = **0.99539**, indicating that **99.539**% of the variation in **Magnitude** is accounted for by **logbright** .

The best estimate for the slope is **-2.39854** +/- **0.13311** at a **95** % confidence level. (The standard error of the slope is **0.0577234**.)

When **logbright** = **5** , the predicted value for a future observation of **Magnitude** is **12.5027** +/- **0.180342**.

5/4/2004 collection
Scatter
Magnitude = -2.504*log bright + 25.34
logbright
16
15
14
13
3.8
4.0
4.2
4.4
4.6
4.8
5.0
5.2

4/29/2004 collection
Scatter
Magnitude = -2.405*log bright + 24.5
logbright
16
15
14
13
3.6
3.8
4.0
4.2
4.4
4.6
4.8

5/4/2004 collection

	star	Bright	MagnituÉ	logbright
=				log (Bright)
1	Cl* NGC 5272 KUST 906	29731	14.21	4.47321
2	Cl* NGC 5272 KUST 928	51173	13.63	4.70904
3	Cl* NGC 5272 KUST 917	32884	14.01	4.51698
4	NGC 5272 1405	7789	15.60	3.89148
5	Cl* NGC 5272 KUST 960	20765	14.62	4.31733
6	Cl* NGC 5272 KUST 69	63704	13.18	4.80417
7	Cl* NGC 5272 KUST 15	39777	13.85	4.59963
8	Cl* NGC 5272 KUST 18	11679	15.14	4.06741
9	Cl* NGC 5272 KUST 20	6902	15.69	3.83897
10	Cl* NGC 5272 KUST 840	22896	14.30	4.35976

Model of 5/4/2004 collection Simple Regression

Response attribute (numeric): Magnitude
Predictor attribute (numeric): logbright

Sample count: **10**

Equation of least-squares regression line:
Magnitude = -2.50403 logbright + 25.335
Correlation coefficient, r = **-0.995646**
r-squared = **0.99131**, indicating that **99.131**% of the variation in **Magnitude** is accounted for by **logbright** .

The best estimate for the slope is **-2.50403** +/- **0.191143** at a **95** % confidence level. (The standard error of the slope is **0.0828892**.)

When **logbright** = **5** , the predicted value for a future observation of **Magnitude** is **12.8149** +/- **0.234414**.

5/11/2004 collection

	star	Bright	MagnituÉ	logbright
=				log (Bright)
1	Cl* NGC 5272 KUST 906	25642	14.21	4.40895
2	Cl* NGC 5272 KUST 928	50643	13.63	4.70452
3	Cl* NGC 5272 KUST 917	31536	14.01	4.49881
4	NGC 5272 1405	6873	15.60	3.83715
5	Cl* NGC 5272 KUST 960	18472	14.62	4.26651
6	Cl* NGC 5272 KUST 69	67113	13.18	4.82681
7	Cl* NGC 5272 KUST 15	35034	13.85	4.54449
8	Cl* NGC 5272 KUST 18	10548	15.14	4.02317
9	Cl* NGC 5272 KUST 20	6871	15.69	3.83702
10	Cl* NGC 5272 KUST 840	22394	14.30	4.35013

Model of 5/11/2004 collection Simple Regression

Response attribute (numeric): Magnitude
Predictor attribute (numeric): logbright

Sample count: **10**

Equation of least-squares regression line:
Magnitude = -2.43615 logbright + 24.971
Correlation coefficient, r = **-0.997495**
r-squared = **0.99500**, indicating that **99.500**% of the variation in **Magnitude** is accounted for by **logbright** .

The best estimate for the slope is **-2.43615** +/- **0.140849** at a **95** % confidence level. (The standard error of the slope is **0.0610792**.)

When **logbright** = **5** , the predicted value for a future observation of **Magnitude** is **12.7902** +/- **0.178539**.

5/18/2004 collection
Scatter
16
15
14
13
3.4
3.6
3.8
4.0
4.2
4.4
logbright
Magnitude = -2.54*logbright + 24.4

5/11/2004 collection
Scatter
16
15
14
13
3.8
4.0
4.2
4.4
4.6
4.8
5.0
5.2
logbright
Magnitude = -2.436*logbright + 24.97

5/18/2004 collection

	star	Bright	MagnituÉ	logbright
=				log (Bright)
1	Cl* NGC 5272 KUST 906	11374	14.21	4.05591
2	Cl* NGC 5272 KUST 928	19858	13.63	4.29794
3	Cl* NGC 5272 KUST 917	13382	14.01	4.12652
4	NGC 5272 1405	3121	15.60	3.49429
5	Cl* NGC 5272 KUST 960	7725	14.62	3.8879
6	Cl* NGC 5272 KUST 69	24106	13.18	4.38213
7	Cl* NGC 5272 KUST 15	15219	13.85	4.18239
8	Cl* NGC 5272 KUST 18	4381	15.14	3.64157
9	Cl* NGC 5272 KUST 20	2767	15.69	3.44201
10	Cl* NGC 5272 KUST 840	9385	14.30	3.97243

Model of 5/18/2004 collection Simple Regression

Response attribute (numeric): Magnitude
Predictor attribute (numeric): logbright

Sample count: **10**

Equation of least-squares regression line:
Magnitude = -2.5355 logbright + 24.434
Correlation coefficient, r = **-0.996401**
r-squared = **0.99282**, indicating that **99.282**% of the variation in **Magnitude** is accounted for by **logbright** .

The best estimate for the slope is **-2.5355** +/- **0.175845** at a **95** % confidence level. (The standard error of the slope is **0.0762554**.)

When **logbright** = **5** , the predicted value for a future observation of **Magnitude** is **11.7564** +/- **0.259176**.

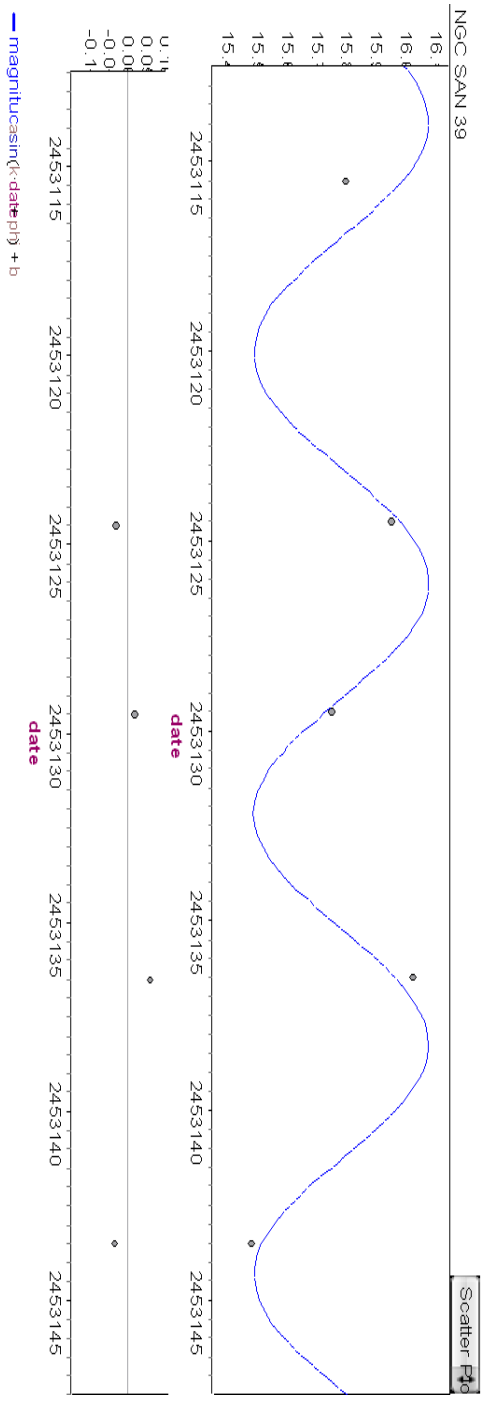
NGC SAN 39
Scatter Plo
2453115
2453120
2453125
2453130
2453135
2453140
2453145
date
magnitude sin(k*date+phi) + b

NGC SAN 39

	date	brightness	logbright	magnitude	plusminus
1	2453115.5	5696	3.75557	15.7987	0.142402
2	2453124.5	3655	3.56289	15.9497	0.168361
3	2453129.5	6723	3.82756	15.7507	0.223951
4	2453136.5	4701	3.67219	16.0249	0.177601
5	2453143.5	3387	3.52982	15.4841	0.195925

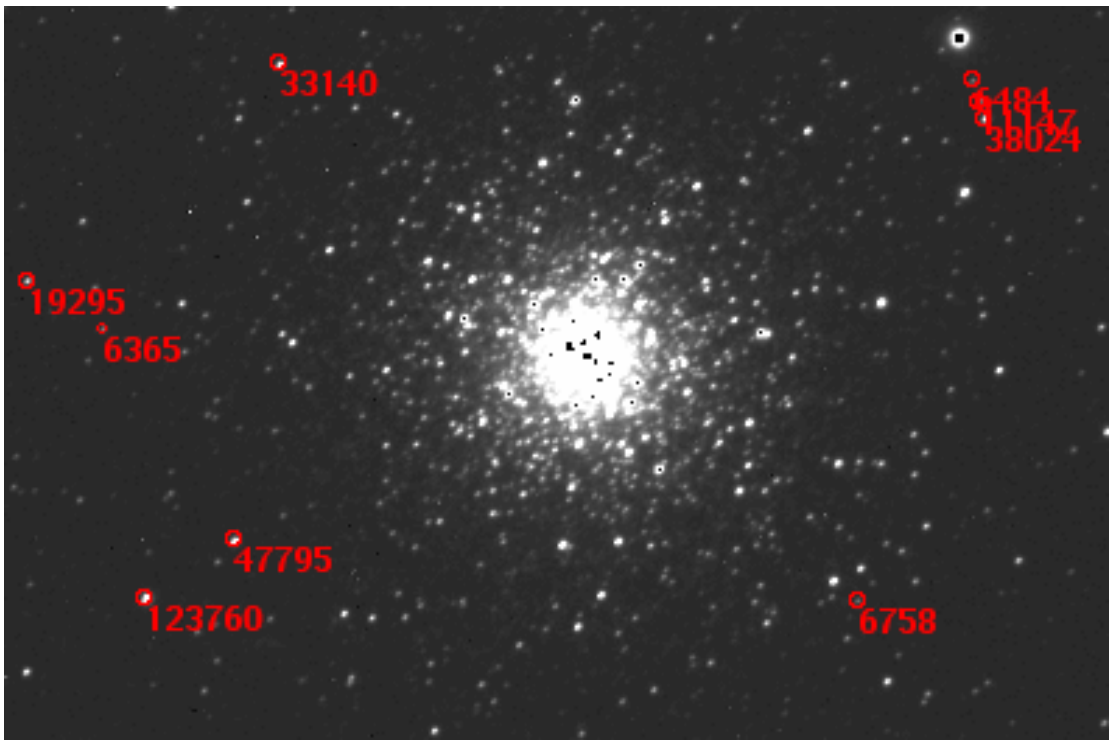

M 92 Data-

Collection 4-29-04

	star	MagnituÉ	BrightnÉ	logbright
=				log (Brightne
1	A	14.060	18974	4.27816
2	B	15.890	2538	3.40449
3	C	12.360	99811	4.99918
4	D	14.600	11056	4.0436
5	E	15.410	4985	3.69767
6	F	13.950	21038	4.323
7	G	13.810	25212	4.40161
8	H	15.160	6011	3.77895
9	I	14.060	17750	4.2492
10	J	12.180	113965	5.05677
11	Variable	15.484	4333	3.63679

Model of Collection 4-29-04 Simple Regression

Response attribute (numeric): Magnitude

Predictor attribute (numeric): logbright

Sample count: **11**

Equation of least-squares regression line:
Magnitude = -2.27732 logbright + 23.766
Correlation coefficient, r = **-0.99884**
r-squared = **0.99768**, indicating that **99.768**% of the variation in **Magnitude** is accounted for by **logbright** .

The best estimate for the slope is **-2.27732** +/- **0.082775** at a **95** % confidence level. (The standard error of the slope is **0.0365912**.)

When **logbright** = **3.63679** , the predicted value for a future observation of **Magnitude** is **15.4836** +/- **0.15202**.

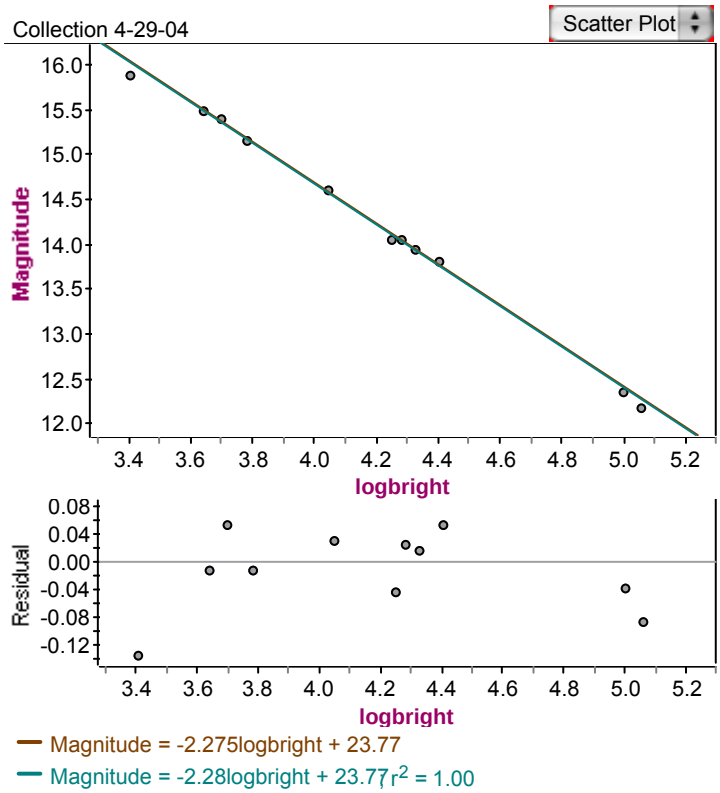
Collection 4-29-04
Scatter Plot
Magnitude
16.0
15.5
15.0
14.5
14.0
13.5
13.0
12.5
12.0
3.4 3.6 3.8 4.0 4.2 4.4 4.6 4.8 5.0 5.2
logbright
Residual
0.08
0.04
0.00
-0.04
-0.08
-0.12
3.4 3.6 3.8 4.0 4.2 4.4 4.6 4.8 5.0 5.2
logbright
Magnitude = -2.275logbright + 23.77
Magnitude = -2.28logbright + 23.77; r2 = 1.00

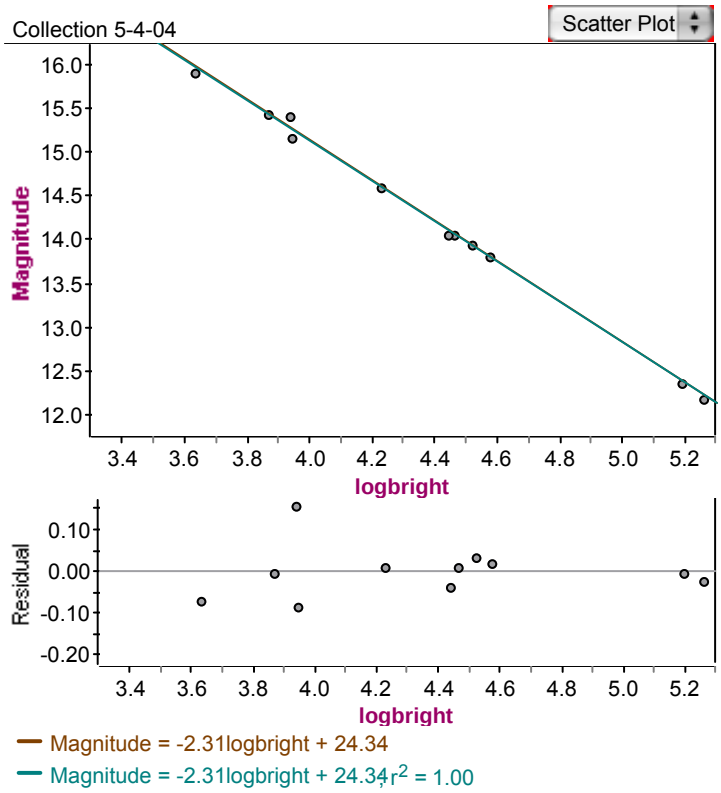
Collection 5-4-04
Scatter Plot
Magnitude
16.0
15.5
15.0
14.5
14.0
13.5
13.0
12.5
12.0
3.4 3.6 3.8 4.0 4.2 4.4 4.6 4.8 5.0 5.2
logbright
Residual
0.10
0.00
-0.10
-0.20
3.4 3.6 3.8 4.0 4.2 4.4 4.6 4.8 5.0 5.2
logbright
Magnitude = -2.31logbright + 24.34
Magnitude = -2.31logbright + 24.34; r2 = 1.00

Collection 5-4-04

	star	MagnituÉ	BrightnÉ	logbright
=				log (Brightne
1	A	14.060	28985	4.46217
2	B	15.890	4295	3.63296
3	C	12.360	155491	5.19171
4	D	14.600	16887	4.22755
5	E	15.410	8691	3.93907
6	F	13.950	33021	4.51879
7	G	13.810	37403	4.57291
8	H	15.160	8783	3.94364
9	I	14.060	27518	4.43962
10	J	12.180	182480	5.26122
11	Variable	15.422	7323	3.86469

Model of Collection 5-4-04 Simple Regression

Response attribute (numeric): Magnitude
Predictor attribute (numeric): logbright

Sample count: **11**

Equation of least-squares regression line:
Magnitude = -2.30605 logbright + 24.338
Correlation coefficient, r = **-0.998623**
r-squared = **0.99725**, indicating that **99.725**% of the variation in **Magnitude** is accounted for by **logbright** .

The best estimate for the slope is **-2.30605** +/- **0.0913479** at a **95** % confidence level. (The standard error of the slope is **0.0403809**.)

When **logbright** = **3.86469** , the predicted value for a future observation of **Magnitude** is **15.4258** +/- **0.164292**.

Collection 5-11-04

	star	MagnituÉ	BrightnÉ	logbright
=				log (Brightne
1	A	14.060	27287	4.43596
2	B	15.890	4337	3.63719
3	C	12.360	151739	5.1811
4	D	14.600	18504	4.26727
5	E	15.410	8882	3.94851
6	F	13.950	33961	4.53098
7	G	13.810	40644	4.609
8	H	15.160	8745	3.94176
9	I	14.060	30408	4.48299
10	J	12.180	189987	5.27872
11	Variable	15.472	7142	3.85382

Model of Collection 5-11-04 — Simple Regression

Response attribute (numeric): Magnitude
Predictor attribute (numeric): logbright

Sample count: **11**

Equation of least-squares regression line:
Magnitude = -2.30246 logbright + 24.350
Correlation coefficient, r = **-0.997752**
r-squared = **0.99551**, indicating that **99.551**% of the variation in **Magnitude** is accounted for by **logbright** .

The best estimate for the slope is **-2.30246** +/- **0.116622** at a **95** % confidence level. (The standard error of the slope is **0.0515535**.)

When **logbright** = **3.85382** , the predicted value for a future observation of **Magnitude** is **15.4772** +/- **0.211352**.

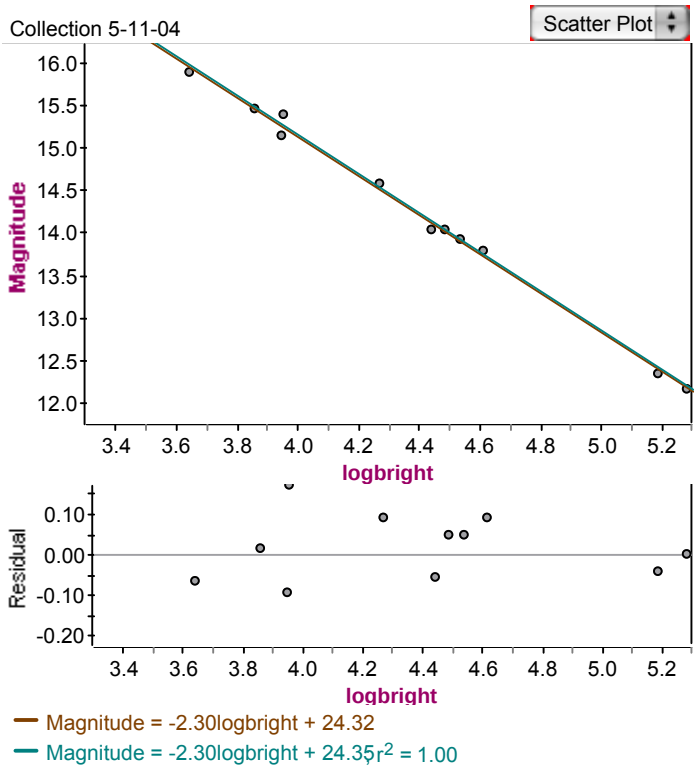
Collection 5-11-04
Scatter Plot
Magnitude
16.0
15.5
15.0
14.5
14.0
13.5
13.0
12.5
12.0
3.4 3.6 3.8 4.0 4.2 4.4 4.6 4.8 5.0 5.2
logbright
Residual
0.10
0.00
-0.10
-0.20
3.4 3.6 3.8 4.0 4.2 4.4 4.6 4.8 5.0 5.2
logbright
Magnitude = -2.30logbright + 24.32
Magnitude = -2.30logbright + 24.35
r2 = 1.00

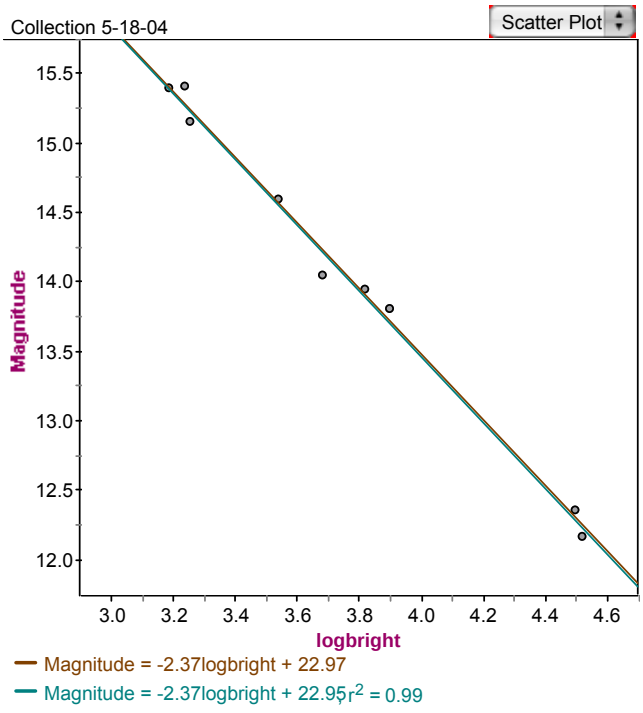
Collection 5-18-04
Scatter Plot
Magnitude
15.5
15.0
14.5
14.0
13.5
13.0
12.5
12.0
3.0 3.2 3.4 3.6 3.8 4.0 4.2 4.4 4.6
logbright
Magnitude = -2.37logbright + 22.97
Magnitude = -2.37logbright + 22.95
r2 = 0.99

Collection 5-18-04

	star	MagnituÉ	BrightnÉ	logbright
=				log (Brightne
1	A	14.060		
2	B	15.890		
3	C	12.360	31082	4.49251
4	D	14.600	3434	3.5358
5	E	15.410	1704	3.23147
6	F	13.950	6559	3.81684
7	G	13.810	7796	3.89187
8	H	15.160	1779	3.25018
9	I	14.060	4750	3.67669
10	J	12.180	32841	4.51642
11	Variable	15.404	1516	3.1807

Model of Collection 5-18-04 Simple Regression

Response attribute (numeric): Magnitude
Predictor attribute (numeric): logbright

Sample count: **9**

Equation of least-squares regression line:
Magnitude = -2.37017 logbright + 22.950
Correlation coefficient, r = **-0.996963**
r-squared = **0.99394**, indicating that **99.394**% of the variation in **Magnitude** is accounted for by **logbright** .

The best estimate for the slope is **-2.37017** +/- **0.165458** at a **95** % confidence level. (The standard error of the slope is **0.0699723**.)

When **logbright** = **3.1807** , the predicted value for a future observation of **Magnitude** is **15.4116** +/- **0.266145**.

Collection 5-27-04

	star	MagnituÉ	BrightnÉ	logbright
=				log (Brightne
1	A	14.060	15091	4.17872
2	B	15.890	2465	3.39182
3	C	12.360	80505	4.90582
4	D	14.600	8904	3.94959
5	E	15.410	4140	3.617
6	F	13.950	17795	4.2503
7	G	13.810	20257	4.30658
8	H	15.160	6561	3.81697
9	I	14.060	15046	4.17742
10	J	12.180	92139	4.96444
11	Variable	15.186	5182	3.7145

Model of Collection 5-27-04 Simple Regression

Response attribute (numeric): Magnitude
Predictor attribute (numeric): logbright

Sample count: **11**

Equation of least-squares regression line:
Magnitude = -2.38835 logbright + 24.072
Correlation coefficient, r = **-0.998027**
r-squared = **0.99606**, indicating that **99.606**% of the variation in **Magnitude** is accounted for by **logbright** .

The best estimate for the slope is **-2.38835** +/- **0.113305** at a **95** % confidence level. (The standard error of the slope is **0.0500869**.)

When **logbright** = **3.7145** , the predicted value for a future observation of **Magnitude** is **15.2006** +/- **0.191008**.

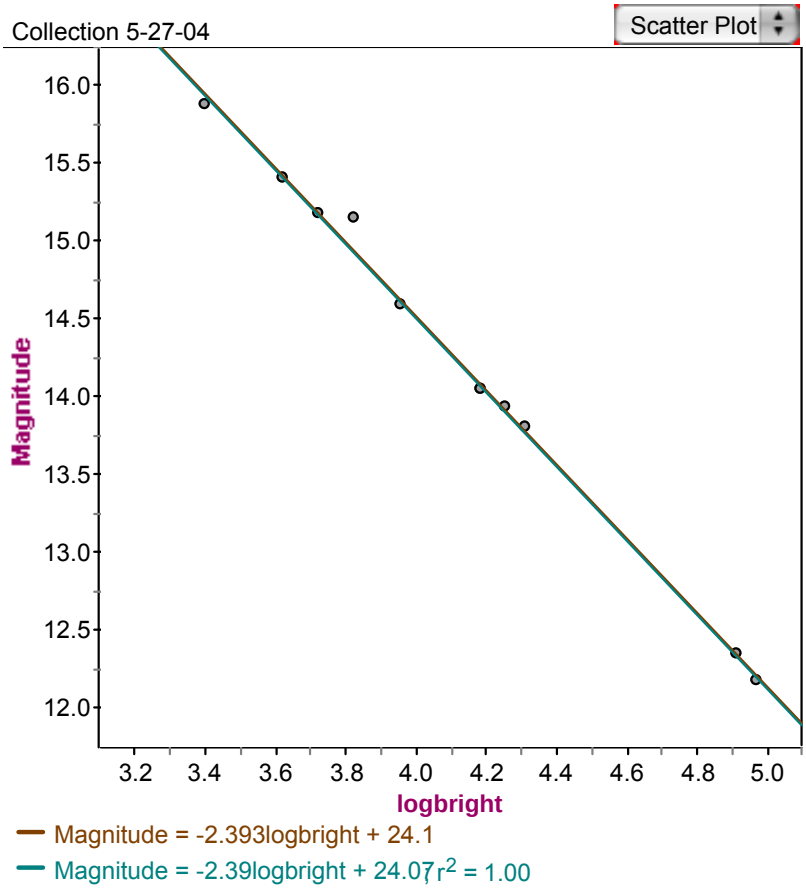
Collection 5-27-04
Scatter Plot
16.0
15.5
15.0
14.5
14.0
13.5
13.0
12.5
12.0
Magnitude
3.2
3.4
3.6
3.8
4.0
4.2
4.4
4.6
4.8
5.0
logbright
Magnitude = -2.393logbright + 24.1
Magnitude = -2.39logbright + 24.07, r2 = 1.00

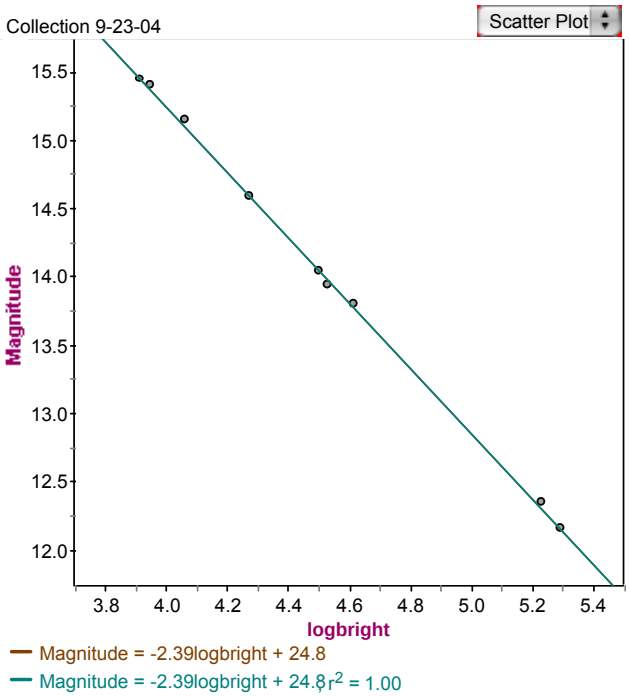
Collection 9-23-04
Scatter Plot
15.5
15.0
14.5
14.0
13.5
13.0
12.5
12.0
Magnitude
3.8
4.0
4.2
4.4
4.6
4.8
5.0
5.2
5.4
logbright
Magnitude = -2.39logbright + 24.8
Magnitude = -2.39logbright + 24.8, r2 = 1.00

Collection 9-23-04

	star	MagnituÉ	BrightnÉ	logbright
=				log (Brightne
1	A	14.060		
2	B	15.890		
3	C	12.360	166431	5.22123
4	D	14.600	18544	4.2682
5	E	15.410	8734	3.94121
6	F	13.950	33322	4.52273
7	G	13.810	40766	4.6103
8	H	15.160	11451	4.05884
9	I	14.060	31095	4.49269
10	J	12.180	194419	5.28874
11	Variable	15.459	8120	3.90956

Model of Collection 9-23-04 Simple Regression

Response attribute (numeric): Magnitude
Predictor attribute (numeric): logbright

Sample count:**9**

Equation of least-squares regression line:
Magnitude = **-2.38825** **logbright** + **24.808**
Correlation coefficient, r = **-0.999711**
r-squared = **0.99942**, indicating that **99.942**% of the variation in **Magnitude** is accounted for by **logbright** .

The best estimate for the slope is **-2.38825** +/- **0.0513518** at a **95** % confidence level. (The standard error of the slope is **0.0217167**.)

When **logbright** = **3.90956** , the predicted value for a future observation of **Magnitude** is **15.4706** +/- **0.0830231**.

Collection 10-26-04

	star	MagnituÉ	BrightnÉ	logbright
=				log (Brightne
1	A	14.060	17542	4.24408
2	B	15.890	3124	3.49471
3	C	12.360	85612	4.93253
4	D	14.600	10670	4.02816
5	E	15.410	5428	3.73464
6	F	13.950	20217	4.30572
7	G	13.810	23857	4.37762
8	H	15.160	7080	3.85003
9	I	14.060	18486	4.26684
10	J	12.180	103988	5.01698
11	Variable	15.238	6210	3.79309

Model of Collection 10-26-04 — Simple Regression

Response attribute (numeric): Magnitude
Predictor attribute (numeric): logbright

Sample count: **11**

Equation of least-squares regression line:
Magnitude = -2.4903 logbright + 24.671
Correlation coefficient, r = **-0.999306**
r-squared = **0.99861**, indicating that **99.861**% of the variation in **Magnitude** is accounted for by **logbright** .

The best estimate for the slope is **-2.4903** +/- **0.0700211** at a **95** % confidence level. (The standard error of the slope is **0.0309532**.)

When **logbright** = **3.79309** , the predicted value for a future observation of **Magnitude** is **15.2252** +/- **0.113864**.

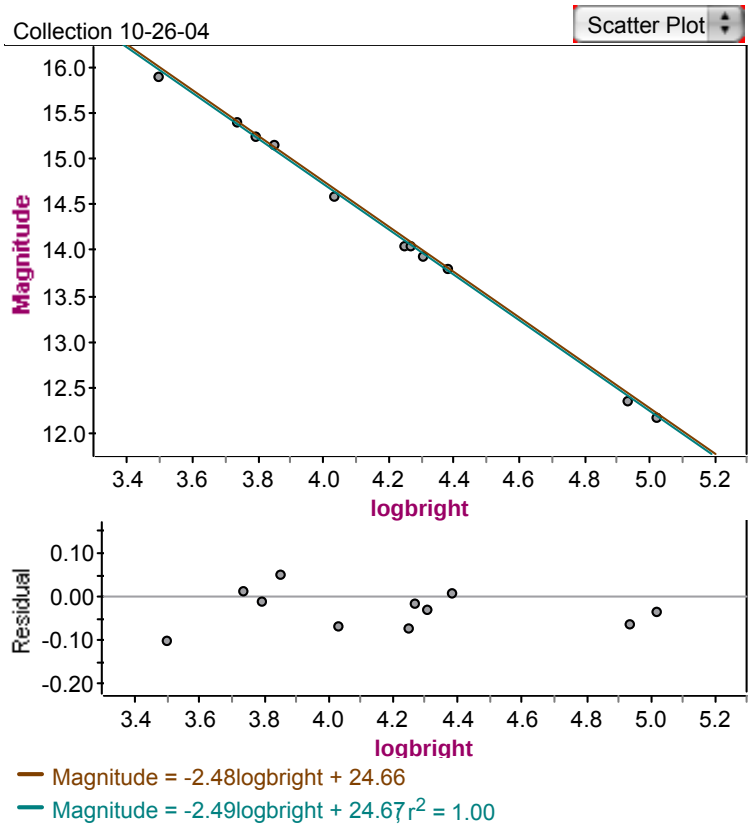

Collection SAW V1

	Date	J_date	MagnituÉ	Error
1	10/26/04	2453304	15.2252	0.1138640
2	9/23/04	2453271	15.4706	0.0830231
3	5/27/04	2453152	15.2006	0.1910080
4	5/18/04	2453143	15.4116	0.2661450
5	5/11/04	2453136	15.4772	0.2113520
6	5/4/04	2453129	15.4258	0.1642920
7	4/29/04	2453124	15.4836	0.1520200

Collection SAW V1
Scatter Plot
15.6
15.5
15.4
15.3
15.2
2453120
2453140
2453160
2453180
2453200
2453220
2453240
2453260
2453280
2453300
2453320
J date
Magnitude = a sin (k·Date + phi) + b

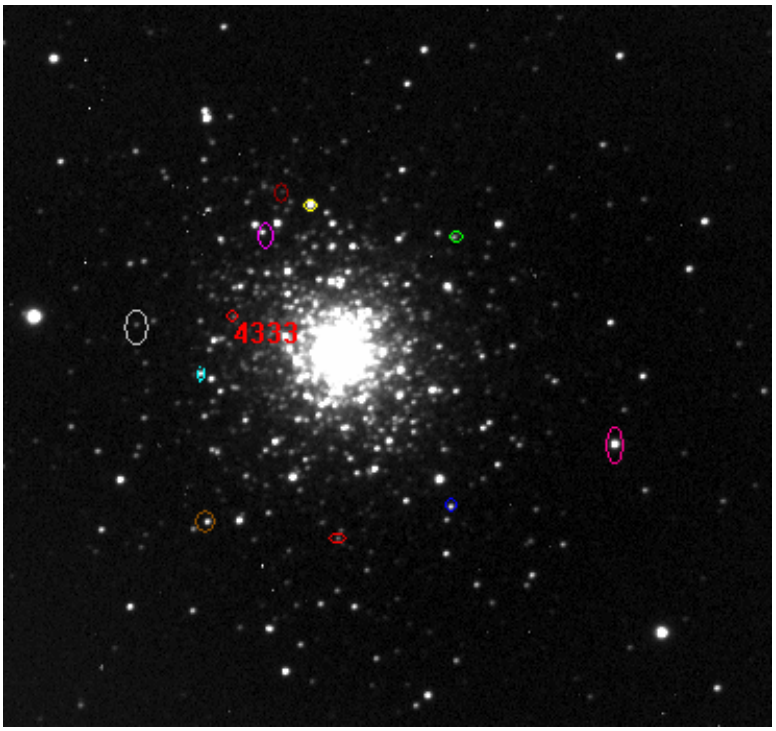

Letter	M 92 - Cl* NGC 6341	V	Color
A	Barn 111	14.06	Purple
B	Buon 57	15.89	Dk. Red
C	Barn 95	12.36	Yellow
D	Buon 111	14.60	Green
E	Buon 257	15.41	Grey
F	Barn 120	13.95	Lt. Blue
G	Buon 551	13.81	Brown
H	Buon 565	15.16	Red
I	Buon 545	14.06	Blue
J	Buon 488	12.18	Pink
Vari.	Saw v1	15.107	N/A variable

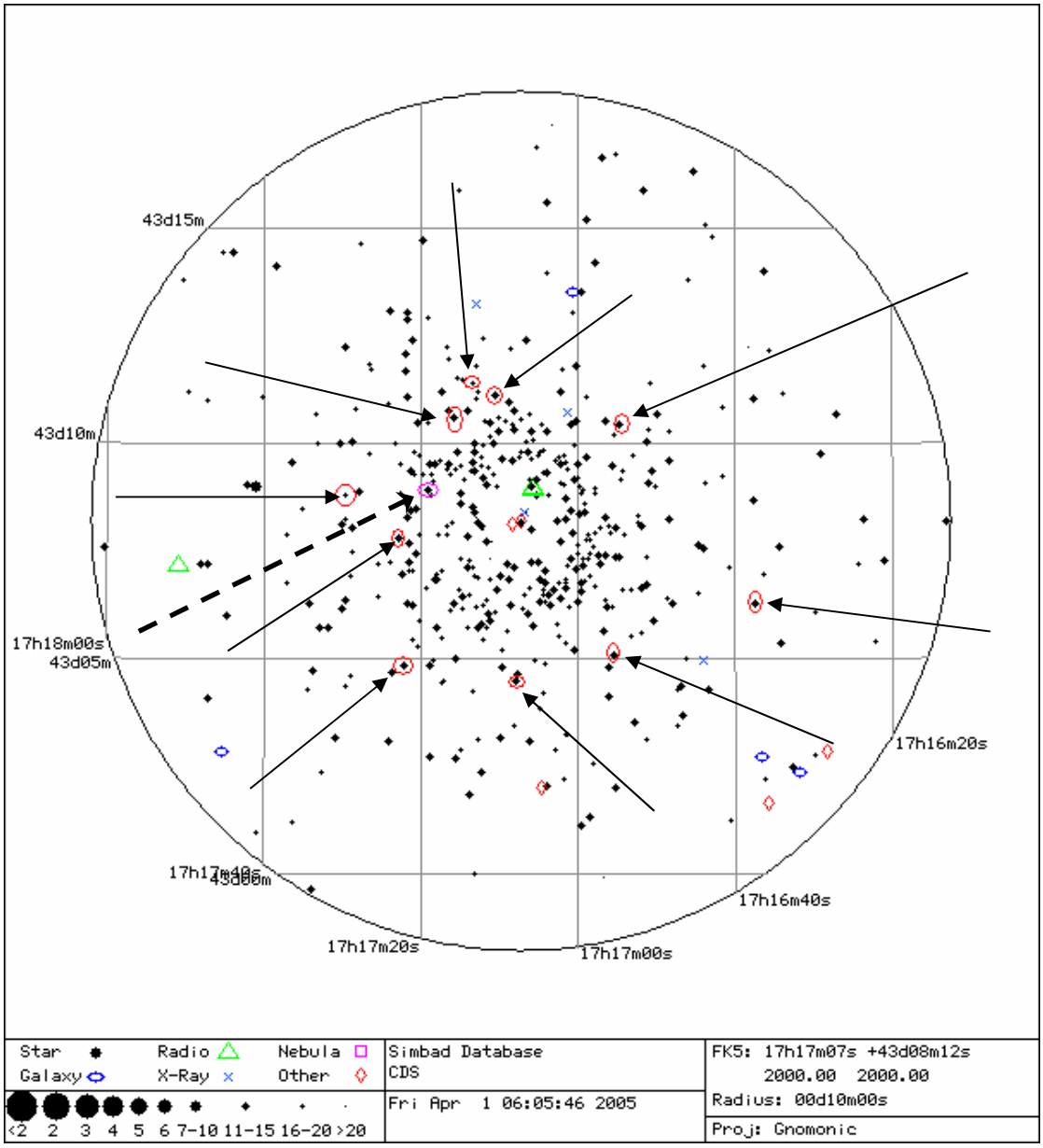
43d15m
43d10m
17h18m00s
43d05m
17h16m20s
17h17m40s
43d00m
17h16m40s
17h17m20s
17h17m00s
Star
Radio
Nebula
Galaxy
X-Ray
Other
<2 2 3 4 5 6 7-10 11-15 16-20 >20
Simbad Database
CDS
Fri Apr 1 06:05:46 2005
FK5: 17h17m07s +43d08m12s
2000.00 2000.00
Radius: 00d10m00s
Proj: Gnomonic

SUMMARY

After analysis, we have concluded that we have not discovered any novae. If we had, it would have been blatantly obvious. However, we used our data to verify our data is reliable. Fluctuations are greater than the probability of error; therefore, we certainly observed the variation of these stars. We checked our data against authenticated amplitudes and periods. Our measurements of SAN 39 in M3 demonstrated a shift in magnitude up to .717611 and M 92's SAW V1 had one of .283. On the matter of the periods, we have little evidence to support what was extrapolated. We have since discovered that the selected variables are of the RR Lyrae type, which have periods less than a day. It would be extremely difficult to attempt to find the correct periods because our observations are sporadic comparatively. We currently plan on doing a study on the micro-variability over the course of a single night, but our previous attempt has been thwarted due to a mechanical error. We will persevere and continue our research until the issues are completely dealt with.

ACKNOWLEDGEMENTS

This project was supported by TLRBSE. This group is running a School-Year Observing Program which has provided the time at NMSO in which we took our pictures to be analyzed. This project also sent us to Kitt Peak Observatory (*http://www.noao.edu/outreach/tlrbse/rct.html*).

NIH Image - *(http://rsb.info.nih.gov/nih-image/download.html*

Fathom 2.0 Beta - *(http://www.keypress.com/fathom/update.html)*

Hands on Universe Image Processing
(http://www.handsonuniverse.org/about_hou/index.html)

NMSkies - (www.telescope2.net) / *(www.nmskies.com)*

Simbad clickable star maps - *(http://simbad.u-strasbg.fr/sim-fid.pl)*

Recent Rediscovery in Variable Star, Z UMa

Kristina M. Olday, Naomi De Mott, Alysia Morgan Turcott
Burchell High School, Wasilla, Ak
Teacher: Tim Lundt, TLRBSE 2003

ABSTRACT

A group of students from Burchell High School were sponsored by TLRBSE to complete a research project on the spectra of variable stars. They were sent to Kitt Peak National Observatory in Tucson, Arizona, to make a more detailed study. They began observations on March 31, 2005 on the 0.9m Coude Feed refractor telescope located on KPNO, and finished on April 1, 2005. While observing, they made a rediscovery on the star, Z UMa. Hydrogen emission was found in the spectra, and had not been seen in the spectra in a very long time. No solid conclusions were made as to why we observed the hydrogen emission, only speculations. It is possible that the hydrogen emission results from the ejection of Z UMa's shell. Further study of Z UMa could possibly unravel that mystery.

INTRODUCTION

Variable stars are stars that can change in brightness, due to a variety of different reasons. Some examples of why these changes occur are: expansion and contraction of surface layers, outbursts of energy from either the surface layers or from deep within the star, eclipses or rotations due to the partner star in binary star systems, flares from the surface of the star (much like the solar flares witnessed from our own Sun). The changes in brightness vary greatly, and can range anywhere from a thousandth of a magnitude to twenty magnitudes. The periods, or time frames, of these changes vary just as much. One can observe changes within a fraction of a second, or several years down the road. Variable stars help to fill in many puzzle pieces of the origin and evolution of stars. Main sequence stars, like the Sun, are considered to be in the "prime" of their lives, like a human in the average adult phase of life. Most stars studied are in this stage.

Z UMa is a semi-regular variable star in the bowl of the Big Dipper, part of the large constellation Ursa Major. It is recognized as part of the M5 spectral type and III luminosity class. The magnitude of Z UMa can range anywhere from its brightest at 6.2 to as faint as 10.2. The mean magnitude of Z UMa happens to vary over time. Currently, the mean range if this star is from 7.2 to 8.9 magnitudes. The semi-regular periodicity of Z UMa results from several different pulsation periods within the star.

According to information found on the AAVSO website, Z UMa was discovered in 1904 by Dr. E. S. King of the Harvard College Observatory. What drew his attention to this variable star was its spectrum, which shows hydrogen emission lines. The spectrum also shows molecular absorption bands of titanium oxide (TiO). These two together in the same spectrum are quite odd, and quite rare. Hydrogen absorption is usually present in these stars, while much cooler temperatures are needed to form molecules in a star, such as the TiO found in Z UMa.

RESEARCH

Research done on Z UMa was mainly through the Internet, where the AAVSO website was the main contributor of information. The TLRBSE group from Burchell High School were studying the spectra of variable stars at Kitt Peak Observatory working on the Coude Feed telescope when they made a discovery. The hydrogen found in Z UMa had not been seen in the spectra of the star in quite some time, as pointed out by astronomer Steve Howell.

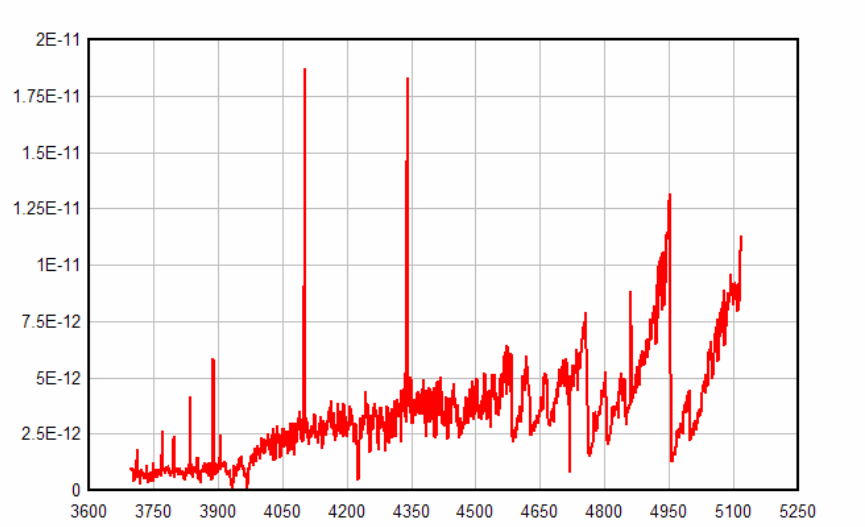

Fig. 1: This is a spectrum of Z UMa taken March 31, 2005 at Kitt Peak National Observatory by the BHS student group. It was taken using a blue grating setting on a 0.9-meter telescope. One can see the TiO molecules quite clearly (shown in wavelength 4951), as well as the hydrogen emission in H delta and H beta.

Element or Molecule Present	Spectral Line
Hydrogen Delta	4101.076
Calcium I	4226.511
Hydrogen Gamma	4340.495
Hydrogen Beta	4860.887
Titanium Oxide	4951.179

Table 1: This is a list of the five strongest lines in the spectra of Z UMa above. The calcium I is an absorption line located between the hydrogen delta and hydrogen gamma lines.

When Dr. E. S. King found hydrogen emission in Z UMa, the star had been believed to be at a peak in its cycle. The BHS student group believes that Z UMa is currently at another peak in its cycle, which lasts roughly 196 days, but can vary greatly over time.

OBSERVATIONS

The TLRBSE group from Burchell High School observed variable stars at Kitt Peak National Observatory on March 31, 2005, and April 1, 2005. They studied the variable stars on the 0.9-meter Coude Feed telescope. The first night of observation, they used a blue grating to record spectra, and on the second night they used a red grating. On April 1 (their second night at KPNO), while observing, they broke the Teacher Observing Project record of 72 stars observed in one night by observing 73 stars.

All the data reduction from the spectra obtained from the two nights of observations was completed by Steve Howell, a TLRBSE staff member. He also assisted the Burchell student group in their study.

RESULTS

Many questions are raised when you examine the fact that, on more than one occasion, hydrogen emission was seen in the star during a cyclic peak, and only during a cyclic peak. What does it mean? One possibility is that Z UMa, nearing the end of its life span, is ejecting a shell at the peak of each brightness cycle.

CONCLUSION

The TLRBSE-sponsored Burchell High School student group was not able to come to any solid conclusions as to why one can only see hydrogen gamma at certain cyclic peaks in the spectra of the semi-regular variable star Z UMa. It is thought that with much further study and dedication to this star, one can possibly find out just exactly what is going on inside Z UMa. Perhaps soon, with concentrated observation, this unusual variable star will not be so much of a mystery.

RESOURCES

http://aa.usno.navy.mil/publications/AstroAlmanac/variables98.html/

http://www.aavso.org/

http://www.astro.uiuc.edu/~kalen/sow/spectra.html

http://www.daviddarling.info/encyclopedia/ETEmain.html/

Brosius, Dr. Jeffery W.; "How Astronomers Use Spectra to Learn About the Sun and Other Stars"

http://www.noao.edu/

http://www.space.com/

Rector, Travis A.; TLRBSE; "Stellar Spectroscopy: The Message of Starlight"; National Optical Astronomy Observatory. September 19, 2001.

Howell, Steve and Croft, Steven; "TLRBSE Research Project: Spectroscopy of Variable Stars: Content Background for Stellar Evolution and Variable Star Research; National Optical Astronomy Observatory

http://wise-obs.tau.as.il/~eran/Wise/Util/Sncalc.html/

The Correlation Between Sunspots and Solar Flares

Samantha J. Breedlove and Leslie A. Curtis
Graves County High School, Mayfield, KY
Teacher: Velvet Dowdy, TLRBSE 2003

ABSTRACT

This paper addresses the extent of the relationship between sunspots and solar flares. We measured approximately one year's worth of sunspots by calculating their area to find out the amount of activity and we used solar flare information already collected by the National Geophysical Data Center to compare to. After putting this information in graphical form we concluded there was a clear correlation between sunspot and solar flare activity.

INTRODUCTION

The Sun's surface, the photosphere, is where sunspots are found and appear as dark areas that are usually about 1800 K cooler than their surroundings. A typical diameter for a large sunspot is around 32,000 km, though small sunspots – called pores – may have a diameter of only a few hundred km. These spots speckle the photosphere more or less constantly, the larger ones lasting for months, and the smaller ones for only a few hours. Where the sunspots occur and how many exist is dictated by an eleven-year sunspot cycle. At the cycle's start, the sunspots multiply and creep closer to the equator until – at the height of the cycle – they've reached their greatest number and have come within 5° of the equator. After that the sunspots begin to die off, particularly the ones furthest from the equator. The cycle ends with a minimum of sunspots before starting over again (Levine). The standard theory suggests that sunspots are created by changes in the solar magnetic field.

The flow of plasma in the sun's convection zone actually creates the Sun's magnetic field. The sun rotates faster at its equator than its poles, and therefore its magnetic fields run east to west as the sun turns. This stretching out inhibits convection, allowing a spot on the Sun to cool – and thus, a sunspot is born (Hathaway). Other recorded instances, such as the poles changing every eleven years, give support that a relationship exists between sunspots and the solar magnetic field. Yet the exact relationship between sunspots and the solar magnetic field remains unclear.

While sunspots are interesting phenomenon in their own right, another occurrence on the Sun has also captured the attention of many scientists: solar flares. A flare is defined as a sudden, rapid, and intense variation in brightness. A solar flare occurs when magnetic energy that has built up in the solar atmosphere is suddenly released. This magnetic energy is released as radiation that varies along the entire electromagnetic spectrum. The first solar flare recorded in astronomical literature was on September 1, 1859.

As the magnetic energy is being released, particles, including electrons, protons, and heavy nuclei, are heated and accelerated in the solar atmosphere. The energy released during a flare is typically around 1027 ergs per second. Large flares can emit up to 1032 ergs of energy. This energy is ten million times greater than the energy released from a volcanic explosion.

On the other hand, it is less than one-tenth of the total energy emitted by the Sun every second (The Corona).

There are typically three stages to a solar flare. First is the precursor stage, where the release of magnetic energy is triggered. Soft x-ray emission is detected in this stage. In the second or impulsive stage, protons and electrons are accelerated to energies exceeding 1 MeV. During the impulsive stage, radio waves, hard x-rays, and gamma rays are emitted. The gradual build up and decay of soft x-rays can be detected in the third, decay stage. The duration of these stages can be as short as a few seconds or as long as an hour (Classification of x-ray Solar Flares).

Solar flares originate in the Sun's corona. The corona is the outermost atmosphere of the Sun, consisting of highly rarefied gas. This gas normally has a temperature of a few million degrees Kelvin. Inside a flare, the temperature typically reaches 10 or 20 million degrees Kelvin, and can be as high as 100 million degrees Kelvin (Solar flare resources). The corona is not uniformly bright, but is concentrated around the solar equator in loop-shaped features. These bright loops are located within and connect areas of strong magnetic field called active regions. It has been found that sunspots are located within these active regions, along with the occurrences of solar flares (The Corona).

The frequency of flares indicates that it coincides with the Sun's eleven year cycle. When the solar cycle is at a minimum, active regions are small and rare and few solar flares are detected. These increase in number as the Sun approaches the maximum part of its cycle.

As distant as they may seem, solar flares have a direct effect on the Earth's atmosphere. As a result of the intense radiation: The Earth's upper atmosphere becomes more ionized and expands, long distance radio signals can be disrupted by the resulting change in the Earth's ionosphere, a satellite's orbit around the Earth can be disturbed by the enhanced drag on the satellite from the expanded atmosphere, satellites' electronic components can be damaged.

As both solar flares and sunspots are activity generated by the Sun, one would assume that there must be a correlation between the two activities, even though, the exact source from where they are generated might differ.

The purpose of our project is to more accurately determine the relationship between sunspot and solar flare activity.

OBSERVATION AND DATA REDUCTION

Observations made from the Kitt Peak Vacuum Telescope were implemented in our process of collecting data. With a disk loaned by instructor Mrs. Velvet Dowdy, the group was able to access images of the sun from August 2000 to September 2001. The data on the disk was made available by funding from NOAO, NSF, and ALLRA. Using the images to calculate first the daily sunspot activity by using the program Scion Image, then to calculate sunspot area, then using Microsoft Excel, the data was input for every day from August to September and thus the calculation was made tabulating the amount of sunspot activity monthly.

ANALYSIS AND RESULTS

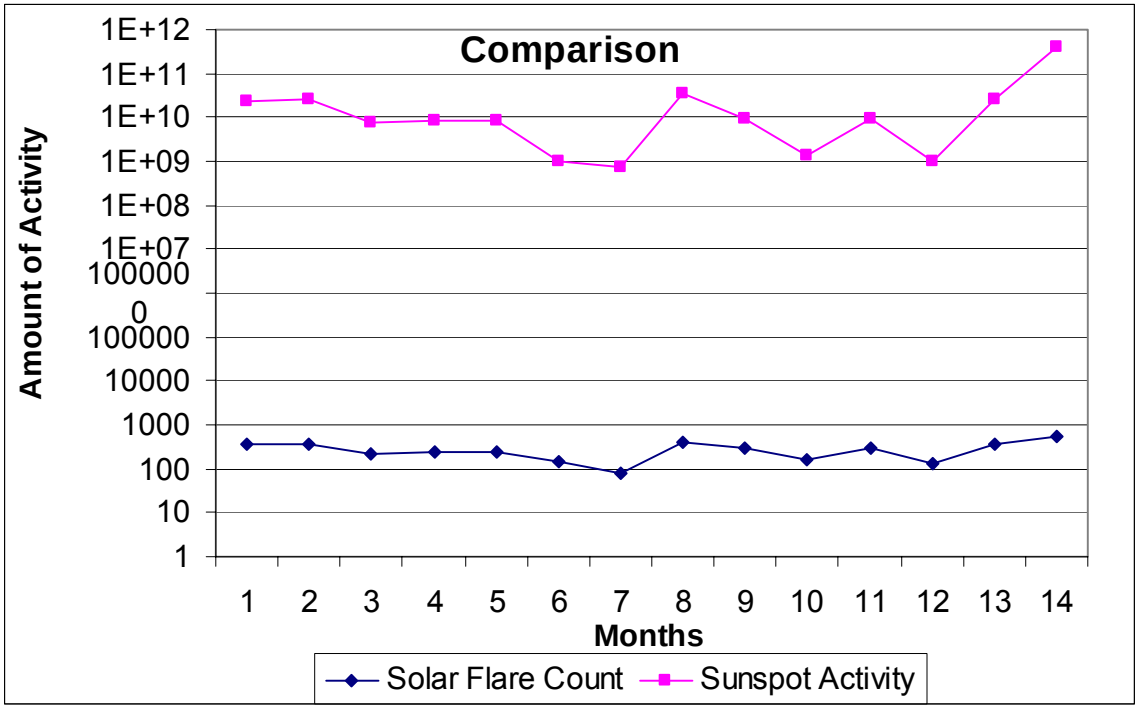

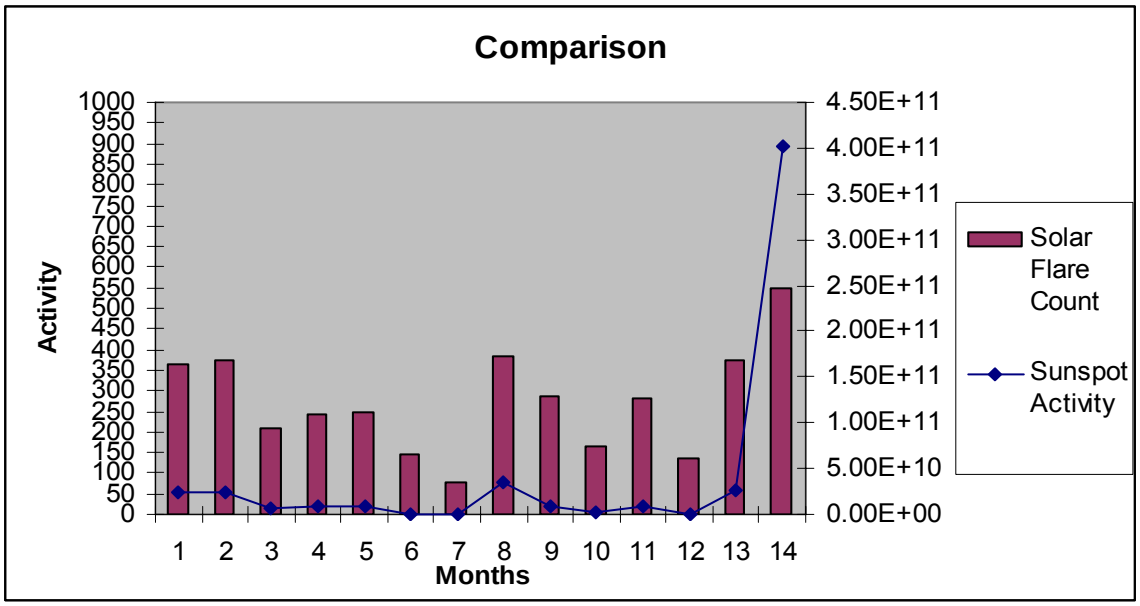

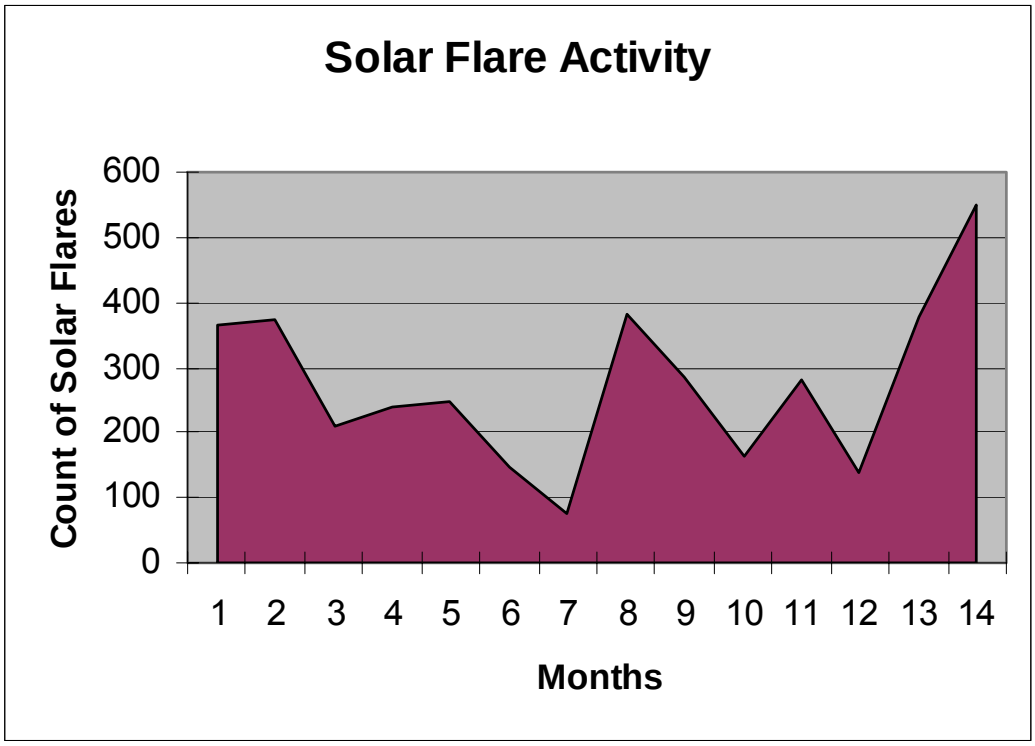

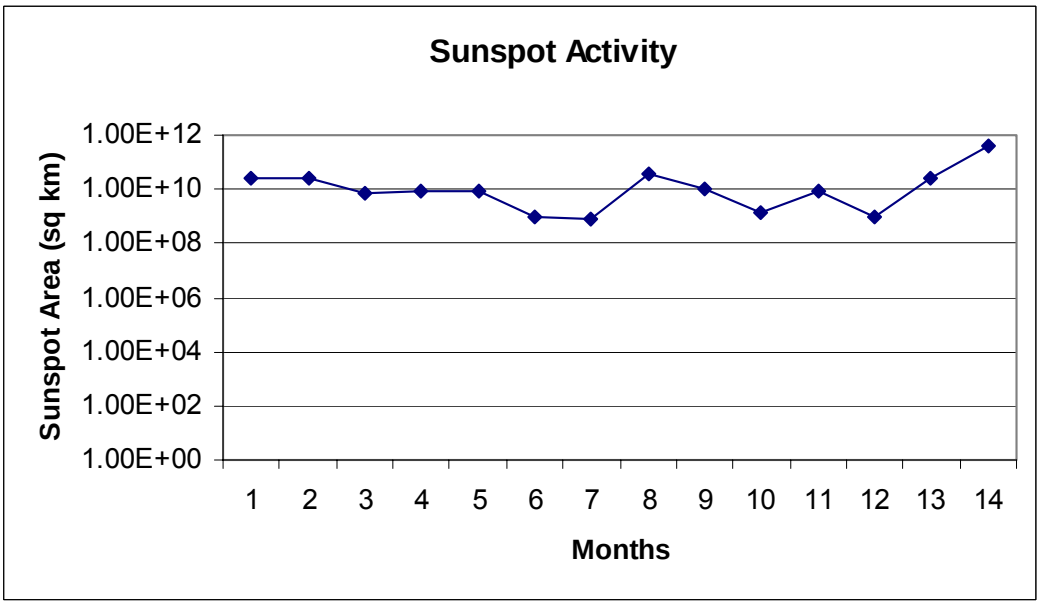

DISCUSSION

After compiling the data of sunspot and solar flare activity the result was an indicated relationship between the two events, as seen in the graph with both sets of data.

Because the research was focused only upon finding the graphical correlation between sunspots and solar flares, a conclusion about the causes of these events cannot be reached through our research. In addition to that problem, it was also possible the results may have

been altered by the addition and collection of data from the Scion Image program through the measurements of each sunspot on all the days of data collection. While typing and inputting data into Microsoft Excel there might have been a numerical error and it could have thus altered the outcome of the project.

Another obstacle we had to overcome was the origin of our original research question. In the amount of time we had allotted to us, we were originally going to compare sunspot and coronal loop activity; however, as data could not be found for coronal loops we had to change our topic to cover solar flares instead.

In order to carry out our project we depended heavily on the data we found from the National Geophysical Data Center. Because of this, it might be that our results were incorrect or slightly off because that data may be incorrect.

SUMMARY AND ACKNOWLEDGEMENTS

Analysis and data from the National Geophysical Data Center and our compilation of data from the program and images from Scion Image demonstrated that there was a correlation between sunspot and solar flare activity.

We wish to thank Mrs. Velvet Dowdy for her time and patience explaining the programs and data we were finding and also in the implementation of the data. For further research one might study the areas of x-ray or gamma ray effects of each of these events and how they affect the earth.

REFERENCES

"Solar indices." Space Weather Data. National Weather Service. 29 Jan. 2006 <*http://www.sec.noaa.gov/ftpdir/indices/old_indices/2005Q1_DSD.txt*>.

Phillips, Dr. Tony. "Space Weather News." News and Information about the Sun-Earth environment. Space Weather. 26 Jan. 2006 <*http://www.spaceweather.com/*>.

Hathaway, Dr. David H. "Solar Physics." The Sunspot Cycle. 25 Nov. 2005. Marshall Space Flight Center. 21 Jan. 2006 <*http://science.nasa.gov/ssl/pad/solar/sunspots.htm*>.

"The Corona." Surfing for Sunbeams: About the Corona. 2001. Yohkoh Public Outreach Project. 21 Jan. 2006 <*http://solar.physics.montana.edu/YPOP/Spotlight/Tour/loops2.html*>.

Hamilton, Calvin J., Coronal Loop Animation. 1995. Views of the Solar System. 21 Jan. 2006 <*http://www.solarviews.com/cap/sun/vtrace01.htm*>.

Levine, Randolph H. "Sun," Microsoft® Encarta® Online Encyclopedia 2005 <*http://encarta.msn.com*> © 1997-2005 Microsoft Corporation (Levine)

Our Star. Mar. 1996. Solar & Heliospheric Observatory. 03 Mar. 2006 <*http://www.cosmiclight.com/imagegalleries/sun.htm*>. Solar index graphs. Solar Influences

Data Analysis Center. 27 Jan. 2006 <*http://sidc.oma.be/sunspot-index-graphics/sidc_graphics.php*>.

"Classification of x-ray Solar Flares." "Solar Flare Alphabet Soup". Space Weather. 27 Jan. 2006 <*http://www.spaceweather.com/glossary/flareclasses.html*>.

"Solar Flares." Solar Data. National Oceanic and Atmospheric Administration. 27 Jan. 2006 <*ftp://ftp.ngdc.noaa.gov/STP/SOLAR_DATA/SOLAR_FLARES/XRAY_FLARES/xray.fm*>.

Resources-Solar Flares. Independence Planetarium. 27 Jan. 2006 <*http://planet.esuhsd.org/resources/photos_jpg/solar_flares.jpg*>.

Sunspot Activity and Amount of Atlantic Hurricanes

Aimée Michaud, Eric Dubois, and Joey White
Biddeford Middle School, Biddeford, ME, Grade 8
Teacher: Barbara A. Fortier, TLRBSE 2004

ABSTRACT

A correlation between the annual number of sunspots and the annual number of hurricanes in the Atlantic Ocean was analyzed. A study of the number of sunspots showed a solar cycle pattern every 11 years from 1955 to 2004. Analysis of the number of hurricanes in the Atlantic showed fluctuation, not comparable to the sunspot cycle. It was therefore determined that a relationship between the annual number of sunspots and the annual number of hurricanes in the Atlantic Ocean could not be verified.

INTRODUCTION

A relationship was examined from 1955 to 2004 between yearly sunspots numbers and the yearly number of hurricanes in the Atlantic Ocean. Over the past 50 years there have been more than 429 hurricanes, with the average being 8.58 hurricanes per season. The normal hurricane season is from June 1st to November 30 of each year. According to the research, there are an average number of 77.956 sunspots per year.

The relationship between sunspot activity and hurricanes was studied. Hurricanes can be strengthened during the day, suddenly, if solar activity is high or if flares occur. Whenever a hurricane is building, it appears that they receive their energy from the warm waters beneath them. In monitoring solar activity, it seems that hurricanes can be heated from above, as well as from below, making it seem that there is a relationship between the two.

The Sun has solar cycles that repeat approximately every 11 years. The discovery of the Sun's cycles started with the discovery of sunspots. A sunspot is a region on the sun's surface (photosphere) that are cooler dark regions of the sun, that sometimes grow to several times the size of earth and then fade away. When sunspots increase in size, the amount of radiation from the sun also increases. This makes earth receive more energy from the sun. When the earth receives more energy from the sun, the theory is that this affects the weather. When there are more sunspots, the sun is decaying more quickly and is giving off more heat.

In 1848, the Swiss astronomer Johann Rudolph Wolf introduced a daily measurement of sunspot numbers. His method, which is still used today, counts the total number of spots visible on the face of the Sun and the number of groups into which they cluster, because neither quantity alone satisfactorily measures sunspot activity.

In regards to hurricanes, there are three terms generally used to describe a hurricane season: frequency, intensity and activity. Hurricane frequency refers to the number of hurricanes that occur. Hurricane intensity is a measure of the strength or maximum wind speed of a hurricane. Hurricane activity is the term used by the National Hurricane Center that encompasses both the frequency and intensity of hurricanes in a season. Additionally, there are different categories

of storms based on their intensity. Hurricanes develop from weaker systems, called tropical storms that have maximum sustained wind speeds of 35-73 mph. All such tropical storms are given names, but not all tropical storms intensify to hurricane strength. The intensity of a hurricane is described based on the Saffir-Simpson Scale. These storms have maximum sustained wind speeds of 74 mph or higher.

OBSERVATIONS AND DATA REDUCTION

Data of annual hurricane numbers in the Atlantic Ocean was obtained from the National Hurricane Center, while data on the yearly number of sunspots was gathered from the Sunspot Index Data Center.

The data was compiled into graphs using Create-a-Graph Software and Microsoft Excel. The first graph (see Figure 1) shows the yearly number of sunspots from 1955 to 2004. The second graph (see Figure 2) shows the yearly number of hurricanes from the same time period. A third graph was created to show both the yearly number of sunspots and the yearly number of Atlantic hurricanes (see Figure 3). Because a conclusion still could not be absolutely determined, a scatter plot was created using Microsoft Excel that compared the independent variable of sunspots on the x axis with the number of Atlantic hurricanes on the y axis (Figure 4).

The graphs were analyzed to determine, if indeed, a relationship between sunspots and the number of hurricanes in the Atlantic does, in fact, exist.

ANALYSIS AND RESULTS

Fig. 1. Graph showing average number of sunspots for 1955-2004.

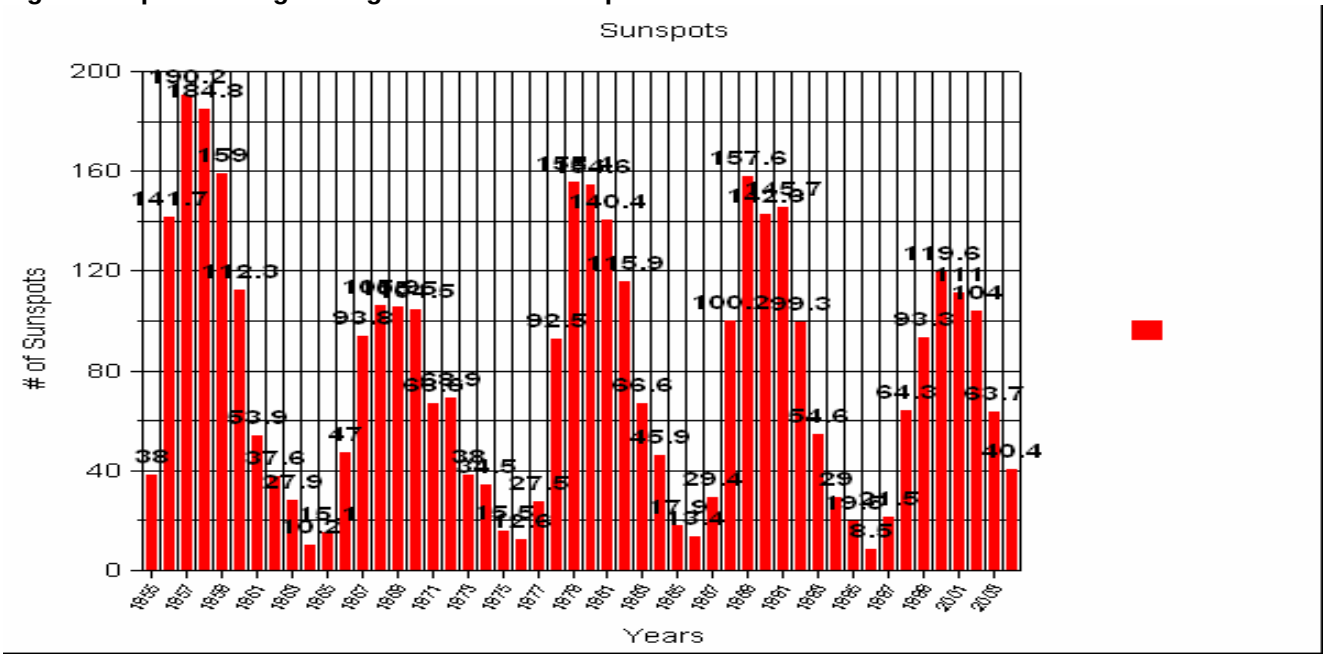

Fig. 2. Graph showing number of Atlantic hurricanes from 1955-2004.

Fig. 3. Graph showing the comparison of the number of sunspots and the number of hurricanes in the Atlantic from 1955-2004

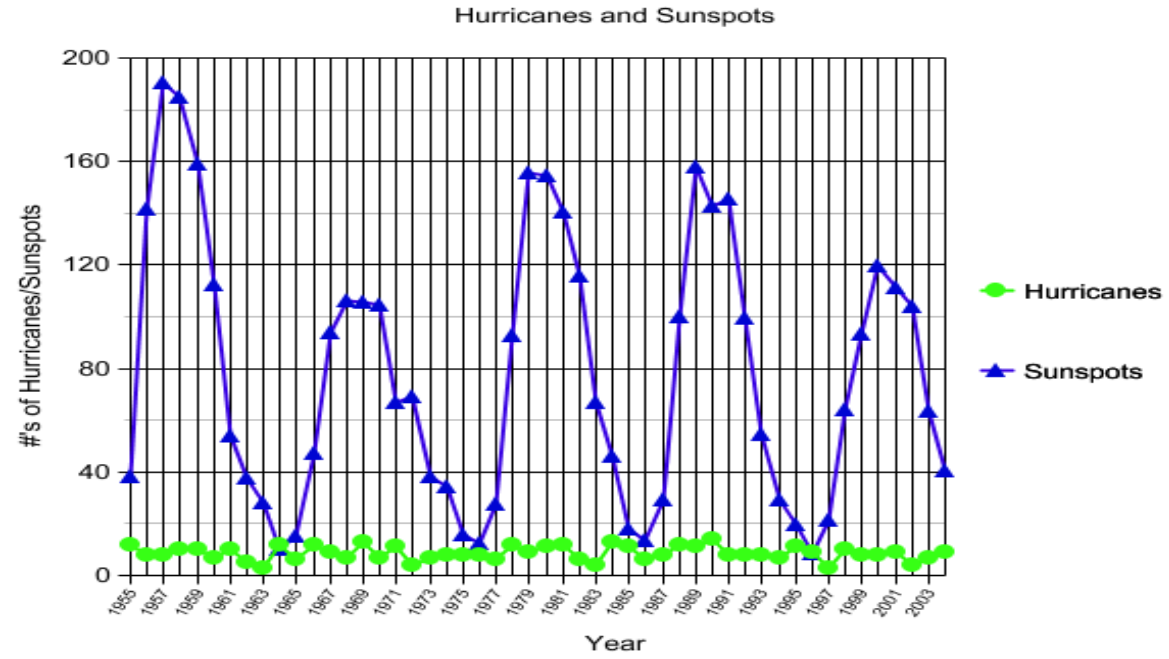

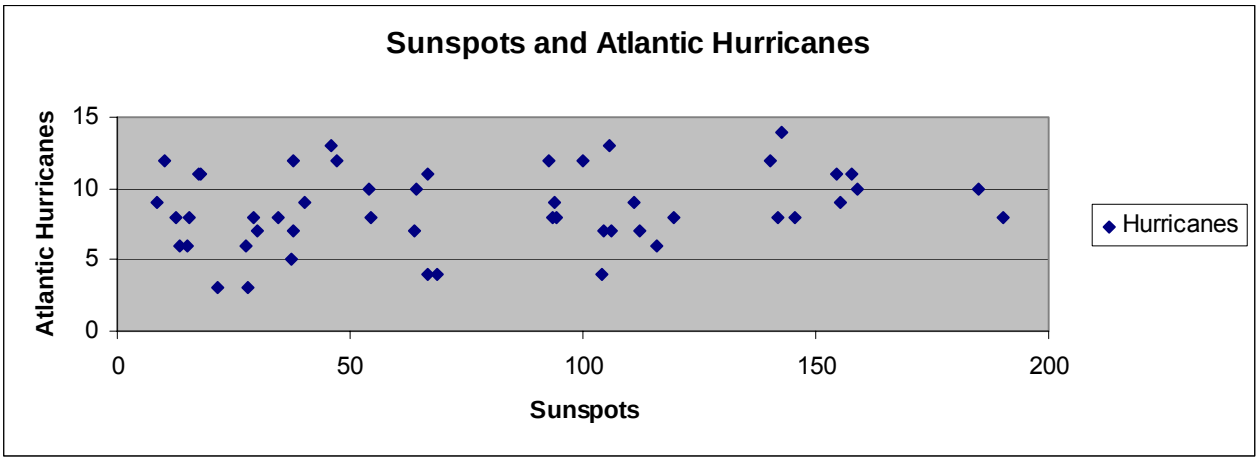

Fig. 4. Graph comparing annual sunspot number and the number of Atlantic hurricanes from 1955-2004.

DISCUSSION

After comparing the data in Figures 1, 2, and 3, it appeared there was no definite relationship between the number of sunspots and the number of hurricanes in the Atlantic Ocean from 1955 to 2004. To be absolutely certain, a scatter plot was constructed to directly compare the number of sunspots with the number of Atlantic hurricanes. When this scatter plot was analyzed, the data points were seen to be completely random and no linear correlation could be determined. Although some prior research suggested that there may have been some relationship between sunspots and the intensity of hurricanes, this research project focused on sunspots and the number of hurricanes in the Atlantic.

Further study may show that sunspots have an indirect role in the number of hurricanes in the Atlantic Ocean. This indirect role could be that the number of sunspots affects the jet stream temperature, sea surface temperatures, or climate, which in turn may have an effect on the number of hurricanes in the Atlantic.

SUMMARY AND ACKNOWLEDGEMENTS

Analysis of data from the National Hurricane Center and the Sunspot Index Data Center determined that a relationship between the number of sunspots and the number of hurricanes in the Atlantic Ocean does not exist.

We wish to acknowledge and thank our mentors, Mrs. Dubois, Mrs. Michaud, and Mrs. White for their guidance, assistance, and support. Without them and their time, we would have struggled even more than we did in completing this project.

Lastly, we would like to extend a special thank you to Connie Walker of the National Optical Astronomy Observatory for her patience and assistance in helping us with our data analysis.

REFERENCES

"Are Hurricanes Becoming Stronger And More Frequent?" [Online] Available *http://www.windows.ucar.edu/tour/link=/earth/climate/hurricaneclimate.html,* September 14, 2005

"Create a Graph." [Online] *http://nces.ed.gov/nceskids/createagraph/index.asp,* April 3, 2004.

"Heliometeorology" [Online] *www.grandunification.com/hypertext/Heliometeorology.html,* October 8, 1997.

"Hurricanes."[Online] *http://hurricanes.noaa.gov,* August 4, 2005.

"Hurricanes." [Online] *www.nhc.noaa.gov*, November 28, 2005.

"Hurricane Season Tropical Cyclone Reports" [Online] Available *www.nhc.noaa.gov/pastall.shtml,* April 14, 2005.

"Sunspot Index Data Center." [Online] *http://sidc.cma.be/index.php3,* January 6, 2004.

"Weather." [Online] *www.wunderground.com,* November 30, 2005.

Sunspots and the Annual Snowfall Amount on Mt. Washington, NH

Nate Lessard
Biddeford Middle School, Biddeford, ME, Grade 8
Teacher: Barbara A. Fortier, TLRBSE 2004

ABSTRACT
A relationship between the annual amount of snowfall on Mt. Washington, New Hampshire, and the annual amount of sunspots from 1935-2004 was studied. To find information about this topic, data was collected from weather observers on the summit of Mt. Washington and from the Sunspot Index Data Center. The data was graphed and analyzed, and it was determined that a relationship does not exist.

INTRODUCTION
A relationship between the annual amount of snowfall on Mt. Washington, New Hampshire and the annual amount of sunspots from 1935-2004 was studied. It was noted that the snowfall amounts varied from a low of 126.7 inches in 1941 to a high of 495.2 inches in 1969 with an average of 306.3 inches of snowfall per year. The average annual sunspot number for those same years was 262.6.

Sunspots are spots on the sun that are cooler than the surrounding area. Most large sunspots are planet-sized. Sunspots are divided into two parts, the outer section is called the penumbra and the darker, inner section, is called the umbra. Most of them are about 6,700 degrees Fahrenheit, while the surrounding area of the sun is about 10,000 degrees Fahrenheit. Even though these spots seem dark, they are actually bright. Sunspots are prime areas for solar flares, which cause solar storms. It is these solar storms that may affect the snowfall on Mt. Washington.

Other scientists have studied this topic. Some of the scientists say that there is a relationship between snowfall amounts and sunspot numbers, while other scientists say there is no relationship. Scientist Dr. Sami Solanki, the director of the renowned Max Planck Institute for Solar System Research in Gottingen, Germany, has studied the sun to see what effect sunspots may have on Earth, like global warming. Global warming might have an effect on the annual snowfall amounts on Mt. Washington.

It was hypothesized that there will not be a relationship between the two sets of data because sunspot numbers increase and decrease in an 11-year cycle while snowfall amounts can vary widely from year to year.

OBSERVATIONS AND DATA REDUCTION
The yearly average sunspot numbers for the years 1935-2005 were gathered from the Sunspot Index Data Center. The yearly average sunspot number was used for this study instead of a seasonal average because, on Mt. Washington, it snows in every month of the year.

Annual snowfall amounts on Mt. Washington for the years 1935-2004 were obtained from Jim Salge of the Mt. Washington Observatory. Of the 70 years that were analyzed, all had snowfall amounts that were greater than 150 inches, but none exceeded 495 inches. Annual snowfall amounts and average annual sunspot numbers for the years 1935-2004 were graphed for analysis using Microsoft Excel. The data was then analyzed to determine if, indeed, a relationship between yearly sunspot number and snowfall amount on Mt. Washington, New Hampshire exists.

ANALYSIS AND RESULTS

Fig. 1. Graph showing average annual number of sunspots and annual amount of snowfall on Mt. Washington from 1935-2004.

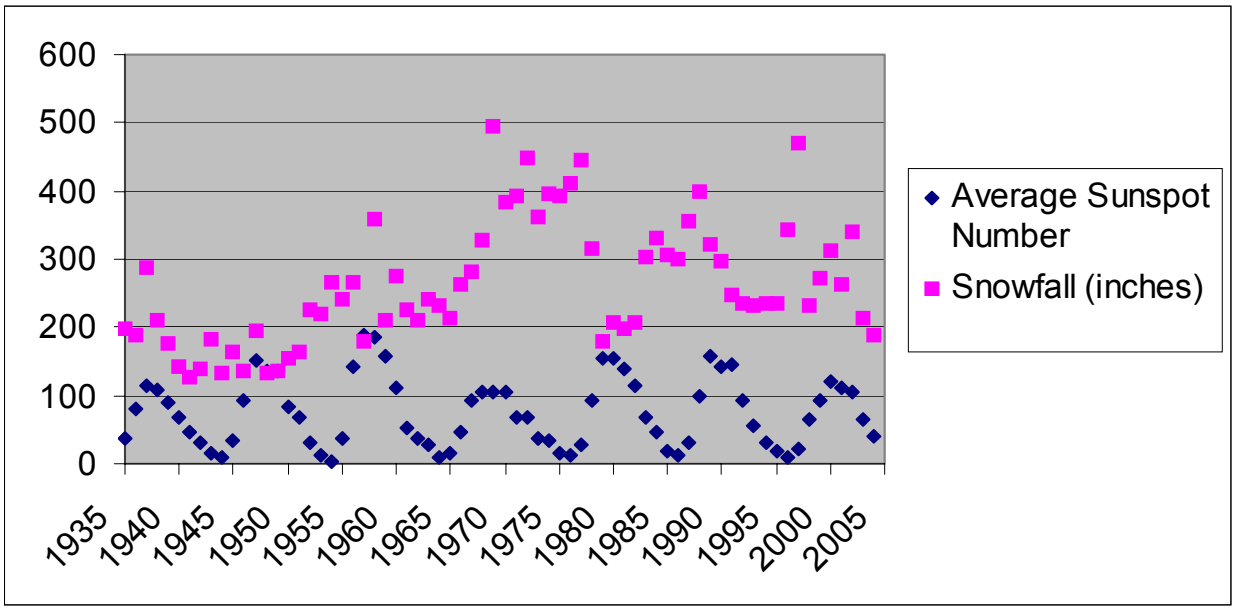

Fig. 2. Graph correlating average annual sunspot number with annual snowfall amounts on Mt. Washington from 1935-2004.

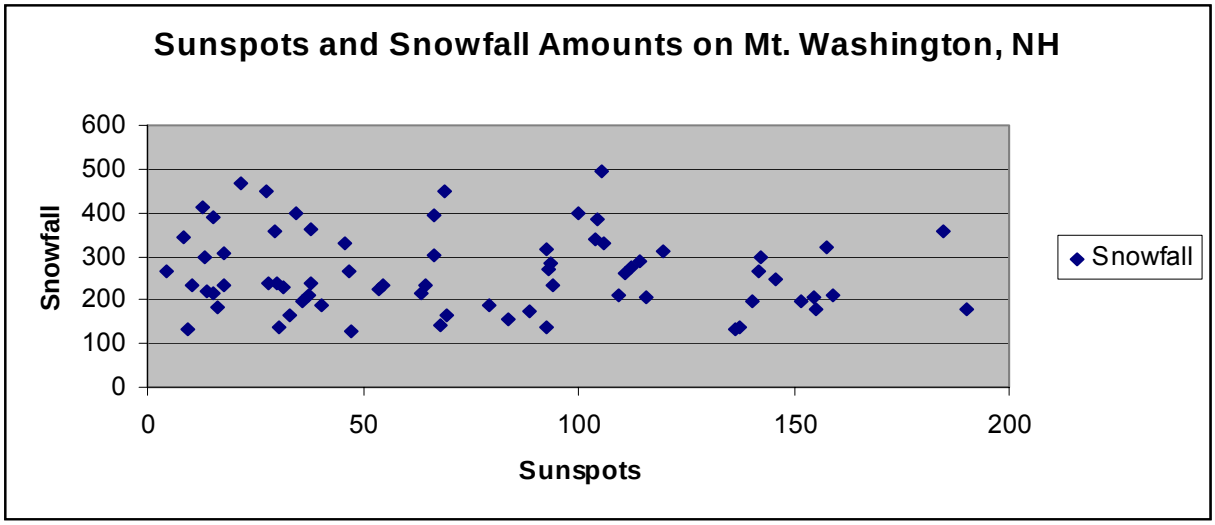

DISCUSSION

After comparing the data sets of yearly snowfall amounts on Mt. Washington from Jim Salge of the Mt. Washington Observatory and of annual average sunspot numbers from the Sunspot Index Data Center, it was determined that a definite relationship between the two does not exist.

Upon initial analysis, it was noted that during sunspot maximums in 1937, there was an increased snowfall amount of 287.7 inches. Again, during sunspot maximum in 1947, there was an increase in snowfall amount of 196.1 inches. The year 1956 also had an increased amount of snowfall of 267.1 inches; however, sunspot maximum actually occurred in 1957 with a high of 190.2 sunspots. The next sunspot maximum occurred in 1968 with 105.9 sunspots; however, the snowfall high occurred in 1969, topping out at 495.2 inches! That year, though, showed a rather high average of 105.5 sunspots. The pattern then showed a great change because during the year of 1979, a sunspot maximum, there were 155.4 sunspots, but only 179.4 inches of snow. Another year for sunspot maximum was 1989 with 157.6 sunspots, but the larger snowfall occurred the year before, in 1988, with 399.7 inches of snow. The last sunspot maximum in the study occurred in 2000 with 119.6 sunspots, and a high of 311.4 inches of snow.

The first sunspot minimum during the timeframe studied occurred in 1944 with an average of only 9.6 sunspots and a low of 134.2 inches of snow. The next sunspot minimum occurred in 1954 with a low of 4.4 sunspots; however, Mt. Washington received 266.1 inches of snow that year. In 1964, there was again a low of 10.2 sunspots, but a respectable 233.0 inches of snow. In 1976, there was a low of 12.6 sunspots, but 410.2 inches of snow. A minimum in 1986 of 13.4 sunspots showed 298.7 inches of snow, lower than the years just preceding and following the minimum, but certainly a fair amount. There were 8.6 sunspots in 1996 with a snowfall amount of 341.9 inches. In 2004, as we approach the next solar minimum, the snowfall amounts on Mt. Washington have again decreased to 187.3 inches.

Upon closer examination, it was determined that the data does not support a definite relationship between annual sunspot numbers and snowfall amounts on Mt. Washington. Although some scientists would say there is a relationship, the pattern does not hold true for the length of the study. Even though some years of solar maximum were also shared by peak numbers of snowfall amounts; other years of solar maximum showed much lesser amounts of snowfall. The same was true with solar minimums. Therefore, no definite pattern could be established.

To be absolutely certain, a scatter plot was constructed to get a true representation of whether or not there was any correlation between annual sunspot number and annual snowfall amount on Mt. Washington (Figure 2). When analyzed, it was apparent that no correlation exists. Although there appeared to be a slightly negative slope, this was not enough to prove a direct correlation. Therefore, it is concluded that no correlation exists between annual sunspot number and annual amount of snowfall on Mt. Washington between 1935 and 2005.

SUMMARY AND ACKNOWLEDGEMENTS

Analysis of data from the Mt. Washington Observatory and the Sunspot Index Data Center revealed there was no relationship between the annual snowfall amount on Mt. Washington, New Hampshire and the annual average sunspot number. While some scientists have indicated that a possible relationship may exist between these two phenomena, this study did not support that theory. In the future, it may be necessary to examine data from a variety of other regions around the world to get a global picture of whether or not a relationship may exist.

I would like to thank Jim Sagle from the Mt. Washington Observatory for providing me with a chart of the annual snowfall amount on Mt. Washington for the past 70 years.

I would also like to thank Connie Walker of the National Optical Astronomy Observatory for her help with the data analysis.

REFERENCES

Sagle, Jim. "Annual Snowfall Chart." E-mail to Nate Lessard. 20 November 2005.

Sunspot Index Data Center. [Online] *http://sidc.oma.be*, 1999.

University Corporation for Atmospheric Research (UCAR). [Online] *http://www.Windows.ucar.edu/tour/link=/sun/atmosphere/sunspots.html*. 1999.

Sunspot Activity and the Amount of Tornadoes in Oklahoma

Kaylie Lachance, Grade 8
Biddeford Middle School, Biddeford, ME
Teacher: Barbara A Fortier. TLRBSE 2004

ABSTRACT

A relationship between the number of sunspots and the number of tornadoes in Oklahoma was analyzed. Information on both topics was looked at over a period of 55 years. After graphing the number of sunspots and the number of tornadoes in Oklahoma, the information was examined. Some years showed an increase in both the number of sunspots and the number of Oklahoma tornadoes, while other years showed a decrease in the number of both. There were many years where the increases and decreases were slightly different. To get a true representation of the data, a scatter plot was created. Close examination of this plot clearly showed that a relationship between annual sunspot number and annual number of Oklahoma tornadoes does not exist.

INTRODUCTION

A relationship was examined between the yearly number of sunspots and the yearly number of tornadoes in Oklahoma. The data used to determine whether sunspots and tornadoes in Oklahoma were related was over a 55 year period (1950-2005). The only years that had over one hundred tornadoes in Oklahoma were 1957, 1981, and 1999. There were 14 years that had over one hundred sunspots.

The relationship between the yearly number of sunspots and the yearly number of tornadoes in North America has been studied before. Rhonda Dicken and Holy Kiefer, student scientists at Fairfield High School in Fairfield, PA, studied a relationship between sunspots and tornadoes in the year 2002. These student scientists came to the conclusion that sunspots do not have an effect on patterns or occurrences of tornadoes in North America. However, these student scientists only studied the relationship between the number of sunspots and tornadoes for two years from January 1999 until December 2000. The data in the report was not referenced.

Astronomers are still trying to figure out how sunspots affect Earth. Sunspots are dark spots, sometimes 50,000 miles in diameter. Sunspots contract and expand as they move. Sunspots appear in groups. Sunspots are made when a concentrated portion of the solar magnetic field pokes through the surface. Sunspots can appear cooler, darker, and lower than the surrounding surface. Sunspots can last days before dying out. The number of sunspots is always changing from a high amount of sunspots to a low amount of sunspots. This is called the sunspot cycle. Sunspots vary in number over a period of approximately eleven years. Sunspots, just like the sun, should never really be directly looked at.

A tornado usually comes from a thunderstorm. A tornado is basically a violently rotating column of air extending from a thunderstorm to the ground. Tornadoes are hard to predict. This is why there are so many deaths when tornadoes occur. The Fujita Tornado Damage Scale is a scale that measures the wind speed of a tornado to determine what level a tornado is.

A tornado can be measured as a F0, F1, F2, F3, F4, F5, F0 being the smallest and F5 being the largest. Tornadoes can last anywhere from several seconds to over an hour.

Even though tornadoes can occur at any time of the year, there is a tornado season. Tornado season begins in late winter and ends in midsummer (May into early June).

It was hypothesized that the data would show a relationship between the yearly number of sunspots and the yearly number of tornadoes in Oklahoma.

OBSERVATIONS AND DATA REDUCTION

Average annual sunspot numbers for the years 1950-2005 were gathered from the Sunspot Index Data Center while the yearly number of Oklahoma tornadoes for the same period was obtained from the National Oceanic and Atmospheric Administration. Both sets of data were graphed using Microsoft Excel.

Originally, three graphs were created. The first graph showed 28 years of data from 1950-1977. The second graph showed the remaining 28 years of data from 1978-2005. The third graph contained both sets of data for all 56 years in the study. It was determined that this graph made it easiest to conclude whether or not there was a relationship between the number of sunspots and the number of tornadoes in Oklahoma. For this reason, the first two graphs were not included in the final analysis.

To obtain a true representation of whether of not a correlation exists between the two phenomena, a scatter plot was generated with annual sunspot number on the x axis and annual number of Oklahoma tornadoes on the y axis. This graph was analyzed and compared with the original graph to form a final conclusion.

ANALYSIS AND RESULTS

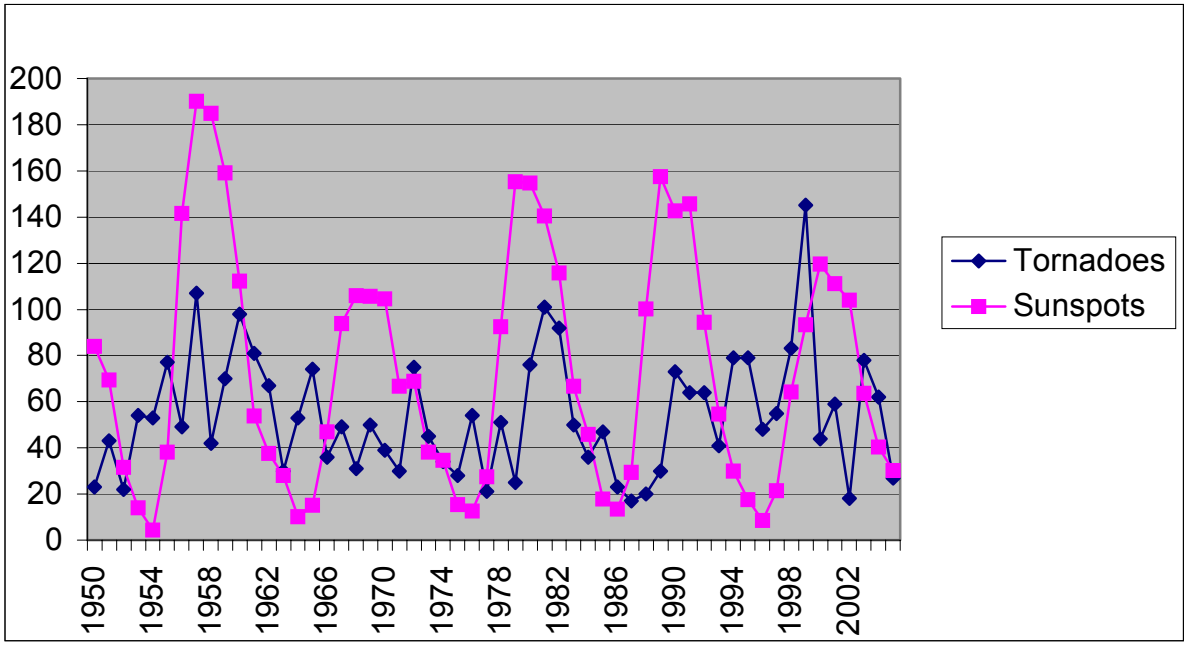

Fig 1. Graph showing average annual sunspot number and number of tornadoes in Oklahoma from 1950-2005.

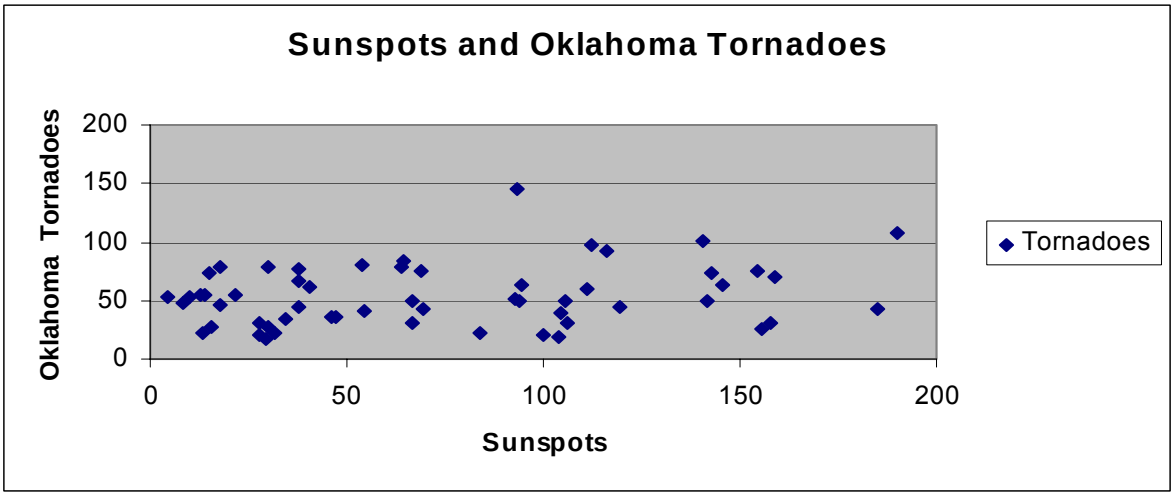

Fig 2. Scatter plot correlating the average annual sunspot number and annual number of tornadoes in Oklahoma from 1950-2005.

DISCUSSION

After initial examination of the data from the Sunspot Index Data Center and the National Oceanic and Atmospheric Administration, it was thought that an inverse relationship possibly exists between the yearly number of sunspots and the yearly number of tornadoes in Oklahoma. Looking carefully at Figure 1, between the years 1987 and1996 when the number of sunspots was low, the number of tornadoes was high.

Some years, such as 1963, 1974, and 2005, showed an almost exact same number of annual sunspots and number of Oklahoma tornadoes. Other years, such as 1952, 1966, 1972, 1973 and 1984, showed only a slight difference. Between the years 1980 and 1986, the relationship was not the relationship found between other years. Between 1980 and 1986 when the sunspot number was high, the tornado number was also high. This indicated the possibility of a direct relationship. The overall pattern, however, initially suggested an indirect relationship between average annual sunspot number and the annual number of tornadoes in Oklahoma.

To be absolutely certain, a scatter plot was produced to show a true representation of the annual sunspot number and the annual number of Oklahoma tornadoes (Figure 2). This showed clearly that no relationship between the two quantities exists. When a linear trend line was added to the plot, it showed a slightly positive slope; however, this was not enough to prove a direct correlation.

Some people may look at Figure 1 and argue the point that there appears to be a relationship between the yearly number of sunspots and the yearly number of tornadoes in Oklahoma. However, Figure 2 clearly shows there is no correlation. It should be noted, however, that this study is limited to the yearly number of tornadoes in only one particular state in the U.S. and that data from other states may need to be analyzed to make a final determination of whether or not there is any relationship between the yearly number of sunspots and tornado activity in North America as a whole.

SUMMARY AND ACKNOWLEDGEMENTS

The analysis of data from the National Oceanic Atmospheric Administration and the Sunspot Index Data Center determined that there is no relationship between the yearly average number of sunspots and the yearly number of tornadoes in Oklahoma. This coincides with the findings of student scientists, Rhonda Dicken and Holly Kiefer, from Fairfield, PA who did not find a relationship between the yearly number of sunspots and occurrences of tornadoes in North America. Although Dicken and Kiefer included tornadoes in all areas of North America, they only analyzed two years of data; this study included 56 years of data but focused only on tornadoes in Oklahoma. Despite these differences in the research, the final conclusion was the same.

I would like to thank Ms. Fortier for her help and support in doing this study and for her advice and suggestions for web sites to visit to gather information. Both are very much appreciated.

I would also like to thank Tad Johnson of the Maine Department of Education and Connie Walker of the National Optical Astronomy Observatory for their time and suggestions regarding data analysis.

REFERENCES

"National Oceanic Atmospheric Administration." [Online] *http://www.noaa*.gov/tornadoes.html. August 9, 2005.

"NOAA Storm Prediction Center" [Online] *http://www.spc.noaa.gov/faq/tornado/*, December 1, 2005.

"SIDC- Solar Influences Data Analysis Center." [Online] *http://sidc.oma.be*, December 15, 2005.

"Sunspots: Magnetic Depressions." [Online] *http://antwerp.gsfc.nasa.gov/apod/ap980322.html*, March 22, 1998.

"Sunspots." [Online] *http://www.exploratorium.edu/sunspots*, 1998.

Proof of Standard Stars

Jennifer Becker
Deer Valley High School, Antioch, CA
Teacher: Jeff Adkins, TLRBSE 2002

ABSTRACT

In doing this research, I hoped to show that a selection of listed standard stars used in a project involving the Andromeda Galaxy (M31) were, in fact, standard. I had never seen any data reference for the standards in the subrasters for the fields of the galaxy, and intended to investigate, looking at ten stars in field 14 of M31. A standard star is a star whose magnitude stays fairly constant over time and is used as a comparison towards the calculation of a target's magnitude. They are used to detect variable stars, black holes, quasars, novas and super novas, polar systems, etc.

The magnitudes for each of the stars in each picture, or epoch, were calculated by isolating one star and using the other nine stars as standards to compare to. This was done for each star in fifty selected epochs. I then made a graph for each of the stars and plotted their magnitude over time. Using these graphs, I was able to determine if the stars stayed within their given error range and therefore show them to be standard stars.

INTRODUCTION

Originally, my project idea was to find a new variable star in the Andromeda galaxy (also known as M31) based on my theory that more variables would be located near the outer edge of a galaxy, as this is where new stars are formed. This proved very difficult to do, with an incredible amount of data, and during a discussion about the project, Mr. Jeff Adkins made a statement that he had never seen actual data on the standard stars, and I was unable to find a data reference, so I decided that I would show that these listed standards were actually standard. I selected field 14 of M31, which contains about ten standards. The reason why I needed a field with more standards in it is because the more standard stars you have, the more accurate your calculations for magnitude will be and therefore your data is more reliable.

The pictures used in this project were taken by Travis A. Rector and George H. Jacoby at the Kitt Peak National Observatory in Arizona. The telescopes used were the KPNO 0.9-meter, MDM 1.3-meter and KPNO 2.1-meter telescopes. The pictures of the Andromeda Galaxy (M31) were taken periodically across nine years (1995-2004). However, there is a gap in each year where no pictures were taken and this is due to the fact that M31 is not visible from Earth from late January to late June. The pictures were taken for a nova search lab to be used in classrooms. The pictures were actually taken of the galaxy as a whole. Each picture of the galaxy was divided into 16 subrasters, or fields, in order to make locating novas easier for the students who would participate in this lab. I used these same pictures to look at a selection of the listed standard stars in the galaxy.

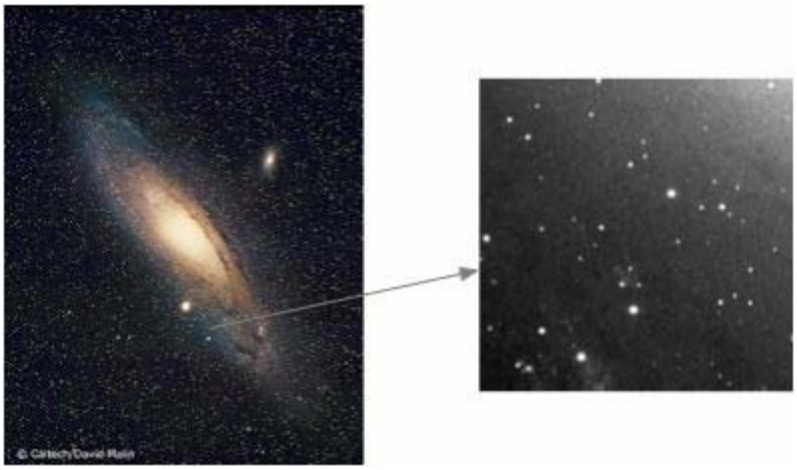

[1]

Above is a picture of the entire Andromeda Galaxy (M31). Above and to the right is the field that I selected to test, field 14.

A standard star is a star whose magnitude stays fairly constant over time. In other words, it shows very little variation. Standard stars are given an error range, because no star can stay perfectly constant as well as the possibility for random measurement error when the calculations for its magnitude were made. This error range is usually not higher than a 0.1magnitude variation. For example, if a standard star has an average magnitude of 16.5 ± 0.08, then that star is still considered constant as its magnitude can change from 0.08 above the average or below 0.08 below the average.

Standard stars are used as comparison to calculate the magnitudes of variable stars, planets, quasars, novas, etc. There are thousands of standard stars- that way, no matter where your target is, you have access to a standard somewhere within the vicinity of your target. Though there are an abundance of standard stars that we know of, there are many others out there that we have not tested. The more standards we have at our disposal, the more accurate our calculations will be when looking at a variable, or black hole, or anything else really. Standard stars are essential in the research of other objects in space. We use them in determining magnitude, and by determining magnitude, we can find out how far away the target is, what it could possibly be made of, and we can make a very close estimate as to how big it is. As you can see, standards are very important, and we all need to be able to trust them and rely on them. That is why I feel that my research is influential and important.

[1] http://www.obspm.fr/messier/Pics/More/m31caltech.jpg

The stars that I selected to test all have about the same average magnitude and similar error ranges. They are as follows:

Subraster #14 Standard Stars

Star #	My #	Magnitude	Error
50	1	16.56	±0.08
51	2	15.13	±0.08
52	3	15.92	±0.09
53	4	16.13	±0.08
54	5	14	±0.08
55	6	16.14	±0.07
56	7	17.18	±0.07
57	8	15.15	±0.06
58	9	16.5	±0.08
59	10	16.18	±0.08

ANALYSIS AND RESULTS

To collect the data on each standard star in field 14, I used a program called Image J to look at about fifty pictures based on dates, or epochs, of the field and used an aperture tool to get the brightness count of each standard star. Some of the pictures had to be skipped or disregarded because they contained bad pixels or because some of the target stars were cut out on the edge of the picture. I then pasted the data onto a spreadsheet, using Microsoft Excel, for fifty different sheets (one for each epoch, or date, observed). I then calculated the log of the brightness count ($\log(B_1)$) and then took that number and divided it by the brightness count ($\log\left(\frac{B_1}{B_1}\right)$) in other words comparing the star to itself. If the data was correct, the result of this calculation should be zero. I then calculated the log of the brightness count divided by the brightness count of each of the other nine standards ($\log\left(\frac{B_1}{B_2}\right)$; $\log\left(\frac{B_1}{B_3}\right)$… $\log\left(\frac{B_1}{B_9}\right)$). In other words, I took one star and used it as a target, and then used the other nine stars as standards. I put my results for the tests in a table, like this:

Test 1	Test 2	Test 3	Test 4	Test 5
0	0.553710078	0.237816476	0.182675653	1.022276757
-0.553710078	0	-0.315893602	-0.371034425	0.468566679
-0.237816476	0.315893602	0	-0.055140823	0.784460281
-0.182675653	0.371034425	0.055140823	0	0.839601104
-1.022276757	-0.468566679	-0.784460281	-0.839601104	0
-0.189971438	0.36373864	0.047845038	-0.007295785	0.832305319
0.115780295	0.669490374	0.353596772	0.298455949	1.138057053
-0.562584932	-0.008874854	-0.324768456	-0.379909279	0.459691825
0.015344651	0.569054729	0.253161127	0.198020304	1.037621408
-0.112567707	0.441142371	0.125248769	0.070107946	0.90970905

Test 6	Test 7	Test 8	Test 9	Test 10
0.189971438	-0.115780295	0.562584932	-0.015344651	0.112567707
-0.36373864	-0.669490374	0.008874854	-0.569054729	-0.441142371
-0.047845038	-0.353596772	0.324768456	-0.253161127	-0.125248769
0.007295785	-0.298455949	0.379909279	-0.198020304	-0.070107946
-0.832305319	-1.138057053	-0.459691825	-1.037621408	-0.90970905
0	-0.305751734	0.372613494	-0.205316089	-0.077403731
0.305751734	0	0.678365228	0.100435645	0.228348002
-0.372613494	-0.678365228	0	-0.577929583	-0.450017225
0.205316089	-0.100435645	0.577929583	0	0.127912358
0.077403731	-0.228348002	0.450017225	-0.127912358	0

(This example of my data was taken from the first epoch.)

I then took the given magnitude of one of the standards and subtracted the numbers calculated in the previous step ($mag - \log\left(\frac{B_1}{B_2}\right)$; $mag - \log\left(\frac{B_1}{B_3}\right)\ldots$ $mag - \log\left(\frac{B_1}{B_9}\right)$). I then took the average of these results and got that the magnitude for star 1 in epoch 01 is 16.573. However, in order to make it accurate, I still needed to include the standard error of the mean for this star in this epoch. To do this, I took the standard deviation of the average magnitude and divided the result by the square root of the number of measurements used in the average. For my calculations, this would be $\sqrt{9}$ =3. So my error for the magnitude of star 1 in epoch one came out to be ±0.043. This was all done for each standard in each epoch. To better explain these instructions, I have included a flow chart on the following page.

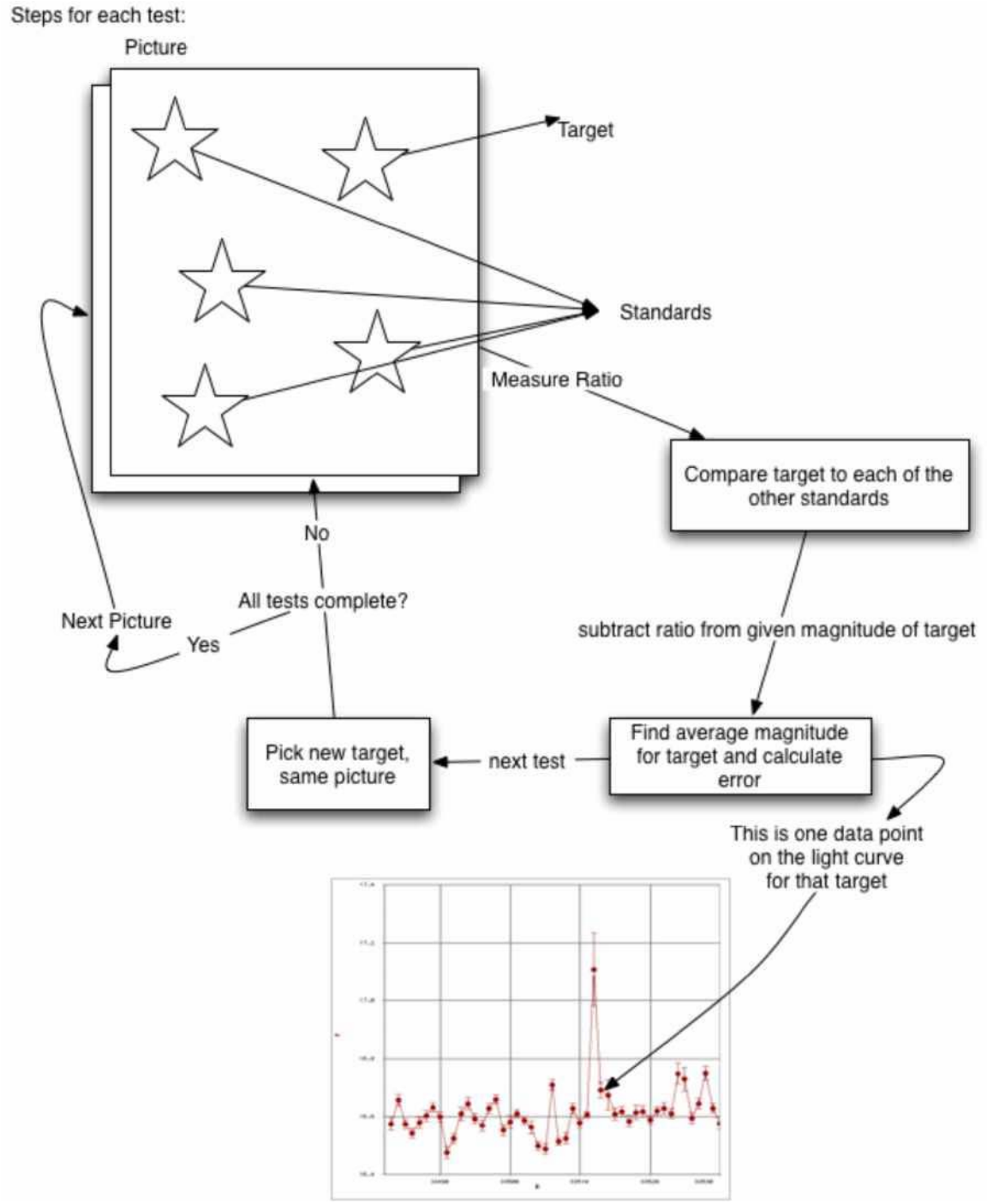

Once I had the average magnitudes and the errors for each standard in each epoch, I then made a graph for each of the ten stars and plotted their calculated magnitudes and error bars over time. Here is an example of one of my graphs:

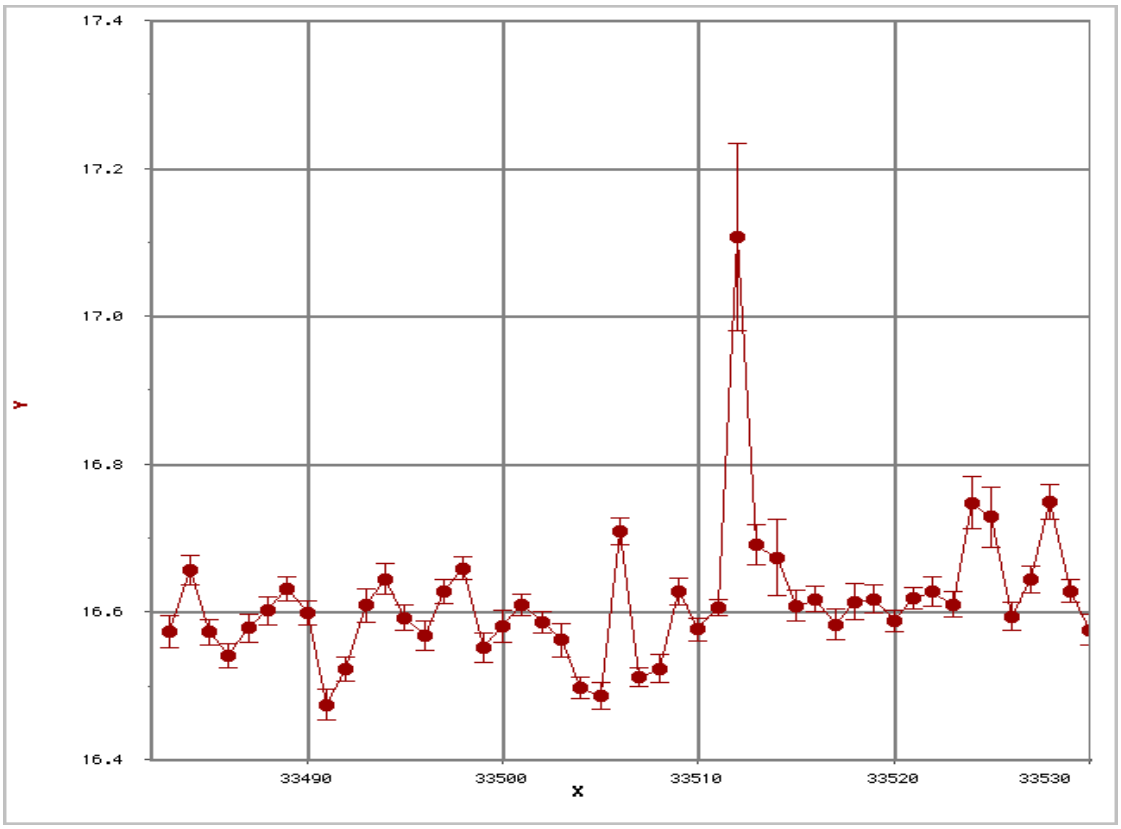

DISCUSSION

As you can see, star 1's light curve is relatively steady; its variations are within its published error range. Each of the points on the graph shows very small errors as well. The stray point at the top of the graph is a point that was off in every one of my graphs. That point is from epoch 31 and there must have been some interference in the picture. (This is something else that could be looked into.) I did attempt to re-measure the brightness counts for the standards in that picture, but I still got the same obscurity.

SUMMARY AND ACKNOWLEDGMENTS

All of my graphs showed that the standards that I tested from field 14 are all standard. Most of the stars stayed fairly constant. According to my calculations, star 3 (or listed 52) surpassed the given range for its error. I believe that a further observance of this star may lead to a better conclusion for it. However, this star's graph showed nearly a flat line, so again I suggest further observance. As I mentioned with the example of one of my graphs, there was one obscure point in every graph and it was all from the same epoch (epoch 31). Because I got the same result after attempting to re-measure the brightness counts for that same epoch, it leads me to believe that there is some sort of interference in the picture itself. I have calculated errors for all these standards, save for one, lie within the given errors, therefore showing nearly every one of these standard.

I would like to thank Mr. Jeff Adkins for all of his help and support throughout this project. Things became very tedious at points and if it were not for him, I would have likely given up.

I would also like to thank my very good friend and peer, Crystal Ewen. Without her pushing forward, I would not have the determination to complete the tasks before me.

REFERENCES

Malin, David. Digital image. [Andromeda Galaxy]. CalTech. 22 Feb. 2006 <*http://www.obspm.fr/messier/pics/More/M31caltech.com*>.

Rector, Travis. Digital images. [Field 14 of the Andromeda Galaxy]. Kitt Peak National Observatory, AZ.

Data collected through he images of Field 14 of the Andromeda Galaxy sponsored by the website *http://www.noao.edu/outreach/tlrbse* for the use of a Nova Search Lab for students.

Rector, Travis. "Cosmic Easter Eggs" Introduction. Nova Search Lab. 2000.